

**IMPROVED RECIPES FOR POLYMER GEL  
DOSIMETERS CONTAINING N-  
ISOPROPYLACRYLAMIDE**

by

Valeria Ilieva Koeva

A thesis submitted to the Department of Chemical Engineering  
in conformity with the requirements for  
the degree of Master of Science (Engineering)

Queen's University

Kingston, Ontario, Canada

(December, 2008)

Copyright © Valeria Ilieva Koeva, 2008

# Abstract

Experimental studies were undertaken to improve the radiation dose response and ease of manufacture of polymer gel dosimeters that use N-isopropyl acrylamide (NIPAM) as the monomer. An alternative carageenan gelling agent was tested in place of gelatin. Although the carageenan did reduce the gelling time for the dosimeter solution, the dose response of the dosimeters was unsatisfactory. An alternative antioxidant system, ascorbic acid and  $\text{Cu}^{2+}$ , was investigated with the aim of reducing the toxicity of dosimeter materials and providing opportunities for commercial production of prepackaged dosimeter kits. Unfortunately, the new antioxidant was ineffective for the NIPAM-based dosimeters that were studied. Three cosolvents, glycerol, N-propanol and isopropanol, were used to increase the solubility of N,N'-methylene-bisacrylamide (Bis) crosslinker in polymer gel dosimeter recipes that use NIPAM. These cosolvents enabled the manufacture of polymer gel dosimeters with higher levels of dissolved crosslinker than was previously possible. Preliminary results using x-ray computed tomography to read the resulting gels are very promising, due to enhancements in dose sensitivity. Dosimeters with high N,N'-methylene-bisacrylamide content that used isopropanol or glycerol as cosolvents had good optical clarity prior to irradiation, but did not produce reliable optical CT results for non-uniformly-irradiated gels. Further experiments and recipe optimization are required to determine whether gels with cosolvents and high levels of N,N'-methylene bisacrylamide can be used effectively for verifying spatially non-uniform dose distributions using x-ray computed tomography.

A mathematical model that includes inhibition of NIPAM-Bis polymerization was developed and the inhibition effects of MEHQ and oxygen in polymer gel dosimeters were simulated. Kinetic parameters were obtained from the literature and were estimated using

experimental data obtained by our research group. Good agreement was obtained between model predictions and experimental data with and without oxygen contamination. Simulation results indicate that MEHQ has little influence on the duration of the inhibition period and the rate of polymerization when no oxygen contamination is present, so that removal of MEHQ from dosimeter recipes is not required. Effective oxygen removal is very important to achieve reliable dosimeter results.

## Co-Authorship

The research that is presented in this thesis was conducted independently by me, under the guidance and supervision of Dr. K. B. McAuley of the Department of Chemical Engineering (Queen's University), and Dr. L. J. Schreiner of the Cancer Centre of Southeastern Ontario and the Departments of Oncology and Physics (Queen's University). Chapter 2, which describes the use of alternative crosslinkers, presents experimental data collected by myself and Mr. R.J. Senden. The manuscripts in and Chapter 4 have been submitted for publication in refereed journals (*Physics in Medicine and Biology (PMB)*, and *Macromolecular Theory Simulations (MTS)*). My cosupervisors and Mr. T. Olding assisted in the preparation and editing of Chapter 3. Dr. A. Jirasek from University of Victoria provided experimental results using x-ray computed tomography. Mr. R.J. Senden helped to develop a portion of the mathematical model described in Chapter 4. Mr. T. Olding and Mr. O. Holmes assisted with irradiation of samples and optical scanning. Mr. Khadimul Imam estimated some of the model parameters that are used in Chapter 4.

# Acknowledgements

Above all, I would like to thank my supervisors Dr. Kim McAuley and Dr. John Schreiner for their guidance throughout my research at Queen's. It was a great learning experience, and a pleasure to work with two such enthusiastic and supportive people.

I would also like to thank Tim Olding and Oliver Holmes of the Cancer Centre of Southeastern Ontario for their assistance in the experimental work, and Dr. Andrew Jirasek and Rob Senden for their invaluable support. Your help and the pleasant discussions we have had were much appreciated. Many thanks also to the faculty, staff and students of the Department of Chemical Engineering, especially my officemates in room G36 (Saeed, Shaohua, Duncan, Dean, Hui, Darmesh and Khadimul), that made my time at Queen's very enjoyable.

I am especially grateful to my husband Atanas for his continuous love and support, and for the courage to follow me to the other side of the world.

# Table of Contents

Abstract.....	ii
Co-Authorship .....	iv
Acknowledgments .....	v
Table of Contents.....	vi
List of Figures.....	ix
List of Tables .....	xiv
Nomenclature.....	xvi
Chapter 1 Introduction .....	1
Chapter 2 Evaluation of a new Gelling Agent, alternative Oxygen-Scavenging System and several Crosslinkers for NIPAM-Based Polymer Gel Dosimeters * .....	7
2.1 Introduction.....	7
2.2 The Influence of Gelatin in Polymer Gel Dosimeters.....	12
2.3 Investigations using Ceambloom 3240 as a Gelling Agent.....	15
2.3.1 .... Methods and Materials.....	19
2.3.1.1 ...CEAMBLOOM 3240.....	19
2.3.1.2 Ascorbic Acid and [Cu <sup>2+</sup> ].....	20
2.3.1.3 Crosslinkers.....	21
2.3.1.4 Gel manufacture.....	24
2.3.2 Results and Discussion.....	26
2.3.2.1 Investigating the setting time for gelatin and CEAMBLOOM 3240.....	26
2.3.2.2 Gels made with CEAMBLOOM 3240.....	27
2.3.2.3 Gels made with Ascorbic Acid and [Cu <sup>2+</sup> ] Oxygen-Scavenging System.....	29

2.3.2.4	Gels made with Alternative Crosslinkers.....	31
2.4	Conclusions .....	32
Chapter 3 Improved Polymer gel dosimeters: the use of cosolvents.....		34
3.1	Chapter Overview.....	34
3.2	Summary.....	35
3.3	Introduction.....	36
3.4	Methods and Materials .....	44
3.4.1	Solubility tests.....	44
3.4.2	Gel Manufacture.....	44
3.4.2.1	Small vials for NMR and optical CT.....	44
3.4.2.2	Vials for X-Ray CT.....	45
3.4.2.3	Large jars.....	46
3.4.3	Gel Irradiation and Measurements.....	46
3.5	Results and Discussion .....	48
3.5.1	Evaluation of Cosolvents for Increasing Bisacrylamide Solubility.....	48
3.5.1.1	Observations during Gel Manufacture.....	48
3.5.1.2	Irradiated Gels Containing Cosolvents.....	53
3.6	Conclusions.....	66
3.7	Acknowledgments.....	67
Chapter 4 Inhibition Effects: Kinetic Model Development.....		68
4.1	Chapter Overview.....	68
4.2	Summary.....	69
4.3	Introduction.....	70
4.4	Influence of THPC on Polymer Gel Dosimeters.....	75
4.5	Previous Kinetic Model.....	78

4.6	Extension of Mathematical Model to Include Oxygen and MEHQ Inhibition.....	88
4.6.1	Modeling of oxygen inhibition.....	88
4.6.1.1	Scavenging of primary radicals.....	89
4.6.1.2	Scavenging of propagating radicals by oxygen.....	89
4.6.2	Modeling of MEHQ inhibition.....	96
4.7	Results and Discussion.....	97
4.7.1	Simulations with oxygen inhibition.....	97
4.7.2	Simulations with MEHQ inhibition.....	98
4.8	Conclusions.....	100
4.9	Acknowledgments.....	101
4.10	References in Chapter 4.....	102
Chapter 5 Conclusions and Recommendations.....		109
5.1	Conclusions.....	109
5.2	Recommendations.....	112
Bibliography.....		114
Appendix A: Problems and recommendations during gel manufacturing.....		123
Appendix B: Experimental procedures.....		125
Appendix C: PREDICI© Input File.....		129



# List of Figures

<b>Figure 1.1:</b> Photograph of uniformly irradiated polymer gel dosimeters. Radiation doses vary from 0 Gy for the vial at the left to 40 Gy for the vial at the right.....	2
<b>Figure 1.2:</b> Dose-response curve of 6%T, 50%C NIPAM/Bis Dosimeter (■).....	3
<b>Figure 2.1:</b> Schematic diagram of an amine unit reacting with THPC molecule from Reeves and Guthrie (1956).....	14
<b>Figure 2.2:</b> Influence of gelling-agent concentration on gel strength for aqueous gels containing Ceambloom 3240 and Gelatin (Laustsen 2006). For a product with the same gel strength of 300 g/cm <sup>2</sup> only 1.2 wt% Ceambloom 3240 is required, compared to 3.5 wt % for gelatin.....	16
<b>Figure 2.3:</b> The most important seaweed types used in carrageenan production (Laustsen 2006).....	16
<b>Figure 2.4:</b> NMR transverse relaxation rate ( $R_2$ ) at 20 °C, determined at various times prior to irradiation for 6% T, 50% C NIPAM/Bis gel dosimeter with 5 wt % gelatin (■) and 2 wt % Ceambloom 3240 (◆). The first $R_2$ measurement was taken 2 hours after the gel phantoms were made. Curves are added to guide the eye.....	27
<b>Figure 2.5:</b> Dose-response ( $R_2$ ) curves showing the results of using Ceambloom as a setting agent for: 6% T 50% C dosimeter containing 2% CEAMBLOOM 3240 and 10 mM THPC (◆), 6% T 50% C dosimeter containing 2% CEAMBLOOM 3240 and 5 mM THPC (▲), and 6% T 50% C dosimeter containing 0.5% CEAMBLOOM 3240 (no THPC) (▲). A 6% T 50% C dosimeter containing 5% Gelatin and 10 mM THPC (■) is added as a reference. Curves are added to guide the eye.....	28
<b>Figure 2.6:</b> Trisodium citrate is used as a pH buffer, stabilizing and anticoagulant agent, antioxidant and firming agent. It is also known as E331.....	28

<b>Figure 2.7:</b> Dose-response (optical attenuation coefficient) determined at 22 °C room temperature, 24 hours post irradiation for 6% T 50% C dosimeter containing 30% isopropanol (◆) and 6% T 50% C dosimeter containing 30% N-propanol (■).....	30
<b>Figure 2.8:</b> Comparison of dose-response curve of 6%T, 50%C Aam/Bis Dosimeter (◆) with dose response of potential Aam/PEGDA258 (○), Aam/PEGDA550 (x), and Aam/PEDGA700 (◇) gel dosimeters. Reproduced from Senden <i>et al</i> (2006) with permission.....	32
<b>Figure 3.1:</b> Chemical structures and representative cartoons for (a) acrylamide (Aam); (b) N,N'-methylene-bisacrylamide (Bis).....	37
<b>Figure 3.2:</b> Simplified reaction scheme in a polyacrylamide gel dosimeter. The mechanism includes propagation (a and b), crosslinking (c) and cyclization (d) reactions. Termination reactions are not shown.....	38
<b>Figure 3.3:</b> Photographs of gels containing cosolvents showing that the clarity of the gel depends on the cosolvent used. a) 6%T, 50%C, 10% Gly NIPAM/Bis gel. b) 10%T, 50%C, 30% IPA NIAPM/Bis gel (on the <b>left</b> ) and 10%T, 50%C, 30% NPA NIPAM/Bis gel (on the <b>right</b> )...	50
<b>Figure 3.4:</b> Photographs of gels containing Sec-Butanol prior to irradiation, showing that the clarity of the gels a) From left to right: i) 4%T, 50%C, NIPAM/Bis gel (no cosolvent); ii) Water, gelatin, 10% Sec-But, 5% Bis, THPC (no NIPAM) iii) Water, gelatin, 10% Sec-But, (no monomers); iv) Water, gelatin, 10% Sec-But, THPC (no monomers); v) 10%T, 50%C, 10% Sec-But NIPAM/Bis gel; vi) Water, gelatin, 10% Sec-But, 5% NIPAM, THPC (no Bis). All gels except iv) contained 10 mM THPC.....	51
<b>Figure 3.5:</b> a) 10%T 50%C, 30% Sec-But NIPAM/Bis gel 48 hours after manufacturing. Notice that the solution separated into two distinct layers (arrows). b) Undissolved lumps formed when gelatin is soaked in an aqueous solution containing sec-butanol.....	52
<b>Figure 3.6:</b> Comparison of dose responses of a standard 6% T 50% C NIPAM/Bis dosimeter with no cosolvent (■) and a similar dosimeter containing 30 wt % isopropanol (◆). NMR responses are shown in a) and optical responses are shown in b). The gels contained 5 mMol THPC...	53

<b>Figure 3.7:</b> Dose response for an 8%T, 50%C dosimeter prepared using 10% glycerol (▲). A standard 6%T, 50%C dosimeter with no co-solvent (◆) is shown for comparison. The dosimeters contained 10 mM THPC.....	54
<b>Figure 3.8:</b> Comparison of dose responses for 10% T 50 %C NIPAM/Bis dosimeters prepared with different amounts of isopropanol co-solvent: 30% isopropanol (▲),10% isopropanol (■), no co-solvent (◆). The dosimeters contained 10 mM THPC.....	55
<b>Figure 3.9:</b> Comparison of dose-response of a 10% T, 50% C dosimeter containing 10% isopropanol (●) with an 8% T 50% C dosimeter containing 10% glycerol (▲). A standard 6%T, 50%C dosimeter with no co-solvent (◆) is shown for comparison. The dosimeters contained 10 mM THPC.....	55
<b>Figure 3.10:</b> a) Influence of time on NMR dose response of 10%T, 50%C NIPAM/Bis dosimeters containing 30 wt% isopropanol 3 hours (◆) 20 hours (■) and 42 hours (▲) after irradiation; (b) Reproducibility dose response for three replicate batches of 10 %T 50 %C NIPAM/Bis dosimeters containing 30 wt% isopropanol 20 hours after irradiation. The dosimeters contained 10 mM THPC. Curves are added to guide the eye.....	57
<b>Figure 3.11:</b> Comparison of dose responses for 10% T, 50 %C NIPAM/Bis dosimeter containing 30 wt% isopropanol (◆) and 30 wt % N-propanol (▲). The NMR a) and optical b) dose responses for a standard 6% T, 50 %C dosimeter without cosolvent (■) are shown for comparison. All dosimeters were prepared using 5 mM THPC.....	58
<b>Figure 3.12:</b> X-ray CT dose response curves for a) 10%T, 50%C NIPAM/Bis dosimeters containing 0 (◆), 10 (▲) and 30 (◆) wt% of isopropanol, and for b) 6% T, 50% C NIPAM/Bis dosimeters containing 0 (◆), 10 (■) and 30 (▲) wt% of glycerol. In Figure 3.12a the dose response for an anoxic PAG dosimeter (6% T 50% C) (●) is included for comparison. The dosimeters contained 5 mM THPC. Curves are added to guide the eye.....	59

**Figure 3.13:** Optical dose-response for a uniformly irradiated 10% T 50% C NIPAM/Bis dosimeter containing 30% isopropanol. This is the same sample used to generate one of the replicate NMR dose-responses in Figure 3.8. The optical results were measured at 22 °C, 24 hours post irradiation. The dosimeter contained 10 mM THPC. Curve is added to guide the eye.....60

**Figure 3.14:** a) Reconstructed Opt CT image for the 4%T 50%C NIPAM/Bis dosimeter with no cosolvent. b) Raw optical dose response data for the 4%T 50%C NIPAM/Bis dosimeter calibration with no cosolvent. c) Gamma map of a 500 cGy treatment plan delivered to a 4% T 50% C NIPAM/Bis dosimeter containing no cosolvent for 3% 3mm criteria.....61

**Figure 3.15:** a) Reconstructed Opt CT image for the 6%T 50%C NIPAM/Bis dosimeter containing 10% Glycerol. b) Raw optical dose response data for the 6%T 50%C NIPAM/Bis dosimeter containing 10% Glycerol, indicating that the calibration curves are unreliable.....63

**Figure 3.16** a) Reconstructed Opt CT image for the 10%T 50%C NIPAM/Bis dosimeter containing 30% isopropanol. b) Raw optical dose response data for the 10%T 50%C NIPAM/Bis dosimeter containing 30% isopropanol indicating that the calibration curves are unreliable. The presented in b) data is produced 2 hours post irradiation (■) and 20 hours post irradiation (■). Note that the points in b) correspond to the blue diamonds curve in Figure 3.20. c) Gamma map of a 500 cGy treatment plan delivered to a 10% T 50% C NIPAM/Bis dosimeter containing 30% IPA indicates regions of significant failure in the dosimetry for 3% 3mm criteria.....63

**Figure 3.17.** a) Raw optical dose response data for 4%T 50%C NIPAM/Bis dosimeter: a) with 12% isopropanol obtained 24 hours post irradiation (■) and 120 hours post irradiation (■) in a non-uniformly irradiated jar and b) without cosolvent obtained 24 hours post irradiation (■) and 4 months post irradiation (■) in a non-uniformly irradiated jar.....64

**Figure 3.18:** a) Optical data obtained from non-uniformly irradiated jars 24 hours post irradiation for: a reference 4%T 50%C dosimeter with no cosolvent (◆), a 4%T 50%C dosimeter

containing 12% isopropanol (♦), a10%T 50%C dosimeter containing 30 wt% isopropanol (♦).....	65
<b>Figure 4.1:</b> Photograph of a non-uniformly irradiated polymer gel dosimeter.....	71
<b>Figure 4.2:</b> Photograph of uniformly irradiated polymer gel dosimeters. Radiation doses vary from 0 Gy for the vial at the left to 40 Gy for the vial at the right.....	71
<b>Figure 4.3:</b> Dose-response curve of 6%T, 50%C NIPAM/Bis Dosimeter (♦).....	73
<b>Figure 4.4:</b> Comparison of the simulated and experimental calorimetric data <sup>[15]</sup> used in the parameters estimation. The samples containing O <sub>2</sub> were irradiated at a dose rate of 1.25 Gy/min to a total dose of 60 Gy and those without O <sub>2</sub> were irradiated at a dose rate of 1.1 Gy/min to a total dose of 15.4 Gy and 8.8 Gy, respectively.....	88
<b>Figure 4.5:</b> Reaction mechanism of oxygen inhibition by scavenging of propagating radicals, where R <sub>n</sub> * is a propagating chain of length n with a monomer (M) end unit, R <sub>n</sub> -O-O* is a propagating chain of length n with a peroxy end unit, and DH is a hydrogen donor (e.g. monomer). <sup>[46]</sup> .....	90
<b>Figure 4.6:</b> Simulation results showing the conversion of vinyl groups in PAG dosimeters with different initial concentrations of oxygen. The 6 %T, 50 % C dosimeters were irradiated at a dose rate of 1 Gy/min to a total dose of 20 Gy. The concentration of O <sub>2</sub> in a dosimeter in equilibrium with air is 2.5 x10 <sup>-4</sup> M.....	98
<b>Figure 4.7:</b> Simulation results comparing the vinyl group conversion over time in dosimeters with and without oxygen and MEHQ contamination. The concentration of O <sub>2</sub> in a dosimeter in equilibrium with air is 2.5 x10 <sup>-4</sup> M. The curves with oxygen were obtained using one tenth of this concentration. The simulated 6%T 50 %C dosimeters were irradiated at a dose rate of 1 Gy/min to a total dose of 10 Gy.....	99

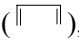
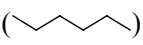
# List of Tables

<b>Table 2.1:</b> Typical 6% T, 50% C Polymer Gel Dosimeter Recipe.....	11
<b>Table 2.2:</b> Different types of Carrageenan and some of their most important properties ( <a href="http://www.ceamsa.com">www.ceamsa.com</a> ).....	17
<b>Table 2.3:</b> Characteristics of CEAMBLOOM 3240.....	19
<b>Table 2.4:</b> Polymer gel dosimeters prepared using different weight percentages of Ceambloom 3240 and different recipes.....	20
<b>Table 2.5:</b> Polymer gel dosimeters prepared using Ascorbic Acid and $[Cu^{2+}]$ as an oxygen scavenger.....	20
<b>Table 2.6:</b> Chemical structures of the crosslinkers, physical state (L=liquid and S=solid), presence of inhibitors, and recipes used in this study. An asterisk (*) is used to indicate crosslinkers that contained monomethyl ether hydroquinone (MEHQ). These crosslinkers were purified using a column with 0.5 g of inhibitor remover for MEHQ.....	22
<b>Table 3.1:</b> Typical 6%T, 50%C normoxic polyNIPAM Gel Dosimeter Recipe (Senden <i>et al</i> 2006, Jirasek <i>et al</i> 2006).....	40
<b>Table 3.2:</b> Solubility (by % weight) of Bis in aqueous solution at 50 °C with different cosolvents.....	49
<b>Table 4.1:</b> Typical 6%T, 50%C Polymer Gel Dosimeter Recipe.....	72
<b>Table 4.2:</b> Simplified reaction scheme in the aqueous phase in a PAG dosimeter. The scheme is illustrated using cartoons: = represents Aam monomer; $\square$ represents Bis, $\sim$ is a polymer chain that can have a radical (*) on either an Aam or Bis end unit. Reaction (2.1) indicates that many different products are generated by water radiolysis. The efficiency factor, $f$ , accounts for the fact that only a fraction of the radical pairs generated by radiolysis can diffuse out of the cage to initiate polymerization. Reactions analogous to (2.9-2.11)	

involving polymer chains with a terminal Bis are included in the model, but are not shown to save space. The model also assumes that polymer chains with a single crosslink precipitate to form a separate phase and that polymerization and crosslinking reactions continue in the precipitated microgels. Details are presented by Fuxman *et al.*<sup>[8,22]</sup>.....79

**Table 4.3:** Optical observations for a variety of unirradiated 6 %T 50% C PAG recipes. The symbol X indicates that a particular component was present. Recipes with gelatin contained 5 wt% gelatin and those with THPC contained 10 mM THPC. The dosimeter that was purged with N<sub>2</sub> was oxygen-free. No radiation, except stray light, was applied to any of the dosimeters so that side reactions could be investigated.<sup>[26]</sup> Samples were wrapped with aluminum foil to prevent polymerization reactions initiated by light and placed in the refrigerator to solidify.....77

**Table 4.4:** Parameters used in Polymer Gel Dosimeter Simulations. The parameters that are in **bold** are new values estimated from experimental data.<sup>[15,25]</sup> The remaining values were used by Fuxman *et al.*<sup>[8,22]</sup> or are from the literature.....84

**Table 4.5:** Proposed simplified reaction scheme for oxygen inhibition by scavenging of propagating radicals using cartoons: acrylamide monomer ( = ), bisacrylamide monomer (  ), AAm/Bis co-polymer chain (  ) that can have a radical (\*) on either an acrylamide, bisacrylamide or peroxy end unit. Q\* is a MEHQ radical, and Q is a dead species. This mechanism is shown in Table 4.7 using the notation of Fuxman *et al.*<sup>[8,22]</sup>.....91

**Table 4.6:** Proposed reaction scheme for oxygen inhibition by scavenging of propagating radicals and for reactions involving MEHQ, where S<sub>i,n</sub> is a short chain radical of length n with acrylamide (i = 1), bisacrylamide (i = 2) or peroxy (i = 3) radical end unit, dead polyperoxides (D<sub>3,n</sub>) and peroxy acids (D<sub>4,n</sub>). Q\* is a MEHQ radical, and Q is a dead species. These reaction equations are added to the original PAG dosimeter model of Fuxman *et al.* (2003).<sup>[8]</sup> The oxygen reactions are assumed to happen only in the aqueous phase.....93

# Nomenclature

---

## Symbols

---

C	Cyclized unit
$D_n$	Dead polymer chain of length n
$D_{3,n}$	Dead polymer chain of length n, containing one or more peroxide groups
$D_{4,n}$	Dead polymer chain of length n, with a peroxy acid end group
DH	Hydrogen donor
$e_{aq}^-$	Hydrated electron
f	Radical efficiency
G	Gelatin
$H^\bullet$	Hydrogen radical
$HO_2^\bullet$	Perhydroxyl radical
$H_2$	Hydrogen molecule
$H_2O^*$	Excited water molecule
$H_3O^+$	Oxonium ion
$H_2O_2$	Hydrogen peroxide molecule
I	Light intensity
k	Reaction rate constant [ $M^{-1}s^{-1}$ ]
$k_c$	Rate constant for intermolecular cyclization reactions [ $M^{-1}s^{-1}$ ]
$k_{f,jk}$	Rate constant for chain transfer reaction of a polymer radical bearing the active radical on an acrylamide unit ( $j = 1$ ), bisacrylamide unit ( $j = 2$ ), or peroxy unit ( $j = 3$ ) to acrylamide monomer ( $k = 1$ ) or bisacrylamide monomer ( $k = 2$ ) [ $M^{-1}s^{-1}$ ]
$k_{f,jG}$	Rate constant for chain transfer reaction of a polymer radical bearing the active



	radical on an acrylamide unit ( $j = 1$ ), bisacrylamide unit ( $j = 2$ ), or peroxy unit ( $j = 3$ ) to gelatin [ $M^{-1}s^{-1}$ ]
$k_{i,k}$	Rate constant for initiation reaction between primary radicals and acrylamide monomer ( $k = 1$ ) or bisacrylamide monomer ( $k = 2$ ) [ $M^{-1}s^{-1}$ ]
$k_{i,3}$	Rate constant for inhibition reaction between primary radicals and oxygen [ $M^{-1}s^{-1}$ ]
$k_{p,jk}$	Rate constant for propagation of a polymer radical bearing the active radical on an acrylamide unit ( $j = 1$ ) or bisacrylamide unit ( $j = 2$ ) with acrylamide monomer ( $k = 1$ ) or bisacrylamide monomer ( $k = 2$ ) [ $M^{-1}s^{-1}$ ]
$k_{p,j3}$	Rate constant for inhibition reaction between oxygen and a polymer radical bearing the active radical on an acrylamide unit ( $j = 1$ ) or bisacrylamide unit ( $j = 2$ ) [ $M^{-1}s^{-1}$ ]
$k_{p,3k}$	Rate constant for re-initiation of a peroxy radical with acrylamide monomer ( $k = 1$ ) or bisacrylamide monomer ( $k = 2$ ) [ $M^{-1}s^{-1}$ ]
$k_{p,Gk}$	Rate constant for re-initiation of a gelatin radical with acrylamide monomer ( $k = 1$ ) or bisacrylamide monomer ( $k = 2$ ) [ $M^{-1}s^{-1}$ ]
$k_{t,jk}$	Rate constant for termination reaction between a polymer radical bearing the active radical on an acrylamide unit ( $j = 1$ ), bisacrylamide unit ( $j = 2$ ), or peroxy unit ( $j = 3$ ) and a polymer radical bearing the active radical on an acrylamide unit ( $k = 1$ ), bisacrylamide unit ( $k = 2$ ), or peroxy unit ( $k = 3$ ) [ $M^{-1}s^{-1}$ ]
$k_{x,j}$	Rate constant for crosslinking reaction between an unreacted pendant double bond and a polymer radical bearing the active radical on an acrylamide unit ( $j = 1$ ) or bisacrylamide unit ( $j = 2$ ) [ $M^{-1}s^{-1}$ ]
$n$	Index of refraction
$M_1$	Acrylamide monomer
$M_2$	Bisacrylamide monomer

$\text{OH}^\bullet$	Hydroxyl radical
$\text{O}_2^{\bullet-}$	Superoxide anion radical
$\text{Q}^*$	MEHQ radical
$\text{Q}$	Dead species
$\text{PR}^\bullet$	Primary radical
$\text{R}^*$	General notation for polymer radical
$\text{R-O-O}^*$	General notation for peroxy radical
$\text{R-O-O-R}$	General notation for polyperoxide
$\text{R-O-OH}$	General notation for peroxy acid
$\text{R}_2$	Transverse relaxation rate [ $\text{s}^{-1}$ ]
$\text{S}_{j,n}$	(short) Propagating radical of length n, bearing the active radicals on an acrylamide unit ( $i = 1$ ), bisacrylamide unit ( $i = 2$ ), or peroxy ( $i = 3$ ) unit.
$\text{T}_2$	Transverse relaxation time [s]
$\nu$	Factor used to reduce the reactivity of radicals on a bisacrylamide unit
$\text{X}$	Crosslinked unit

---

#### Subscripts

---

n, or m	Number that indicated chain length
1	Acrylamide
2	Bisacrylamide
3	Peroxy

---

#### Superscripts

---

$\bullet$ , or $*$	Radical species
--------------------	-----------------

---

Greek

---

$\alpha$	Light attenuation coefficient
$\gamma$	Gamma radiation
$\theta$	Fraction of gelatin radicals that can re-initiate polymerization

---

Acronyms

---

AAM	Acrylamide monomer
BHT	Butylated hydroxytoluene stabilizer
Bis	N,N'-methylene-bisacrylamide crosslinker
CPMG	Carr-Purcell-Meiboom-Gill pulse sequence
CT	Computed Tomography
FT	Fourier Transform
Gy	Unit for radiation dose ( = J/kg)
HQ	Hydroquinone inhibitor
MAc	Methacrylic acid monomer
MEHQ	Hydroquinone monomethyl ether inhibitor
Mn	(number average) Molecular weight
MRI	Magnetic Resonance Imaging
MSDS	Material Safety Data Sheet
NIPAM	N-isopropylacrylamide monomer
NMR	Nuclear Magnetic Resonance
PAG	Polyacrylamide gel
PAGAT	Polyacrylamide gel with THPC antioxidant

PDB	Pendant double bond
ppm	Parts per million
SSD	Source-to-surface distance
TDB	Terminal double bond
THPC	Tetrakis (hydroxymethyl) phosphonium chloride

---

### Cartoons

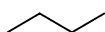
---



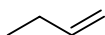
Acrylamide unit



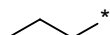
N,N'-methylene-bisacrylamide unit



Polymer chain



Polymer chain with vinyl group



Polymer chain with radical

---

# Chapter 1

## Introduction

According to the Canadian Cancer Society (Statistics Canada, 2006) more than 50% of new cancer patients will require radiation therapy as part of their treatment. It is imperative to deliver the correct dose of radiation to the tumour, without harming surrounding healthy tissue. In recent years, polymer gel dosimeters have been developed for detecting 3-dimensional radiation dose distributions delivered by radiation therapy equipment. The most widely used dosimeter for verification of spatial dose distribution is the Polyacrylamide Gel (PAG) dosimeter (Maryanski *et al* 1994b, De Deene *et al* 2006). PAG dosimeter recipes are usually referred to by the concentrations of monomers in the solution prior to irradiation. The specifications most commonly used are %T, the total mass percent of monomers (acrylamide, AAm, and N,N'-methylene-bisacrylamide, Bis) in the gel system and %C, the mass percent of the monomer mixture that is crosslinker. When the dosimeter is irradiated, in place of the patient, radiolysis of the water creates free radicals that induce polymerization and crosslinking. As shown in Figure 1.1, more crosslinked polymer forms and precipitates at locations where the radiation dose is high than where the dose is low. Note that radiation doses are specified in units of Gray (Gy), where 1 Gy corresponds to 1 Joule of ionizing radiation delivered per kg of sample.

Highly crosslinked microgels precipitate from the solution and can be detected using a variety of imaging techniques including Magnetic Resonance Imaging (MRI) (Maryanski *et al* 1993), x-ray Computed Tomography (CT) (Hilts *et al* 2000) and optical scanning techniques (Maryanski *et al* 1996a). Uniformly irradiated vials, like those shown in Figure 1.1, can be used to construct NMR, x-ray or optical dose response curves.

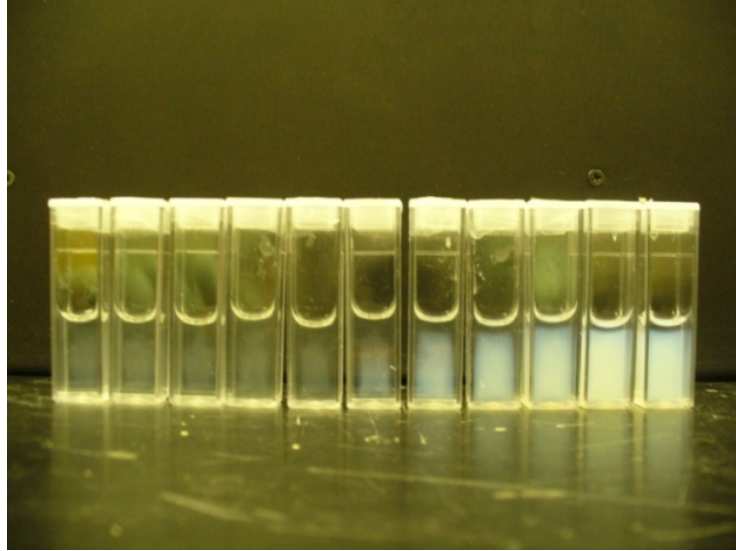


**Figure 1.1:** Photograph of uniformly irradiated polymer gel dosimeters. Radiation doses vary from 0 Gy for the vial at the left to 40 Gy for the vial at the right.

Figure 1.2 shows an NMR dose response curve for a typical polymer gel dosimeter. Dose sensitivity is the slope of linear low-dose portion of the dose-response curve. The vertical axis on this figure is  $R_2$ , the transverse relaxation rate, measured by  $^1\text{H}$  NMR. The horizontal axis is the radiation dose. Note that Magnetic Resonance Imaging (MRI) can be used to obtain local values of  $R_2$  in polymer gels that have received spatially non-uniform radiation doses like those used to treat cancer patients. Figure 1.2 can then be used to determine the radiation dose at locations of interest within the non-uniformly irradiated gel and to confirm (or not) that the radiation-delivery equipment is delivering the expected dose to the correct position.

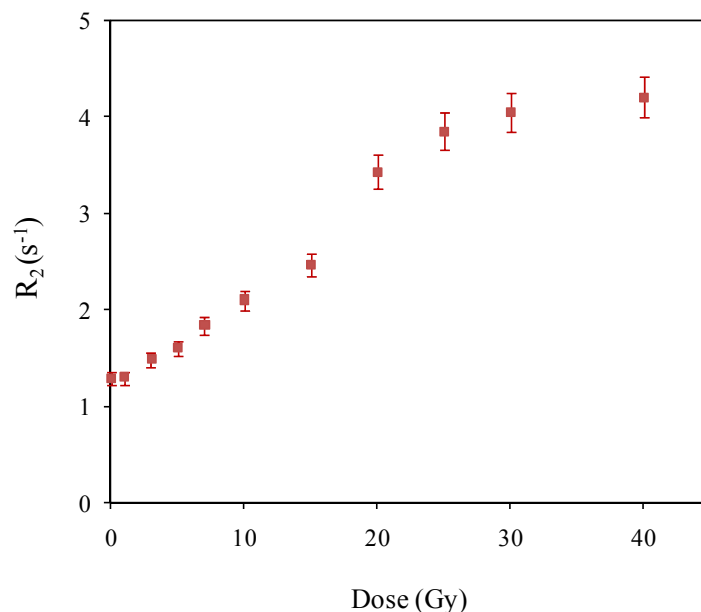


**Figure 1.2:** Dose-response curve of 6%T, 50%C NIPAM/Bis Dosimeter (■).

Over the years, much effort has gone into developing improved polymer gel dosimeter recipes. The Acrylamide (Aam) monomer in PAG dosimeters is a dangerous neurotoxin and suspected human carcinogen that requires careful handling (Ibbott 2004, Papagianis *et al* 2006). Recently it was shown by Senden *et al* (2006) that acrylamide can be successfully replaced with N-isopropylacrylamide (NIPAM), thereby reducing considerably the safety concerns with handling chemicals in the clinical environment. NIPAM-based dosimeters are safer to use, because NIPAM is a larger less-toxic molecule with less chance of accidental contact for the user because it has a lower vapour pressure and it cannot pass easily through the skin. The radiation-dose response of NIPAM-based dosimeters is very similarly to PAG dosimeters. They produce a similar dose-sensitivity when the dosimeter is examined using NMR and optical techniques. Fortunately, the dosimeter response does not appear to be sensitive to changes in the dose rate or temperature during irradiation (Senden *et al* 2006). NIPAM has good water solubility and is relatively inexpensive for clinical use.

Oxygen is a well-known inhibitor of free-radical polymerization (Rudin 1982, Odian 1991), which can have a significant effect on the performance of polymer gel dosimeters (Hepworth *et al* 1999, McJury *et al* 1999, Salomons *et al* 2002). The rates of the chemical reactions between oxygen and free radicals are sufficiently high that even small amounts of oxygen can consume enough radicals to inhibit or significantly retard polymerization reactions, influencing the response of polymer gel dosimeters. Moreover, the level of dissolved O<sub>2</sub> in polymer gel dosimeters can vary depending on manufacturing procedures and storage conditions prior to irradiation, resulting in variable dosimetry results. It is therefore important to remove oxygen from polymer gel dosimeters. Traditionally this was done by bubbling the dosimeter solution with an inert gas in a glove box (Baldock *et al* 1998) during phantom preparation.

In recent years, “normoxic” polymer gel dosimeters have become popular due to their low sensitivity to oxygen and convenient preparation (e.g. Fong *et al* 2001, De Deene *et al* 2002b, Venning *et al* 2005, De Deene *et al* 2006, Jirasek *et al* 2006, Senden *et al* 2006). Normoxic dosimeters can be manufactured and stored under normal atmospheric conditions because they include an oxygen scavenger. Tetrakis (hydroxymethyl) phosphonium chloride (THPC) is a preferred antioxidant due to its high reactivity in scavenging oxygen (De Deene *et al* 2002b). Recently, Jirasek *et al* (2006) and De Deene *et al* (2006) showed that there are fundamental differences between polyacrylamide gels with and without THPC antioxidant that affect their dose-response behaviour. Jirasek *et al* (2006) presented a chemical mechanism that explains oxygen consumption by THPC. THPC can also participate in a large number of side reactions. Jirasek *et al* (2006) used Raman spectroscopy to confirm that THPC reacts with gelatin. There is no appreciable consumption of acrylamide and bisacrylamide monomers by reactions with THPC in the absence of free radicals. THPC can, however, react with free radicals in polymer gel dosimeters, resulting in reduced polymerization rates and reduced dose sensitivity (De Deene *et al* 2006).



Gelatin is currently the preferred gelling agent in dosimeter recipes because of its good optical clarity (Maryanski *et al* 1993, Maryanski *et al* 1994b). Increasing gelatin concentration in PAG dosimeters leads to lower dose sensitivity. Also higher gelatin levels lead to higher values of  $R_2$  at zero dose, because more gelatin leads to stiffer gels, which have higher relaxation rates (DeDeene *et al* 2002). Changes in background stiffness of the gel can be also caused by crosslinking reactions involving gelatin and THPC (DeDeene *et al* 2002, Jirasek *et al* 2006). Aqueous gelatin solutions require time (up to 12 hours) to set and it would be beneficial if a better, faster-setting gelling agent could be identified so that polymer gel dosimeters could be used soon after they are made.

Limited water solubility and low crosslinking efficiency are the main concerns with the use of N,N'-methylene-bisacrylamide (Bis) in polymer gel dosimeters. Low crosslinking efficiency arises due to primary cyclization, which is abundant due to the formation of a favorable seven-membered ring, so that as much as 80% of the bisacrylamide is consumed by this reaction (Tobita *et al* 1990, Naghash *et al* 1996). Vinyl groups consumed by primary cyclization are not available for crosslinking reactions. Replacing the relatively inefficient Bis crosslinker is worth investigating, because a more efficient crosslinker could increase the performance and the accuracy of gel dosimeters.

The goal of this research is to improve current polymer gel dosimeter recipes, and ameliorate the overall performance of “normoxic” PAG and NIPAM-based dosimeters. Chapter 2 describes the investigation of a new gelling agent, an alternative oxygen scavenger system and 10 potential crosslinkers. Unfortunately, none of these proposed improvements was successful. Because the search for a better crosslinker was unsuccessful, cosolvents are used (in Chapter 3), to increase the solubility of bisacrylamide (Bis) in the polymer gel solution. Three different cosolvents (glycerol, isopropanol and N-propanol) are shown to be effective for increasing the solubility of Bis, enabling the manufacture of dosimeters with enhanced dose sensitivity. In addition to attempts to improve the recipe of polymer gel dosimeters, existing mathematical

models are extended to describe the kinetic processes that occur in irradiated polymer gel dosimeters that are contaminated by oxygen and MEHQ inhibitor (Chapter 4). Synergistic inhibition effects of MEHQ and oxygen on the NIPAM-Bis polymerization in uniformly-irradiated dosimeter are simulated to show that the level of MEHQ does not influence polymerization if the oxygen has been removed. Conclusions based on the experimental work and simulation results, and recommendations for future studies are presented in Chapter 5.

## **Chapter 2**

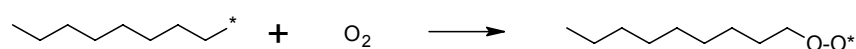
# **Evaluation of a new Gelling Agent, alternative Oxygen-Scavenging System and several Crosslinkers for NIPAM-Based Polymer Gel Dosimeters\***

### **2.1 Introduction**

This chapter describes the testing of several alternative NIPAM-based polymer gel dosimeter recipes that are aimed at reducing the time and effort required for the manufacture of dosimeter phantoms and at improving dosimeter sensitivity and accuracy. Gelatin is currently the preferred gelling agent in dosimeter recipes because of its better optical clarity compared to agarose (Maryanski *et al* 1993, Maryanski *et al* 1994b) the original gelling agent that was first used. In addition to keeping the precipitated microgels at the location where they form, gelatin also has other effects on the behavior of polymer gel dosimeters. The strong dependence of polymerization rate on gelatin concentration in PAG (and related dosimeters) suggests that one of the most important polymer-radical-consuming reactions involves gelatin (Fuxman *et al* 2003). Because aqueous gelatin solutions require time to set, polymer gels are usually manufactured one day before the dosimeters are irradiated. It would be beneficial if a better, faster-setting gelling agent could be identified so that polymer gel dosimeters could be used soon after they are made.

\*Note that some of the research results presented in this chapter have been published in Koeva *et al*, 2008a

Early polymer gel dosimeters were prepared in glove boxes in an oxygen-free environment to prevent contamination by oxygen, which inhibits free-radical polymerization (Maryanski *et al* 1994b). Even small amounts of oxygen can inhibit free radical copolymerization reactions in polymer gel dosimeters (Hepworth *et al* 1999). The peroxy radicals created by reactions of oxygen with growing polymer chains are generally unreactive for further polymerization reactions, but can participate in bimolecular termination reactions (Kishore *et al* 1981).



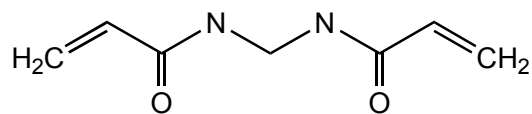
In recent years, oxygen scavengers (also called antioxidants) have been included in polymer-gel-dosimeter recipes. A variety of antioxidants and their effects on the dose-response characteristics have been studied. De Deene *et al* (2002b) studied the following oxygen scavengers: ascorbic acid, gallic acid, trolox, N-acetyl-cysteine, and THPC for use in PAG dosimeters. Among these antioxidants, the most promising results were shown by THPC. Before adapting polyacrylamide dosimeters for preparation in regular atmospheric conditions through the addition of THPC Fong *et al* (2001) introduced a formulation that permitted gel dosimeters to be prepared under normal atmospheric conditions. This new type of dosimeter was termed methacrylic and ascorbic acid in gelatin initiated by copper, or MAGIC, and was said to be less toxic than acrylamide-based dosimeters. De Deene *et al* (2002b) showed that some initial polymerization takes place in MAGIC gels due to the creation of radicals from the ascorbate-copper-oxygen complex. Copper acts as a catalyst in the oxygen scavenging by oxidation of ascorbic acid. The polymerization reaction can be terminated by a redox reaction in which  $\text{Cu}^{2+}$  is reduced if high concentrations of  $\text{CuSO}_4 \cdot 5\text{H}_2\text{O}$  are used. Adding oxygen scavengers to polymer gel dosimeters leads to higher dose responses at low scavenger levels and to reduced dose responses at high scavenger levels (Hurley *et al* 2005, Haraldsson *et al* 2006). THPC is widely used to make “normoxic” PAG and

\*Note that some of the research results presented in this chapter have been published in Koeva *et al*, 2008a

methacrylic-acid-based dosimeters, since it is a more rapid oxygen scavenger than ascorbic acid (Jirasek *et al* 2006). It also helps to improve temporal and spatial stability of polyacrylamide gel dosimeters, mostly because long-lived radicals are consumed by reactions with THPC. However THPC is known to be highly toxic and viscous liquid, which makes it non-attractive to use. Reactions between THPC and oxygen are reasonably well understood, but these are not the only reactions in which THPC participates. THPC leads to chemical and physical changes in the gelatin matrix, which causes changes in  $R_2$  of irradiated and non irradiated polymer gels. Reactions between THPC and polymer radicals also reduce polymerization rates and dose sensitivity. Jirasek *et al* (2006) suggested that the difference in the dose sensitivities of a “normoxic” PAG dosimeter and an anoxic dosimeter may be due to a reduction in monomer mobility due to more crosslinked gelatin. They calculated that a 5 mM THPC solution contains about five times as much THPC as is needed to consume all of the oxygen. It seems that much of the remaining 80 % of the THPC is consumed by reactions with gelatin, including additional crosslinking of the gelatin network. Recently, Luci *et al* (2007) recently reported effective oxygen scavenging in a methacrylic-acid-based dosimeter recipe using ascorbic acid in combination with  $[Cu^{2+}]$  as the oxygen-scavenging system. It will be beneficial to study the behavior of this scavenging system in NIPAM-based dosimeters. This will allow us to reduce the overall toxicity of the gels and to avoid reactions with gelatin. Also nontoxic ascorbic acid and  $Cu^{2+}$  could be added as solids. Since all of the components in the standard recipe (Senden *et al* 2006, De Deene *et al* 2002b) are solids, except for the water and THPC solution, there may be an opportunity for a company to prepare and sell pre-weighed packets of water-free dosimeter contents. The physicists and technicians who use the dosimeters could “just add water” and then use the dosimeters without careful weighing or special training.

As summarized by Senden *et al* (2006) all dosimeters described in the literature use Bis (shown below) as the crosslinker.

\*Note that some of the research results presented in this chapter have been published in Koeva *et al*, 2008a



N,N'-methylene-bisacrylamide crosslinker

The only exception is the polymethacrylic acid gel dosimeter, which does not require a crosslinker (De Deene *et al* 2006) because linear polymethacrylic acid polymer precipitates from solution when it is produced in the presence of gelatin. Limited water solubility and low crosslinking efficiency are the main concerns with the use of Bis in PAG and related polymer gel dosimeters. Low crosslinking efficiency arises due to primary cyclization, which is abundant due to the formation of a favorable seven-membered ring, so that as much as 80% of the bisacrylamide is consumed by this reaction (Tobita *et al* 1990, Naghash *et al* 1996). Vinyl groups consumed by primary cyclization are not available for crosslinking reactions. A large number of different monomers have been used in place of acrylamide (Aam), with N-isopropylacrylamide (NIPAM) being particularly effective because it has similar chemical properties as Aam, but is much safer to use (Senden *et al* 2006).

Design of polymer gel dosimeter recipes is based on a set of important considerations. The gels must be tissue-equivalent to radiation. The gelling agent (i.e., gelatin) must ensure that the crosslinked polymer remains at the location where it forms. The monomers must be highly reactive at room temperature, and a high crosslink density must be achieved to ensure precipitation of the polymer (Maryanski *et al* 1997). Relatively nontoxic and inexpensive components are preferred. Maryanski *et al* (1997) showed that PAG dosimeters with high Bis concentrations (i.e., high %C and %T) lead to large dose sensitivities when MRI is used for imaging the gels. Dose sensitivity is the slope of the initial linear portion of the  $R_2$  vs. dose plot (see Figure 1.2). A large slope is an important factor for obtaining accurate dose calibration

\*Note that some of the research results presented in this chapter have been published in Koeva *et al*, 2008a

results. Unfortunately, Bis has only limited solubility in aqueous systems. The 6% T 50% C dosimeter recipe in Table 2.1, where Bis is at its solubility limit, enjoys widespread use for dosimeters that are probed using MRI (Baldock *et al* 1998, DeDeene *et al* 2002b). It may be possible to produce more effective dosimeters if higher levels of crosslinking can be obtained.

**Table 2.1:** Typical 6% T, 50% C Polymer Gel Dosimeter Recipe.

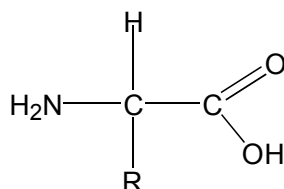
<b>Monomer</b>	<b>Acrylamide (Aam) or N-isopropylacrylamide (NIPAM)</b>	<b>3 g</b>
<b>Crosslinker</b>	N,N'-methylene-bisacrylamide (Bis)	3 g
<b>Gelatin</b>		5 g
<b>Water</b>		89 ml
<b>Antioxidant</b>	Tetrakis (hydroxymethyl) phosphonium chloride (THPC)	10 mM

The aim of the current work is to develop improved NIPAM-based polymer-gel-dosimeter recipes that will be easier to use and will produce higher dose sensitivities. First, a new carrageenan-based gelling agent (CEAMBLOOM 3240<sup>®</sup> available from P.L. Thomas & Co., Inc. USA), which sets more quickly than gelatin, is evaluated for use in dosimeter recipes in the hope that the time between gel preparation and irradiation can be reduced. Second, an alternative antioxidant system, ascorbic acid with [Cu<sup>2+</sup>], recently used by Luci *et al* (2007) for methacrylic-acid-based dosimeters, is tested for use for in NIPAM dosimeters. Finally, several alternative crosslinkers are evaluated and new techniques for increasing the solubility of Bis are tested. It would be beneficial to replace Bis with an alternative crosslinker that does not undergo primary cyclization, or one that is more soluble in water. The former may be achieved by using crosslinking agents that have a larger number of covalent bonds between the vinyl groups (Gopalan *et al* 1982), because 8-,9- or 10-membered rings are less geometrically favored than 7 membered rings. Another advantage

to selecting larger crosslinker molecules is that they should diffuse more slowly, reducing edge enhancement, which occurs due to diffusion of monomer and crosslinker from unirradiated to irradiated zones within the dosimeter (McAuley 2004, Vergote *et al* 2004 and Fuxman *et al* 2005) during the polymerization process. Experimental results related to testing of the new gelling agent, the alternative antioxidant and alternative crosslinkers are described in this chapter. Results related to increasing the solubility of Bis using cosolvents are presented in Chapter 3.

## 2.2 The Influence of Gelatin in Polymer Gel Dosimeters

Gelatin is a mixture of water-soluble proteins derived primarily from collagen (Digenis *et al* 2006). It contains specific amounts of 18 different amino acids (AA) which are joined together in sequences to form polypeptide chains of ca. 1000 AA per chain, scientifically known as the primary structure. The general structure of an alpha amino acid is:



Where "R" represents a side chain specific to each amino acid.

Most amino acids in gelatin have this alpha structure, wherein the amine group and carboxyl group are attached to the same carbon. Several studies have been performed to elucidate the influence of gelatin on the response of polymer gel dosimeters (Baldock *et al* 1998, DeDeene *et al* 2002b). In PAG-type gels, increasing gelatin levels result in decreased dose sensitivity due to radical-consuming chain-transfer reactions between growing polymer chains and gelatin (Fuxman *et al* 2003).



Chain transfer reaction:



The gelatin-centered radicals that form are slow to reinitiate polymerization, but can participate in termination reactions. It is important that the main chain-stopping reactions in PAG (and related) dosimeters involve only one growing polymer chain (i.e., chain-transfer to gelatin involves a single polymeric radical and so does termination between a gelatin radical and a polymeric radical). If the main chain-stopping reaction were bimolecular termination between two polymeric radicals (or a polymeric radical and a primary radical), then the rate of polymerization would be dose-rate dependent. Fortunately, the response of PAG (and related) dosimeters is quite dose-rate independent, compared to other competing gel systems, such as polymethacrylic acid gels (DeDeene et al, 2006, Karrlson *et al*, 2007). In polymethacrylic acid gels, increasing gelatin results in increasing NMR dose sensitivity, and the presence of gelatin is required to induce polymerization (De Deene *et al* 2006, Hayashi *et al* 2008). In PAG-type gels, it is thought that the crosslinked polyacrylamide (or polyNIPAM) forms an interpenetrating polymer network with the gelatin (Lepage *et al* 2001d, Jirasek and Duzenli 2001), while in the methacrylic-acid-based gel dosimeter the polymer may be chemically grafted onto the gelatin matrix (De Deene *et al* 2006).

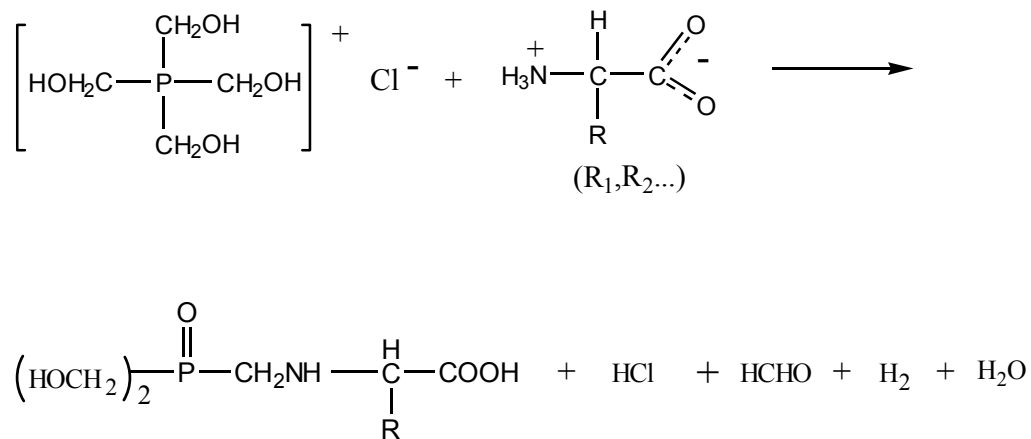
Babic and Schreiner (2006) obtained NMR dose-response curves for a series of gelatin-free PAG dosimeters. As expected, these dose-response curves had an initial linear region at low radiation doses and the response leveled off (saturated) at higher doses where there was less unreacted monomer (and crosslinker) available for polymerization. The dose-response curves for these gelatin-free dosimeters saturated at much lower radiation doses than corresponding gelatin-containing PAG dosimeters. The reason for this difference in behavior is that no polymerization-inhibiting gelatin was present to consume polymeric free radicals, and larger amounts of monomer and comonomer were consumed at lower radiation doses. The strong dependence of

\*Note that some of the research results presented in this chapter have been published in Koeva *et al*, 2008a

polymerization rate on gelatin concentration in nPAG (and related dosimeters) results in lower dose sensitivities than could be obtained using a gelling agent that does not consume radicals appreciably.

Gelatin can also participate in side reactions with oxygen scavengers (antioxidants) that are used in normoxic dosimeter recipes. In their study about the role of Tetrakis (hydroxymethyl) phosphonium chloride (THPC) as an antioxidant in polyacrylamide gel dosimetry, Jirasek *et al* (2006) revealed that THPC can react with gelatin and thus induce changes to the gelatin matrix. It was proved that the addition of THPC in the solution leads to chemical changes to the gelatin solution. Even though the density of the solution was not changed, the form of the gelatin matrix is altered by increasing the gelling of the polymer solution. These side reactions consume THPC and make less of it available for oxygen scavenging.

Each gelatin molecule will have an amine unit at one end, and may have some pendant amine groups resulting from amino acids with two amine groups. Reeves and Guthrie (1956) have shown that THPC can react with these groups present in gelatin chains, thereby increasing the coagulation and cross-linking of the gelatin (See Figure 2.1).



or

\*Note that some of the research results presented in this chapter have been published in Koeva *et al*, 2008a

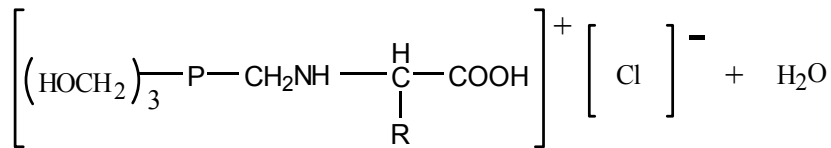


**Figure 2.1:** Schematic diagram of an amine unit reacting with THPC molecule from Reeves and Guthrie (1956).

Increased gelatin crosslinking leads to stiffer gels with higher values of  $R_2$  at zero radiation dose. This high initial value of  $R_2$  can make it more difficult to detect changes in  $R_2$  that are caused by the radiation-induced polymerization and microgel precipitation.

In summary, it would be beneficial to identify a suitable replacement for gelatin in polymer gel dosimeter applications. Among the most important considerations are: setting time, chain-transfer reactions that consume polymer radicals and influence dose sensitivity, reactions with THPC that influence gel stiffness and consume THPC, need for refrigeration and controlled cooling rates during setting, and optical clarity.

### 2.3 Investigations using Ceambloom 3240 as a Gelling Agent

In an attempt to find a suitable replacement for gelatin, as other researchers did in the past (Bussche *et al* 2004), the scientific literature on gelling agents used in food preparation was surveyed. These gelling agents are commercially available, reasonably priced and often optically clear. We found that Ceambloom 3240, an attractive alternative to traditional gelling agents, was recently introduced in the global marketplace. This new product results from a new separation technology developed by a Spanish carrageenan company (CEAMSA, [www.ceamsa.com](http://www.ceamsa.com)). This new purified carrageenan extract possesses desirable properties that include: optical clarity, fast

\*Note that some of the research results presented in this chapter have been published in Koeva *et al*, 2008a

setting time, high gel strength compared to gelatin (See Figure 2.2), good heat stability and gel formation without the need for refrigeration.

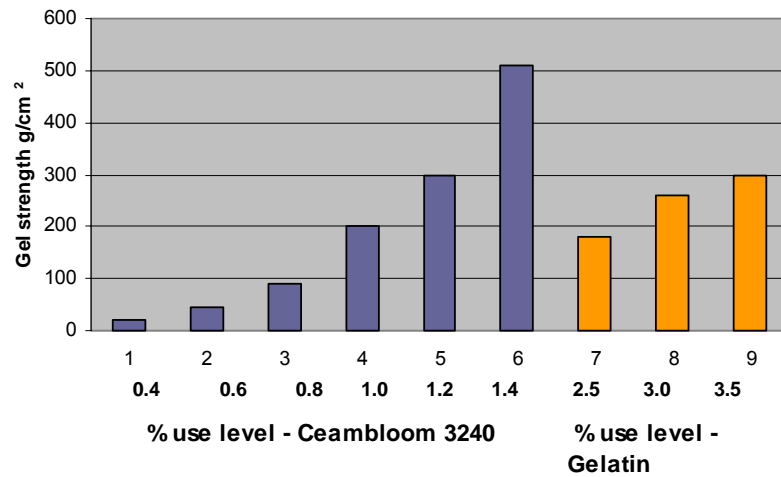


**Figure 2.2:** Influence of gelling-agent concentration on gel strength for aqueous gels containing Ceambloom 3240 and Gelatin (Laustsen 2006). For a product with the same gel strength of 300 g/cm<sup>2</sup> only 1.2 wt% Ceambloom 3240 is required, compared to 3.5 wt % for gelatin.

This carrageenan-based product is a natural hydrocolloid extracted from red seaweed of the Rhodophyceae class (Figure 2.3).

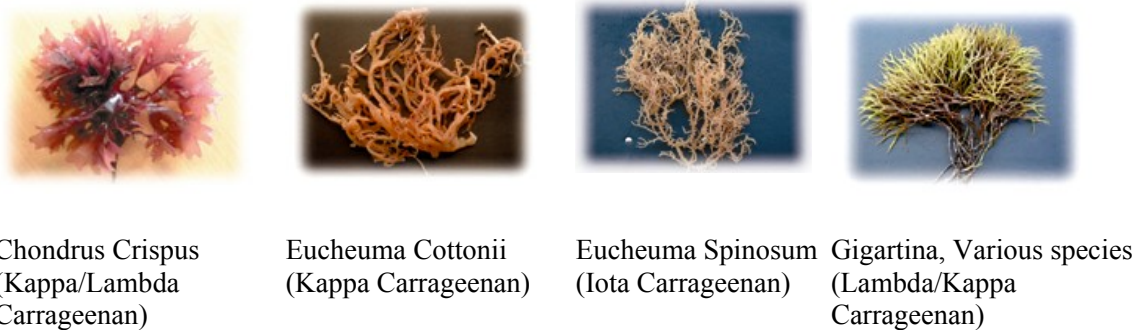


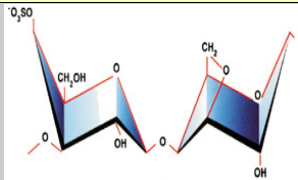
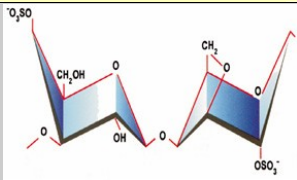
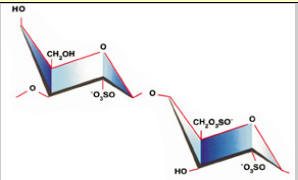
**Figure 2.3:** The most important seaweed types used in carrageenan production (Laustsen 2006).

\*Note that some of the research results presented in this chapter have been published in Koeva *et al*, 2008a

Carrageenan is a high-molecular-weight linear polysaccharide made from repeating galactose units and 3,6 anhydrogalactose units, both sulphated and non-sulphated and joined by alternating  $\alpha$ 1-3 and  $\beta$ 1-4 glycosidic linkages. Since Carrageenan is a large molecule (molecular weight >500.000 daltons) composed of some 1000 monomer units, there are many structural variations. There are three main types of commercial carrageenan that have been identified. These are known as KAPPA, IOTA and LAMBDA which are idealized molecules assigned a definitive structure (Table 2.2) [www.ceamsa.com](http://www.ceamsa.com). Seaweed does not yield these ideal types of Carrageenan, but is composed of a range of intermediate structures.

**Table 2.2:** Different types of Carrageenan and some of their most important properties

([www.ceamsa.com](http://www.ceamsa.com))

	KAPPA	IOTA	LAMBDA
<b>Raw Material</b>	<b>Cottonii</b>	<b>Spinosum</b>	<b>Gigartina/Chondrus</b>
<b>Molecule Structure</b>			
<b>3,6 anhydro-D galactose</b>	Yes	Yes	No
<b>SO<sub>4</sub>-content</b>	25%	35%	40%
<b>Texture type</b>	Brittle, firm gel with a tendency to syneresis	Cohesive and thixotropic gel with no syneresis	No gelling agent. Will thicken the solution only.

<b>Solubility</b>			
Hot water	Soluble at 70°C	Soluble at 70°C	Soluble
Cold water	Na <sup>+</sup> salts soluble, Ca <sup>++</sup> and K <sup>+</sup> salts insoluble	Na <sup>+</sup> salts soluble, Ca <sup>++</sup> salts gives thixotropic dispersions	Soluble
Organic solvents	Insoluble	Insoluble	Insoluble
<b>Gelation</b>			
Strongest gel with:	K <sup>+</sup> ion	Ca <sup>++</sup> ion	No gel
Gel texture	Brittle	Elastic	
Re-gelation after shear/thixotropy	No	Yes	No
Freeze/thaw stable.	No	Yes	Yes
<b>Stability</b>			
At neutral pH and alkaline pH	Stable	Stable	Stable
At acid pH	Hydrolyzed in solutions when heated. Stable in gelled form.	Hydrolyzed in solutions when heated. Stable in gelled form.	Hydrolyzed.

According to the supplier's MSDS Ceambloom 3240 is a clear beige powder, which is odorless and tasteless. It is dispersible in cold water and totally soluble above 70 °C. It is insoluble in organic solvents. When using Ceambloom 3240, the following methods should be used to obtain good results ([www.ceamsa.com](http://www.ceamsa.com)).

- The filling temperature should be above 55 °C;
- In an acid medium, gel strength degradation increases with the temperature and heating time. It is recommended that Ceambloom 3240 should be used in neutral or alkali media;
- The powder should be poured over the water, while it is quickly stirred;
- For complete dissolution the solution should be heated up to 70-80 °C.

Other characteristics of Ceambloom 3240 are shown in Table 2.3.

**Table 2.3:** Characteristics of CEAMBLOOM 3240.

<b>pH</b>	<b>7-9.5 (1.0% at 20°C in aqueous solution)</b>
<b>Particle size</b>	98% gum below 250 microns (60 US mesh, DIN 24)
<b>Density</b>	700 kg/m <sup>3</sup>

## 2.3.1. Methods and Materials

### 2.3.1.1. Ceambloom 3240

Three batches of Polymer gel dosimeters were manufactured, using N-iso propylacrylamide (NIPAM) as a monomer and N,N'-methylene-bisacrylamide (Bis) as a crosslinker (both from Sigma- Aldrich Canada, Ltd.). The recipes in Table 2.4 with 3% NIPAM and 3% Bis are commonly referred to as 6 %T, 50 %C dosimeters. The quantity of Ceambloom 3240 was varied

from 0.5 to 2 wt% along with the concentration of Tetrakis hydroxymethyl phosphonium chloride (THPC), which varied from 0 mM to 10 mM (Sigma- Aldrich Canada, Ltd.).

**Table 2.4:** Polymer gel dosimeters prepared using different weight percentages of Ceambloom 3240 and different recipes.

	<b>Experiment 1</b>	<b>Experiment 2</b>	<b>Experiment 3</b>
<b>Water</b>	92 wt%	93.5 wt%	92 wt%
<b>Ceambloom 3240</b>	2 wt%	0.5 wt%	2 wt%
<b>NIPAM</b>	3 wt%	3 wt%	3 wt%
<b>Bis</b>	3 wt%	3 wt%	3 wt%
<b>THPC</b>	10mM	0	5mM

### 2.3.1.2. Ascorbic Acid and [Cu<sup>2+</sup>]

Two batches of 6% T 50% C polymer gel dosimeters were manufactured using standard manufacturing procedures (Senden *et al* 2006). The THPC oxygen scavenger from the standard recipe (Senden *et al* 2006) was replaced with ascorbic acid in combination with [Cu<sup>2+</sup>] as an oxygen-scavenging system. Either isopropanol or n-propanol (Sigma- Aldrich Canada, Ltd.) was added to the recipe (See Table 2.5).

**Table 2.5:** Polymer gel dosimeters prepared using Ascorbic Acid and [Cu<sup>2+</sup>] as an oxygen scavenger.

	<b>30 wt% Isopropanol</b>	<b>30 wt% n-propanol</b>
<b>Water</b>	59 wt%	59 wt%
<b>Gelatin</b>	5 wt%	5 wt%

\*Note that some of the research results presented in this chapter have been published in Koeva *et al*, 2008a



<b>NIPAM</b>	3 wt%	3 wt%
<b>Bis</b>	3 wt%	3 wt%
<b>Ascorbic Acid</b>	0.305 g	0.305 g
<b>CuSO<sub>4</sub>·5H<sub>2</sub>O</b>	0.00043 g	0.00043 g

### 2.3.1.3 Crosslinkers

Using the standard gel dosimeter recipe shown in Table 2.1, tests were performed using several alternative crosslinkers (Table 2.6). Note that crosslinkers d) and e) had lower solubility than Bis, so 3%T, 50%C recipes were tested for these crosslinkers, and it is possible that a portion of the crosslinkers used did not dissolve in these dosimeters. Initially several other commercially-available crosslinkers with chemical structures similar to Bis were considered, but they were not pursued because they are too insoluble in water (e.g., 1,4- cyclohexanedimethanol divinyl ether and divinylbenzene), or they have suspected chronic health hazards (e.g., 1,6-hexanediol diacrylate and neopentyl glycol diacrylate). Acrylamide (electrophoresis grade) was used in experiments involving crosslinkers a)-e), but NIPAM (97%) was used with crosslinkers h) to j). The latter experiments were performed after we had confirmed that NIPAM is an effective and safer-to-use replacement for Aam (Senden *et al* 2006). Crosslinkers f) and g) were too insoluble in water to warrant testing in dosimeter recipes. Chemicals were used as received from Sigma-Aldrich Canada, Ltd., except for the crosslinker j) N,N'- ethylene-bisacrylamide (98%), which was purchased from Fluka, Germany and i) calcium diacrylate, which was donated by Sartomer, USA. The PEG divinyl ethers (d and e in Table 2.6) are liquids that were shipped and stored without any inhibitor, which could be a sign that they are relatively unreactive for polymerization and crosslinking. N,N'-diallyltartardiamide, calcium diacrylate and N,N'- ethylene-bisacrylamide are all solids, with no inhibitors, and were used as they were received.

**Table 2.6:** Chemical structures of the crosslinkers, physical state (L=liquid and S=solid), presence of inhibitors, and recipes used in this study. An asterisk (\*) is used to indicate crosslinkers that contained monomethyl ether hydroquinone (MEHQ). These crosslinkers were purified using a column with 0.5 g of inhibitor remover for MEHQ

Crosslinker structure	State	Inhibitor	Monomer	Recipe
<b>Poly(ethylene glycol) diacrylate (PEGDA),</b> <b>with:</b> <b>a) Average Mn=258</b> <b>b) Average Mn=550</b> <b>c) Average Mn=700</b> $\text{CH}_2=\underset{\text{H}}{\text{C}}-\overset{\text{O}}{\parallel}{\text{C}}-\left(\text{O}-\underset{\text{H}_2}{\text{C}}-\underset{\text{H}_2}{\text{C}}\right)_n-\text{O}-\overset{\text{O}}{\parallel}{\text{C}}-\underset{\text{H}}{\text{C}}=\text{CH}_2$	L	100 ppm MEHQ*	Aam	6%T, 50%C
	L	400-600 ppm MEHQ*	Aam	6%T, 50%C
	L	100 ppm MEHQ* and 300 ppm BHT (butylated hydroxytoluene )	Aam	6%T, 50%C
	L	no inhibitor	Aam	3%T, 50%C

\*Note that some of the research results presented in this chapter have been published in Koeva *et al*, 2008a

$\text{H}_2\text{C}=\underset{\text{H}}{\text{C}}-\text{O}-\left(\underset{\text{H}_2}{\text{C}}-\underset{\text{H}_2}{\text{C}}-\text{O}\right)_2-\underset{\text{H}}{\text{C}}=\text{CH}_2$				
<b>e) Tri(ethylene glycol) divinyl ether (TEGDVE), 98%</b>	L	no inhibitor	Aam	3%T, 50%C
$\text{CH}_2=\underset{\text{H}}{\text{C}}-\left(\underset{\text{H}_2}{\text{O}}-\underset{\text{H}_2}{\text{C}}-\underset{\text{H}_2}{\text{C}}\right)_3-\underset{\text{H}}{\text{O}}-\underset{\text{H}}{\text{C}}=\text{CH}_2$				
<b>f) Ethoxylated (14) Trimethylolpropane triacrylate (EthTT)</b>	L	500 ppm MEHQ		Insoluble in water
$\left[\text{CH}_2=\underset{\text{H}}{\text{C}}-\overset{\text{O}}{\parallel}{\text{C}}-\text{O}-\left(\underset{\text{H}_2}{\text{C}}-\underset{\text{H}_2}{\text{C}}-\text{O}\right)_n-\overset{\text{H}_2}{\text{C}}\right]_3-\underset{\text{H}_2}{\text{C}}-\underset{\text{H}_2}{\text{C}}-\text{CH}_3$ <p style="text-align: center;"><math>n+n+n=14</math></p>				
<b>g) 1,3,5-Triacryloylhexahydro-1,3,5-triazine (THT),98%</b>	S	no inhibitor		Insoluble in water
<b>h) N,N'-diallyltartardiamide</b>	S	no inhibitor	NIPAM	6%T, 50%C

$\text{CH}_2=\underset{\text{H}}{\text{C}}-\underset{\text{H}_2}{\text{C}}-\text{N}-\underset{\text{O}}{\overset{\text{OH}}{\text{C}}}-\underset{\text{H}}{\overset{\text{H}}{\text{C}}}-\underset{\text{OH}}{\overset{\text{O}}{\text{C}}}-\text{N}-\underset{\text{H}_2}{\text{C}}-\underset{\text{H}_2}{\text{C}}=\text{CH}_2$				
<b>i) Calcium Diacrylate</b>	S	no inhibitor	NIPAM	6%T, 50%C
$\text{CH}_2=\underset{\text{H}}{\text{C}}-\overset{\text{O}}{\parallel}{\text{C}}-\text{O}-\text{Ca}-\text{O}-\overset{\text{O}}{\parallel}{\text{C}}-\underset{\text{H}}{\text{C}}=\text{CH}_2$				
<b>j) N,N'-ethylenebis(acrylamide),98%</b>	S	no inhibitor	NIPAM	6%T, 50%C
$\text{CH}_2=\underset{\text{H}}{\text{C}}-\underset{\text{H}_2}{\text{C}}-\text{N}-\underset{\text{H}_2}{\text{C}}-\underset{\text{H}_2}{\text{C}}-\text{N}-\underset{\text{H}_2}{\text{C}}-\underset{\text{H}_2}{\text{C}}=\text{CH}_2$				

### 2.3.1.4 Gel manufacture

The polymer gel dosimeters were manufactured inside a fume hood, under normal atmospheric conditions using standard experimental procedures (De Deene *et al* 2002b, Baldock *et al* 1998). Gelatin (300 Bloom Type A) was allowed to swell in 80% of the de-ionized water for 10 minutes at room temperature, before heating to 50 °C. A water bath was used to ensure uniform temperature around the flask. Alternatively, for gels that were prepared with the carrageenan-based gelling agent (CEAMBLOOM 3240<sup>®</sup> available from P.L. Thomas & Co., Inc. USA ([www.plthomas.com](http://www.plthomas.com))), the gelling agent was allowed to swell for 10 minutes and was then heated to 80 °C, which is the temperature suggested by the manufacturer. While stirring continuously,

the crosslinker was dissolved, requiring between 15 and 25 minutes for dissolution, depending on the crosslinker. After the gelatin-crosslinker mixture was cooled (to approximately 32-33 °C for recipes with gelatin and to approximately 50 °C for recipes with carrageenan to prevent premature setting), the monomer (Aam or NIPAM) was added. A solution of the antioxidant (THPC or Ascorbic acid + CuSO<sub>4</sub>·5H<sub>2</sub>O) was prepared with the remaining 20% of the water, and added to the solution. The resulting solution was transferred into small plastic vials, which were filled to a height of 2 cm and then capped. The caps were wrapped with sealing film to prevent additional oxygen from entering the samples. The samples were wrapped with aluminum foil to prevent photo-polymerization, and placed in a refrigerator to set. The dosimeters were irradiated up to 40 Gy, at room temperature, 24 hours after gel manufacture. Note that in chapter 3, experiments are described where larger containers were used for some experiments.

NMR relaxation rates ( $R_2$ ) were determined between one and three days after irradiation, so that polymerization reactions involving long-lived radicals would have stopped (Baldock *et al* 1998). Note that the proton NMR response  $R_2$  can be obtained at various locations in non-uniformly irradiated gels using Magnetic Resonance Imaging (MRI), which is also used for 3-dimensional imaging of tumours. Polymer gel samples with higher crosslinking levels and higher monomer conversion result in a higher  $R_2$  measurement due to enhanced magnetization transfer resulting from higher rigidity of the gel system (Babic and Schreiner 2006, Schreiner 2008, De Deene 2008). Experimental procedures to irradiate and image polymer gel dosimeters with different crosslinkers were identical to those described by Senden *et al* (2006). Polymer formation alters the visual properties of the gel due to the creation of polymer micro-particles that scatter light. The change in optical properties enables non-uniformly irradiated gels to be scanned using optical CT (See chapter 3). For the uniformly-irradiated gels produced in this chapter, an Ultrospec 1000 UV/Visible Spectrophotometer was used to quantify the fraction of light that

could pass through the samples. Attenuation coefficients of the irradiated polymer gels were determined using transmission readings from the spectrophotometer.

## **2.3.2 Results and Discussion**

### **2.3.2.1 Investigating the setting time for gelatin and CEAMBLOOM 3240**

Figure 2.4 shows the influence of setting time on  $R_2$  for an un-irradiated NIPAM-based gel phantoms containing gelatin and containing CEAMBLOOM 3240. The gelatin continues to set for a long time, resulting in increasing  $R_2$  for many hours after the phantom is made. As a result, dose-response curves that are made soon after gel manufacture can be significantly different from dose-response curves obtained several hours or days later (De Deene *et al* 2002a). In addition, the rate at which the gel sets depends on the thermal conditions during setting (Lepage *et al* 2001d). Since large gel phantoms cool at different rates than small phantoms, different  $R_2$  values can be obtained from different phantoms due to differences in size and geometry (De Deene *et al* 2007). Although this problem is less severe when gels are probed using optical and x-ray CT methods, it would be beneficial to replace gelatin with a fast-setting gelling agent that would produce constant dose response curves within an hour of phantom manufacture, regardless of the phantom size. The faster setting time for dosimeter phantoms with CEAMBLOOM 3240 as a gelling agent was confirmed in preliminary experiments using unirradiated gel phantoms (See Figure 2.4). These results were encouraging enough so that a series of gels was produced and irradiated to test the potential of CEAMBLOOM 3240 as a replacement for gelatin.

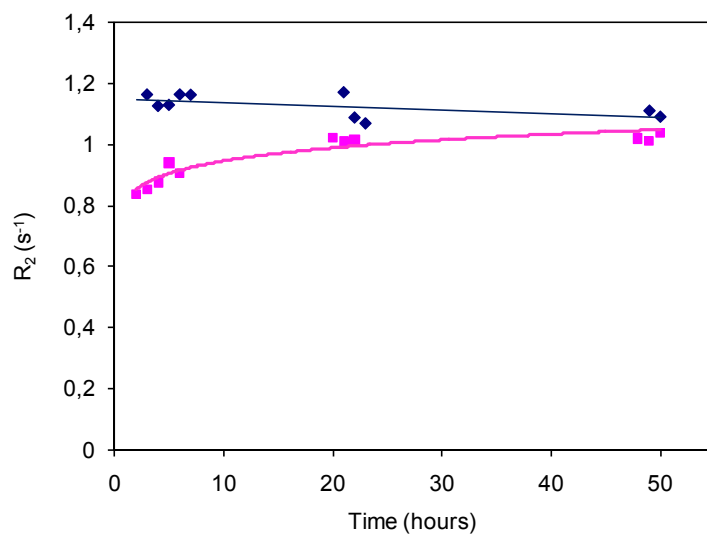


**Figure 2.4:** NMR transverse relaxation rate ( $R_2$ ) at 20 °C, determined at various times prior to irradiation for 6% T, 50% C NIPAM/Bis gel dosimeter with 5 wt % gelatin (■) and 2 wt % Ceambloom 3240 (◆). The first  $R_2$  measurement was taken 2 hours after the gel phantoms were made.

### 2.3.2.2 Gels made with CEAMBLOOM 3240

Three batches of 6 %T, 50 %C NIPAM/Bis gel dosimeters were prepared using different concentrations of Ceambloom 3240 and THPC. For all of the dosimeters prepared using Ceambloom, the transverse relaxation rate  $R_2$  is very low compared to that for the standard dosimeter prepared using gelatin. For some of the dosimeters prepared using Ceambloom, significant polymerization was detected at high radiation doses beyond 30 Gy (Figure 2.5).

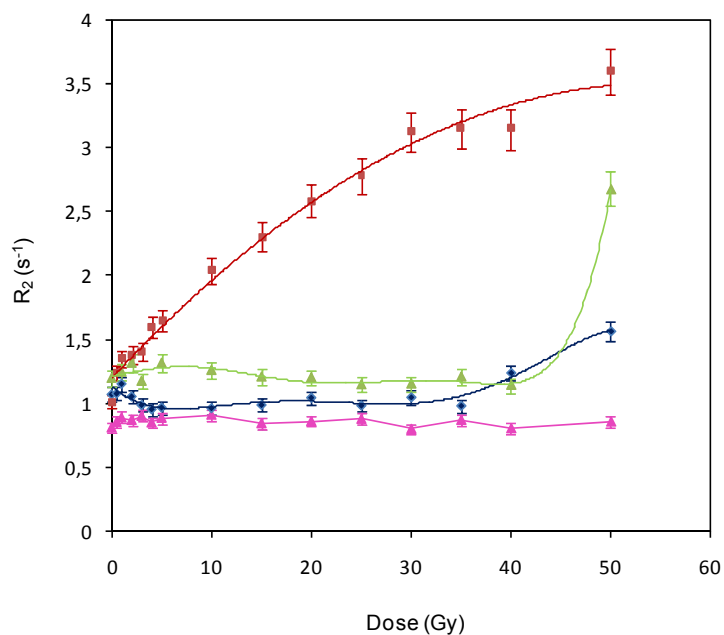


**Figure 2.5:** Dose-response ( $R_2$ ) curves showing the results of using Ceambloom as a setting agent for: 6% T 50% C dosimeter containing 2% CEAMBLOOM 3240 and 10 mM THPC (◆), 6% T 50% C dosimeter containing 2% CEAMBLOOM 3240 and 5 mM THPC (▲), and 6% T 50% C dosimeter containing 0.5% CEAMBLOOM 3240 (no THPC) (▲). A 6% T 50% C dosimeter containing 5% Gelatin and 10 mM THPC (■) is added as a reference. Curves are added to guide the eye.

It should be noted that Ceambloom 3240 contains unknown amounts of sodium citrate (Figure 2.6) and also some potassium chloride (0.3 %), which are known to be very strong preservatives and cation scavengers ([www.chemicaland21.com](http://www.chemicaland21.com)) that may inhibit the polymerization process.

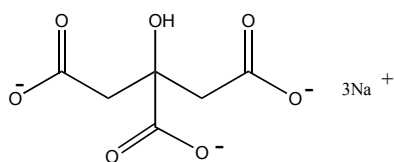


**Figure 2.6:** Trisodium citrate is used as a pH buffer, stabilizing and anticoagulant agent, antioxidant and firming agent. It is also known as E331.

\*Note that some of the research results presented in this chapter have been published in Koeva *et al*, 2008a



Although the gels produced using CEAMBLOOM 3240 set very quickly, radiation dose-response curves showed that CEAMBLOOM 3240 is not an effective gelling agent for use in polymer gel dosimetry, because it results in inhibition of the dose response. It is recommended that carrageenan-based gelling agents should be tested again if gelling agents without additives (or with lower levels of additives) become available.

### **2.3.2.3 Gels made with Ascorbic Acid and [Cu<sup>2+</sup>] Oxygen-Scavenging System**

THPC oxygen scavenger from the standard recipe was replaced with ascorbic acid in combination with [Cu<sup>2+</sup>] as an oxygen-scavenging system. Despite the promising results obtained for methacrylic-acid-based dosimeter recipe (Luci *et al* 2007), this new formulation did not work for the NIPAM-based dosimeters (See Figure 2.7). Even for radiation doses in the range of 30-40 Gy no polymerization was observed. Both R<sub>2</sub> and the optical attenuation coefficient remained small, indicating that the oxygen was not scavenged from the system, or that some other species inhibited the polymerization.

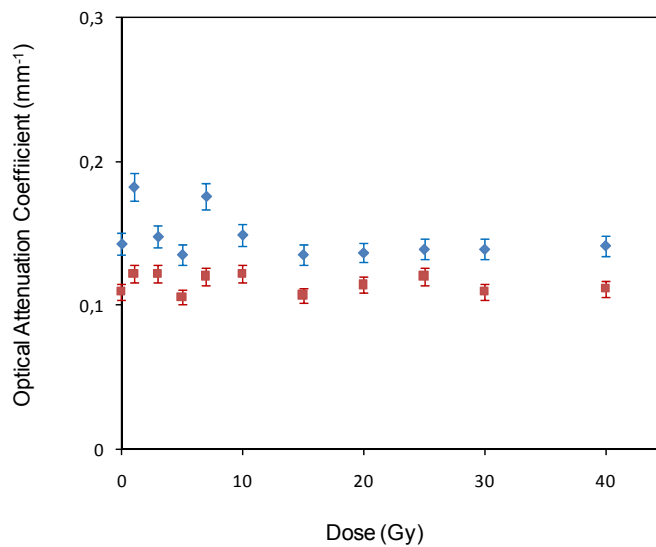


**Figure 2.7:** Dose-response (optical attenuation coefficient) determined at 22 °C room temperature, 24 hours post irradiation for 6% T 50% C dosimeter containing 30% isopropanol (♦) and 6% T 50% C dosimeter containing 30% N-propanol (■).

An additional problem that was encountered is that the gels with ascorbic acid were very weak. The gelatin was unable to form a sufficiently strong gel, and the gels became liquid at room temperature after they were removed from the refrigerator. One of the reasons that liquefaction of gels was not reported by Luci *et al* (2007) could be that their methacrylic-acid-based dosimeter contained 9% gelatin (because gelatin improves dose response in polymethacrylic gels) whereas typical recipes for NIPAM-based dosimeters (and also PAG) contain only 5 % gelatin. Note that the failure of the ascorbic acid and  $\text{Cu}^{2+}$  oxygen-scavenging system may have been due to imperfect mixing of the gel content. Other research groups have experienced problems with the ascorbic acid oxygen-scavenging system in polymethacrylic acid gels when they did not use very vigorous mixing (i.e., when they mixed with a magnetic stirrer rather than with a household hand mixer) (ref., Personal Communication with Dr. Andreas Berg, October, 2008).

### 2.3.2.4 Gels made with Alternative Crosslinkers

New polymer gel dosimeters were prepared and irradiated using either Aam or NIPAM as the monomer and different crosslinking agents (Table 2.6). The dose-response plots of the dosimeters with polyethylene glycol diacrylates of different chain lengths are shown in Figure 2.8. The  $R_2$  response is very low compared to that of the standard dosimeter prepared using Bis (shown by  $\blacklozenge$  symbols). Precipitation of white polymer, which formed upon irradiation at room temperature was only visible for the Bis dosimeter and the PEGDA258 (crosslinker a) dosimeter. PEGDA550 and PEGDA700 both contained a substantial amount of MEHQ that may (or may not) have been removed effectively by the inhibitor remover column. In addition to MEHQ, PEGDA700 contains the radical inhibitor and antioxidant BHT, which cannot be removed with a simple packed column. The poor  $R_2$  vs. dose responses for dosimeters containing crosslinkers a), b) and c) are compared with the desirable response of the standard PAG dosimeter in Figure 1.9. Polymer gel dosimeters containing di- or tri- (ethylene glycol) divinyl ether (crosslinkers d and e) did not respond to radiation at all. Crosslinkers h) and i) also did not lead to any noticeable production of crosslinked polymer. As anticipated, crosslinker j), (N,N'-ethylenebisacrylamide) was an effective crosslinking agent. Unfortunately, the  $R_2$  response was not noticeably better than that of Bis. Since N,N'-ethylenebisacrylamide is approximately 70 times more expensive than regular N,N'-methylenebis(acrylamide), we do not recommend it for use as a crosslinker in polymer gel dosimeters.

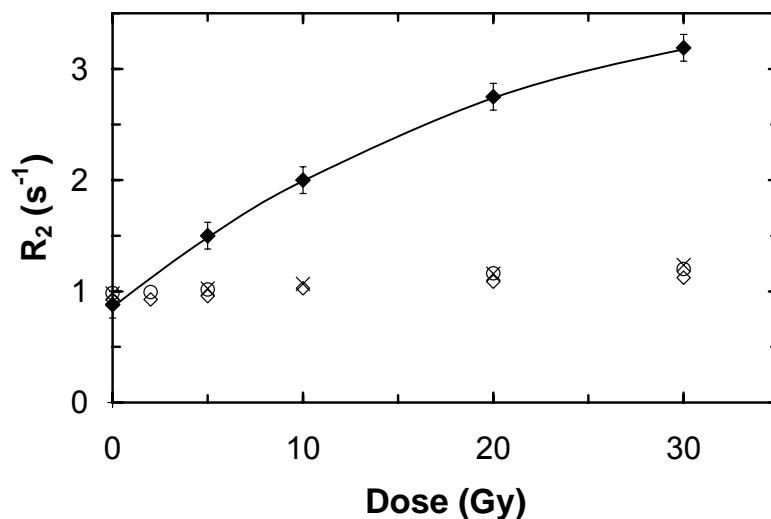


**Figure 2.8:** Comparison of dose-response curve of 6%T, 50%C Aam/Bis Dosimeter ( $\blacklozenge$ ) with dose response of potential Aam/PEGDA258 ( $\circ$ ), Aam/PEGDA550 ( $\times$ ), and Aam/PEGDA700 ( $\diamond$ ) gel dosimeters. Reproduced from Senden *et al* (2006) with permission.

Unfortunately, none of the alternative crosslinkers investigated are suitable replacements for Bis in polymer gel dosimeter systems. The main problems were low reactivities of the crosslinkers at ambient temperature, stabilization of crosslinking agents with inhibitors and limited water solubility. Since a good replacement for Bis could not be found, further investigation was aimed toward increasing the solubility of Bis (to promote additional crosslinking) by adding cosolvents to the recipe.

## 2.4 Conclusions

Several different modifications to the standard recipe for PAG and NIPAM-based dosimeters were tested, with the objective of producing more accurate and easy-to-use dosimeters. CEAMBLOOM 3240 was tested as an alternative gelling agent to gelatin. Although the gels produced using CEAMBLOOM 3240 set very quickly, radiation dose-response curves showed

\*Note that some of the research results presented in this chapter have been published in Koeva *et al*, 2008a

that CEAMBLOOM 3240 is not an effective gelling agent for use in polymer gel dosimetry, because it results in inhibition of the dose response. It is recommended that carrageenan-based gelling agents should be tested again if gelling agents without additives (or with lower levels of additives) become commercially available, because the poor radiation-dose response may result from the citric acid and potassium chloride additives rather than from the carrageenan gel.

Ascorbic acid, in combination with  $\text{Cu}^{2+}$  was evaluated as a potential replacement for Tetrakis (hydroxymethyl) phosphonium chloride (THPC) as an oxygen scavenger. Ascorbic acid and  $\text{Cu}^{2+}$  would be preferred because they are less toxic than THPC and they are available as solids, which could be included in pre-measured packets of dosimetry ingredients. Radiation dose-response curves and visual observations indicate that no precipitated polymer was formed when this alternative oxygen scavenger was used. In addition, the alternative oxygen-scavenging system resulted in very poor gel stiffness. Some of the gels became liquid at room temperature. It is not clear why this alternative oxygen-scavenging system worked well for a polymethacrylic acid dosimeter, but not for the NIPAM-based dosimeters tested here.

A variety of chemical and physical phenomena including primary cyclization reactions and low water solubility influence the performance of crosslinkers in polymer gel dosimetry. Several candidates for replacing N,N'-methylene-bisacrylamide (referred to as Bis throughout this thesis), the crosslinker that is currently used in polymer gel dosimeter recipes, were tested. Unfortunately, recipes using 9 of the candidate crosslinkers were shown to provide less-satisfactory dose-response behaviour than the standard dosimeter recipe using N,N'-methylene-bisacrylamide. The tenth dosimeter, using N,N'-ethylene-bisacrylamide, produced results that are similar to those obtained using N,N'-methylene-bisacrylamide crosslinker, but N,N'-ethylene-bisacrylamide is not recommended because it is considerably more expensive than N,N'-methylene-bisacrylamide.

# **Chapter 3**

## **Improved Polymer gel dosimeters: the use of cosolvents**

### **3.1 Chapter Overview**

In this chapter, several cosolvents were investigated for use in polymer gel dosimeter recipes. Glycerol and isopropanol were studied in detail for their potential to increase the solubility of N,N'-methylene-bisacrylamide, the crosslinker used in existing polymer gel dosimeters. The work presented in this chapter includes a series of experiments conducted to determine the response of the new dosimeters to radiation using different read-out techniques such as nuclear magnetic resonance, x-ray computed tomography and optical scanning. This chapter has been submitted to *Physics in Medicine and Biology*, and appears in manuscript form.

# **Preliminary investigation of the NMR, optical and x-ray CT dose-response of polymer gel dosimeters that use cosolvents to increase crosslinker levels**

**V.I. Koeva<sup>1</sup>, T. Olding<sup>2</sup>, A.Jirasek<sup>3</sup>, K. B. McAuley<sup>1\*</sup>, L.J. Schreiner<sup>4,5</sup>**

<sup>1</sup> Department of Chemical Engineering, Queen's University, Kingston, ON, Canada, K7L 3N6

<sup>2</sup> Department of Physics, Queen's University, Kingston, ON, Canada, K7L 3N6

<sup>3</sup> Department of Physics and Astronomy, University of Victoria, Victoria, BC, Canada, V8W 6V5

<sup>4</sup> Cancer Centre of Southeastern Ontario, Kingston, ON, Canada, K7L5P9

<sup>5</sup> Departments of Oncology and Physics, Queen's University, Kingston, ON, Canada, K7L 3N6

Submitted to: *Physics in Medicine and Biology*

## **3.2 Summary**

The potential of several different cosolvents is investigated, with the aim of increasing the solubility of N,N'-methylene-bisacrylamide crosslinker in polymer gel dosimeters used for detecting radiation dose distributions generated by cancer radiation therapy equipment. Using glycerol and isopropanol increases the limit for the crosslinker solubility from approximately 3 to 5 % and 10 % by weight respectively, enabling the manufacture of polymer gel dosimeters with much higher levels of crosslinking than was previously possible. New dosimeter recipes containing up to 5 wt % N,N'-methylene-bisacrylamide were subjected to spatially uniform radiation and were probed using Nuclear Magnetic Resonance (NMR), as well as x-ray and

optical CT (Computed Tomography) techniques. The resulting dosimeters produced higher dose sensitivities than previously obtained when using typical dosimeters with 3 % N,N'-methylene-bisacrylamide produced without cosolvent. Two potential cosolvents (n-propanol and sec-butanol) were deemed unsuitable for practical dosimeters due to incompatibility with gelatin, cloudiness prior to irradiation, and immiscibility with water when large quantities of cosolvent were used. The dosimeters with high N,N'-methylene-bisacrylamide content that used isopropanol or glycerol as cosolvents had good optical clarity prior to irradiation, but did not produce reliable optical CT results for non-uniformly-irradiated gels. Further experiments are required to determine whether cosolvents can be used to manufacture reliable gels with high dose sensitivity for readout using x-ray computed tomography.

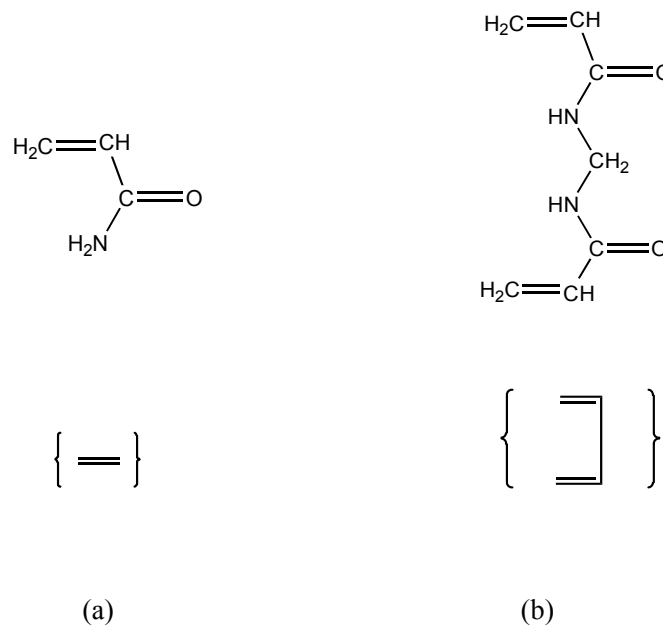
### **3.3 Introduction**

In recent years, polymer gel dosimeters have been developed for detecting high resolution 3-dimensional radiation dose distributions delivered by modern radiation therapy techniques. These dosimeters exhibit the high resolution required to measure the complex conformal dose delivery achieved in modern intensity modulated radiation therapy techniques which are often characterized by non-uniform doses with large dose gradients in small spatial displacement. Furthermore, these tissue equivalent dosimeters are able to measure under dynamic delivery when specific points in the irradiated volumes receive their final dose over a total treatment time. The most-studied and widely-used dosimeter for verification of spatial dose distributions is the Polyacrylamide Gel (PAG) dosimeter (Maryanski *et al* 1994b, De Deene *et al* 2006) which contains acrylamide (Aam) monomer and N,N'-methylene-bisacrylamide (Bis) crosslinker in an aqueous gelatin matrix. When the dosimeter is irradiated radiolysis of the water creates free



radicals that induce polymerization. More crosslinked polymer forms and precipitates at locations where the radiation dose is high than where the dose is low.

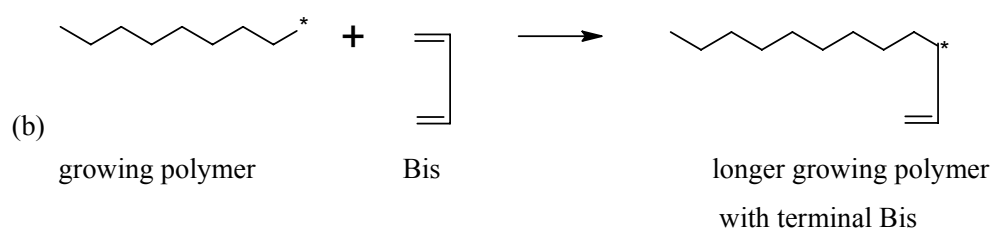
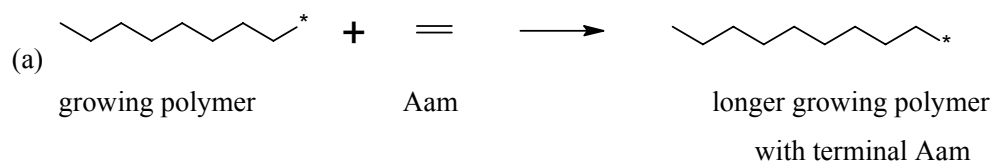
As shown in Figure 3.1, each Aam molecule has one vinyl group (carbon-carbon double bond) that can react with free radicals on the growing polymer chains, and each Bis molecule has two vinyl groups that can react. The simplified symbols in the parentheses, showing the vinyl groups, will be used to indicate Aam and Bis in Figure 3.2.



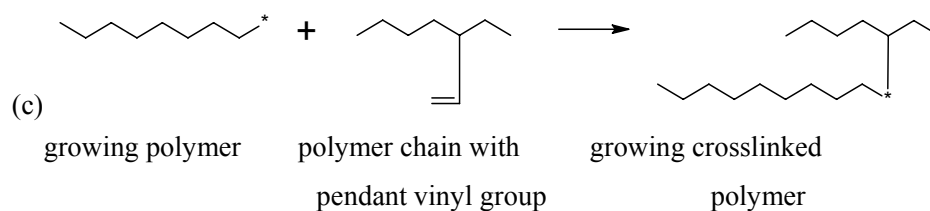
**Figure 3.1:** Chemical structures and representative cartoons for (a) acrylamide (Aam); (b) N,N'-methylene-bisacrylamide (Bis)

Figure 3.2 shows simplified reaction schemes involving the various propagation reactions (a) and (b), crosslinking reactions (c), and primary cyclization (d).

*Propagation:*



*Crosslinking:*



*Primary cyclization:*

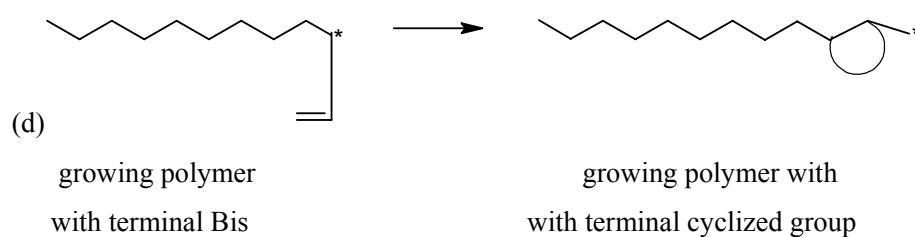
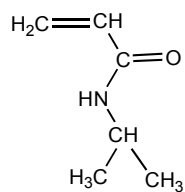


**Figure 3.2:** Simplified reaction scheme in a polyacrylamide gel dosimeter. The mechanism includes propagation (a and b), crosslinking (c) and cyclization (d) reactions. Termination reactions are not shown.

The crosslinking reactions are particularly important in polymer gel dosimeters because linear polyacrylamide molecules (without crosslinks) are water soluble. Crosslinking reactions lead to

the formation of microgels (Teymour and Campbell 1994) that precipitate from the solution and can be detected using a variety of imaging techniques including Magnetic Resonance Imaging (MRI) (Maryanski *et al* 1993), x-ray Computed Tomography (CT) (Hilts *et al* 2000) and optical scanning techniques (OptCT) (Maryanski *et al* 1996a). Although MRI is the most successful and most studied gel readout method, recent research has been devoted to developing dosimeter systems that can be accurately imaged using optical and x-ray CT, because these methods could be much more readily available in clinical settings (Hilts *et al* 2000, Oldham 2001 *et al*, DeJean *et al* 2006a, DeJean *et al* 2006b). Hilts *et al* (2000) have shown that the dose values and high dose gradients of the derived profiles match very well using CT and MRI methods (Hilts *et al* 2000, Babic and Schreiner 2006) and that, unlike MRI, the x-ray CT response is relatively insensitive to the gel temperature during imaging (Hilts *et al* 2000).

Over the years, much effort has gone into developing improved polymer gel dosimeter recipes. The Aam monomer in PAG dosimeters is a dangerous neurotoxin and suspected human carcinogen that requires careful handling (Ibbott 2004, Papagianis *et al* 2006). Recently, Senden *et al* (2006) investigated the dose-response behaviour of new gel dosimeter recipes using N-isopropylacrylamide (NIPAM) in place of Aam. The reaction scheme in Figure 3.2 is exactly the same when NIPAM, which has one vinyl group, is used in place of Aam.



N-isopropylacrylamide (NIPAM)

NIPAM-based dosimeters are safer to use, and behave very similarly to PAG dosimeters, because Aam and NIPAM are chemically similar. They produce similar dose-sensitivities, when the dosimeters are examined using NMR and optical techniques, and the dose response curves do not appear to be very sensitive to changes in the dose rate or temperature during irradiation (Senden *et al* 2006). NIPAM is less toxic than Aam, has good water solubility, and is relatively inexpensive for clinical use. A typical composition of a NIPAM/Bis dosimeter recipe is shown in Table 3.1.

**Table 3.1:** Typical 6%T, 50%C normoxic polyNIPAM Gel Dosimeter Recipe (Senden *et al* 2006, Jirasek *et al* 2006).

Monomer	N-isopropylacrylamide (NIPAM)	3 g
Crosslinker	N,N'-methylene-bisacrylamide (Bis)	3 g
Gelatin		5 g
Water		89 ml
Antioxidant	Tetrakis (hydroxymethyl) phosphonium chloride (THPC)	10 mMol

Gelatin is included in the dosimeter recipe to keep the polymer in the location in which it forms. Several other gelling agents have been used including agarose (Maryanski *et al* 1993). Gelatin is currently the preferred gelling agent in dosimeter recipes because of its better optical clarity compared to agarose (Maryanski *et al* 1994b). Because aqueous gelatin solutions require many hours to set, polymer gels are usually manufactured one day before the dosimeters are irradiated. It would be beneficial if a better, faster-setting gelling agent could be identified so that polymer gel dosimeters could be used soon after they are made. Recently our research group tried a carrageenan-based gelling agent (CEAMBLOOM 3240<sup>®</sup> available from P.L. Thomas & Co., Inc.

USA [www.plthomas.com](http://www.plthomas.com)), because carrageenan gels set more quickly than gelatin. Unfortunately, when this carrageenan gelling agent was used in place of gelatin in the recipe in Table 3.1, no precipitated polymer was observed for radiation doses up to 30 Gy, indicating that CEAMBLOOM 3240<sup>®</sup> is not suitable for dosimetry applications (See Chapter 2). Note that Ceambloom 3240<sup>®</sup> contains several additives, including sodium citrate, which may have inhibited the polymerization process. We recommend that carrageenan-based gelling agents be tested again in future if additive-free carrageenan becomes commercially available at a reasonable price.

Early polymer gel dosimeters were prepared in glove boxes in an oxygen-free environment, because oxygen inhibits free-radical polymerization (Maryanski *et al* 1994b). Recently, oxygen scavengers (also called antioxidants) have been included in polymer-gel-dosimeter recipes, so that these normoxic dosimeters can be manufactured under normal atmospheric conditions (Fong *et al* 2001). A variety of antioxidants and their effects on the dose-response characteristics have been studied. De Deene *et al* (2002b) studied the following oxygen scavengers: ascorbic acid, gallic acid, trolox, N-acetyl-cysteine, and tetrakis (hydroxymethyl) phosphonium chloride (THPC). Among these antioxidants, the most promising results were shown by THPC. However, Luci *et al* (2007) recently obtained excellent results in a methacrylic-acid-based dosimeter recipe using ascorbic acid in combination with [Cu<sup>2+</sup>] as an oxygen-scavenging system. Unfortunately, when our research group made NIPAM-based dosimeters using this ascorbic acid scavenging system, no polymer formation was observed for radiation doses below 40 Gy (See Chapter 2), so THPC is used as the oxygen scavenger in experiments described in this article.

Unlike PAG and NIPAM-based dosimeters, dosimeters that use methacrylic acid as the monomer do not require a crosslinker, because linear (poly)methacrylic acid molecules precipitate when they are produced in the presence of gelatin. Recently, De Deene *et al* (2006)

compared normoxic polymer gel dosimeters based on methacrylic acid (nMAG) with normoxic polyacrylamide gel (nPAG) dosimeters. They showed that nPAG recipes result in a less sensitive gel dosimeter than nMAG recipes, but nPAG dosimeters (and presumably normoxic NIPAM-based dosimeters) have other properties that make them superior to nMAG gel dosimeters. Unfortunately, nMAG dosimeters exhibit problems with temperature sensitivity, energy dependence, and dose-rate dependence (De Deene *et al* 2006, Karlsson *et al* 2007), which are not as problematic in nPAG dosimeters.

As summarized by Senden *et al* (2006) all polymer gel dosimeters that have been investigated (except polymethacrylic-acid-based dosimeters) use Bis as the crosslinker. Limited water solubility and low crosslinking efficiency are the main concerns with the use of Bis in polymer gel dosimeters. Low crosslinking efficiency arises due to primary cyclization (reaction (d) in Figure 3.2), which readily occurs due to the formation of a favorable seven-membered ring (Gopalan *et al* 1982) so that as much as 80% of the bisacrylamide is consumed by this reaction (Tobita and Hamialec 1990, Naghash and Okay 1996). Vinyl groups consumed by primary cyclization are not available for crosslinking reactions.

In our research group, several new polymer gel dosimeters were prepared and irradiated using Aam and NIPAM and 10 different crosslinking agents {Poly(ethylene glycol) diacrylate (PEGDA), N,N'-diallyltartardiamide, Calcium Diacrylate, N,N'-ethylenebis(acrylamide) etc.} (Koeva *et al* 2008). Unfortunately, none of the alternative crosslinkers investigated is a suitable replacement for Bis in polymer gel dosimeter systems. The main problems are low reactivities of the crosslinkers at ambient temperature and limited water solubility. Since a good replacement for Bis could not be found, we directed our investigations toward increasing the solubility of Bis by adding co-solvent to the recipe. Additional Bis in the recipe should result in higher levels of crosslinking.

In PAG, and related dosimeters (De Deene *et al* 2006, Jirasek and Duzenli 2001), changing %C (the mass fraction of the monomers that is crosslinker) while maintaining constant %T (the total mass fraction of monomer and comonomer in the recipe) influences the NMR dose sensitivity (the slope of dose response curves like those shown in Figure 3.6). High dose sensitivity is desirable because it may lead to more accurate dose detection. Increasing %C results in increasing dose sensitivity, up to approximately 50% (for a 6%T dosimeter), followed by decreasing dose sensitivity beyond that point (Maryanski *et al* 1997). The value of %C where the change from increasing to decreasing dose sensitivity occurs is at or near the solubility limit of Bis in the aqueous gel solution at room temperature. When experiments are conducted using dosimeters that contain Bis beyond its solubility limit (approximately 3 wt% in water), dose-response curves tend to have different shapes than when all of the Bis is soluble, with the curve flattening out at a higher dose (De Deene *et al* 2006). As the dissolved portion of Bis is consumed by polymerization, precipitated Bis can dissolve and becomes available for polymerization at higher absorbed doses. Increasing %T while holding %C constant at 50% (in the range from 0 to 8%T) results in an increase in dose sensitivity for PAG and related dosimeters (De Deene *et al* 2006, Babic and Schreiner 2006).

In summary, design of polymer-gel-dosimeter recipes is based on a variety of considerations. The gels should be tissue-equivalent to radiation, and their response should depend on the total radiation dose absorbed, but not on the dose rate (Karlsson *et al* 2007). The gelling agent (i.e., gelatin) must ensure that the crosslinked polymer remains at the location where it forms. The monomers must be reactive at room temperature, and a high crosslink density must be achieved to ensure precipitation of the polymer (Maryanski *et al* 1997). Less-toxic and inexpensive components are preferred. The dosimeter should be easy to manufacture, and should produce accurate and reproducible results using a variety of imaging techniques. The aim of the

current work is to develop improved polymer-gel-dosimeter recipes that will lead to higher crosslinking levels and, hence, better dose sensitivity. Since our attempts to find better crosslinkers than Bis have been unsuccessful thus far, our focus is on improving the solubility of Bis using several common cosolvents (i.e., glycerol, n-propanol, isopropanol and sec-butanol). The dosimeters are then probed using NMR and spin-spin relaxation measurement optical, and x-ray CT scanning.

## **3.4 Methods and Materials**

### **3.4.1 Solubility tests**

Preliminary tests were conducted in a fume hood, under normal atmospheric conditions, to test the influence of the cosolvents on the solubility of Bis in aqueous solutions (without gelatin or NIPAM monomer). Water and cosolvent were mixed at room temperature before heating to 50 °C. While stirring continuously, the crosslinker (Bis) was added to the solution. The solution was considered saturated when we observed that the mixture contained solid Bis that could not be dissolved at 50 °C.

### **3.4.2 Gel Manufacture**

#### **3.4.2.1 Small vials for NMR and optical CT**

The polymer gel dosimeters were manufactured inside a fume hood, under normal atmospheric conditions using standard experimental procedures (De Deene *et al* 2002b, Baldock *et al* 1998, Senden *et al* 2006). Gelatin (300 Bloom Type A, 5% by weight, Sigma-Aldrich) was allowed to swell in a solution containing 80% of the de-ionized water and all of the cosolvent (if used) for 10 minutes at room temperature, before heating to 50 °C. While stirring continuously, the Bis



(Sigma-Aldrich, Oakville, Ontario, Canada) was dissolved in the gelatin solution, requiring between 5 and 25 minutes, depending on whether a cosolvent was used. After the crosslinker mixture was cooled to approximately 37 °C, the monomer (NIPAM, TCI Chemicals, Portland, OR, USA) was added. A solution of the antioxidant (THPC, Sigma-Aldrich) was prepared with the remaining 20% of the water, and added to the solution after it had cooled to approximately 35 °C. The resulting solution was transferred into 4.5 ml polystyrene cuvettes (Fisher Scientific, Canada), which were filled to a height of 2.3 cm and then closed with rubber septa and sealing film. The samples were wrapped with aluminum foil to prevent photo-polymerization, and placed in a refrigerator to set.

### **3.4 2.2 Vials for X-Ray CT**

Polymer gels were manufactured in a fume hood and placed in 20 mL scintillation vials (Wheaton Scientific, Millville NJ, USA) using slightly different techniques (Jirasek *et al* 2006) than for the 4.5 mL vials above. Gels were composed of NIPAM, Bis, gelatin, glycerol (Sigma-Aldrich), and de-ionized water. 5mM of THPC was used as oxygen scavenger. To begin gel manufacture, the water was heated to 27°C at which point gelatin and NIPAM were added. The solution was further heated (and stirred) to 43°C, then cooled to 35°C at which point Bis was added. After ≈ 10 min of stirring, the glycerol was added. The full solution was then stirred for a further 20 min prior to addition of THPC as the final step. The final gel solution was transferred to 10, 20 mL scintillation vials (Wheaton Scientific, Millville, NJ, USA), which were capped and placed in individualized, custom acrylic vessels in order to minimize oxygen contamination.

### **3.4.2.3 Large jars**

The gel solutions were prepared as for the small vials, except that the gelatin/crosslinker solution contained only 60% of the deionized water. The NIPAM monomer was dissolved in the remaining 40% of the water at room temperature, and THPC was added to this solution immediately before it was mixed with the gelatin/crosslinker solution. Gels were poured into 1 L polyethylene terephthalate (PET) jars (9.2 cm in diameter from Modus Medical, Canada). Note that careful manufacturing procedures are required to make large jars of gel with high transparency. A description of problems that were observed using different manufacturing conditions and recommendations for future students who will optimize gel recipes and preparation techniques are provided in Appendix A.

### **3.4.3 Gel Irradiation and Measurements**

The dosimeters were irradiated up to 50 Gy, at room temperature, using a T780 Cobalt-60 unit (MDS Nordion, Kanata, Canada), three to 24 hours after gel manufacture using a 10x10 cm<sup>2</sup> field directed perpendicular to their length. Each vial was rotated 180° at the half way point of the irradiation to ensure that a uniform dose was delivered along the diameter of the vial. Experimental procedures to irradiate and to image the uniformly-irradiated vials by NMR were identical to those described by Senden *et al.* (2006), and are provided in Appendix B.

NMR relaxation rates ( $R_2$ ) were determined between three hours and three days after irradiation, so that the time evolution of polymerization reactions could be studied. The uniformly irradiated gel dosimeters were characterized using an Oxford Instruments MARAN 20/35 benchtop NMR spectrometer operating at 20 MHz.

For the uniformly-irradiated gels, an Ultrospec 1000 UV/Visible Spectrophotometer (Biochrom Ltd., Cambridge, England) was used to quantify the fraction of light that could pass through the samples. Attenuation coefficients of the irradiated polymer gels were determined using transmission readings from the spectrophotometer and calibrated against a known standard.

For X-ray CT imaging experiments, gel vials were housed in custom designed vessels immersed in an in-house-built water tank. Gels were irradiated with a Varian Clinac linear accelerator (Varian Inc, Palo Alto, CA, USA) using 6MV x-rays, a 15x20 cm<sup>2</sup> field size, and a dose rate of 400 cGy/min at 1.5 cm depth in water. Gels were irradiated at a range of 5 depths along the central axis of the beam, giving doses between 3 - 50 Gy. Each vial was rotated 180° at the half way point of the irradiation to ensure that a uniform dose had been delivered along the diameter of the vial. All gels were irradiated 2- 4 hours post manufacture.

X-ray CT images were acquired using a GE HiSpeed X/i scanner (GE Medical Systems, Milwaukee WI, USA) operating at 140 kVp. Gels were imaged 24 hrs post irradiation. 16 image averages were used for signal to noise enhancement and an averaged blank (background) image was used for image subtraction to produce the final CT images. Dose response curves were calculated by taking the mean (and standard deviation) of a region of interest within each vial.

Gels made in the large jars were subjected to spatially non-uniform radiation using a T780 Cobalt-60 unit, modified by the addition of a tomotherapy benchtop (Schreiner 2006) (MDS Nordion, Kanata, Canada) approximately 24 hours post-manufacture using three overlapping 1x1cm<sup>2</sup> pencil beams. These gels were evaluated using the VISTA cone beam OptCT scanner. Reference and data scans were taken using 633 nm LED illumination and a 1024x768 pixel CCD camera (410 projections over 360°). Reconstructions were completed via Feldkamp back projection with a Hamming filter to a 0.5 mm voxel size (See Figures 3.15 and 3.16). The entire procedure took approximately 20 minutes to scan and reconstruct.

## **3.5 Results and Discussion**

### **3.5.1 Evaluation of Cosolvents for Increasing Bisacrylamide Solubility**

#### **3.5.1.1 Observations during Gel Manufacture**

Seven cosolvents (glycerol, isopropanol, n-propanol, sec-butanol, n-butanol, methylethyl ketone and ethyl acetate) were investigated in an attempt to increase the amount of crosslinker that could be dissolved in the aqueous gelatin solution. Cosolvents are often mixed with the main solvent of a solution to adjust the solubility of solutes. For example, isopropanol-water mixtures have been used for the solution copolymerization of vinylbenzyl thymine and vinylphenylsulfonic salt (Garcia *et al* 2006). The seven cosolvents were selected because they are readily available solvents that contain polar and nonpolar groups that make them effective as cosolvents, and their atomic compositions indicate that they will not interfere with the tissue-equivalence of the polymer gel dosimeters. It is also important to choose a cosolvent that is relatively non-toxic and easy to handle and that will not alter the pH of the solution significantly, as it has been found that  $R_2$  can be influenced by the pH of the recipe components (Kennan *et al* 1996). After testing the behaviour of the different cosolvents in a water-gelatin solution we determined that n-butanol, methylethyl ketone and ethyl acetate are not suitable for further investigation due to immiscibility with water at concentrations higher than 10 % by weight. The effects of the remaining four cosolvents (glycerol, n-propanol, isopropanol and sec-butanol) on the solubility of Bis in the aqueous solutions were tested using various ratios of water and co-solvent. These experiments were performed at 50 °C to be consistent with the dissolution temperature used during the gel manufacture. Note that the solubility of Bis at room temperature is lower than at 50 °C. The

purpose of this test was to determine the influence of the quantity of cosolvent used on the amount of Bis that can be completely dissolved. For a 100 ml solution, when using a water-to-isopropanol volumetric ratio of 7:3 we determined that 7 grams of Bis was the maximum amount of crosslinker that could be dissolved completely (no phase separation observed). As shown in Table 3.2, glycerol is an effective cosolvent, which increases the solubility of Bis from 3 wt % to 5 wt%, but isopropanol, n-propanol and sec-butanol are even more effective, increasing the solubility of Bis to 10, 17 and 23 wt %, respectively.

**Table 3.2:** Solubility (by % weight) of Bis in aqueous solution at 50 °C with different cosolvents.

Water : cosolvent volumetric ratio	Glycerol (Gly)	Isopropanol (IPA)	N-Propanol (NPA)	Sec-Butanol (SBA)
10:0	3	3	3	3
9:1	4.5	7	7	9
8:2	5	8	10,5	14
7:3	5	10	14	19
6:4	5	10	17	23

Unfortunately, the solutions containing more than 10% sec-butanol phase separated into two distinct layers as the solutions cooled from 50 °C to room temperature, indicating that gels containing large quantities of sec-butanol as a cosolvent would not be effective (See Figure 3.4b).

These four cosolvents were used to produce gels with different %T and water-to-cosolvent ratios. Gels were made in 1L jars so that they could be subsequently scanned using

Optical CT. Figure 3.3a shows a 6%T 50%C 10% glycerol gel, which was very clear prior to irradiation. Figure 3.3b shows two 10%T 50%C gels (the one on the left containing 30% IPA and the one on the right containing 30% NPA). The gel containing IPA was uniform and clear 24 hours after manufacture, but the gel containing NPA was very cloudy, even without irradiation, and therefore is not suitable for optical scanning. The cloudiness prior to irradiation was also a problem for the gels made with sec-butanol. We studied the causes of cloudiness by producing a series of different gels containing sec-butanol, and compared them to a 4%T 50%C reference gel without any cosolvent.

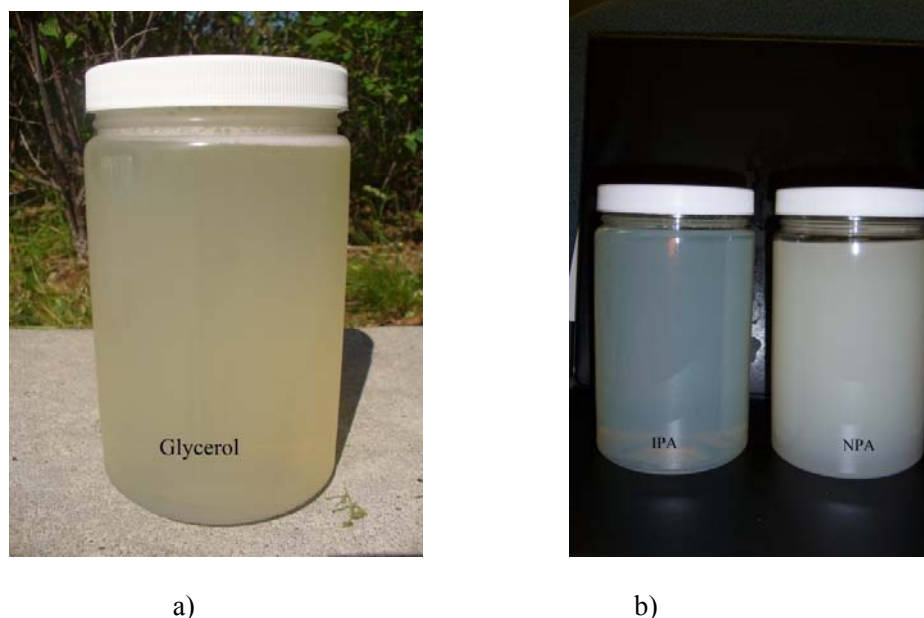


**Figure 3.3:** Photographs of gels containing cosolvents showing that the clarity of the gel depends on the cosolvent used. a) 6%T, 50%C, 10% Gly NIPAM/Bis gel. b) 10%T, 50%C, 30% IPA NIAPM/Bis gel (on the **left**) and 10%T, 50%C, 30% NPA NIPAM/Bis gel (on the **right**).

Figure 3.4 shows that even when no monomers are added to the solution it is cloudy and not as clear as the transparent gel with no cosolvent (4%T 50%C gel). This result may be due to the immiscibility of water and large amounts of sec-butanol cosolvent, which is less polar than

the other cosolvents that were considered. As shown in Figure 3.4, the addition of Bis to the solution does not appear to change the opacity of the gel, since Bis is highly soluble in mixtures of water and sec-butanol (see Table 3.2). The situation changes when NIPAM is added to the gel mixture. As seen in Figure 3.4, both gels containing NIPAM are visibly more opaque than the other gels.

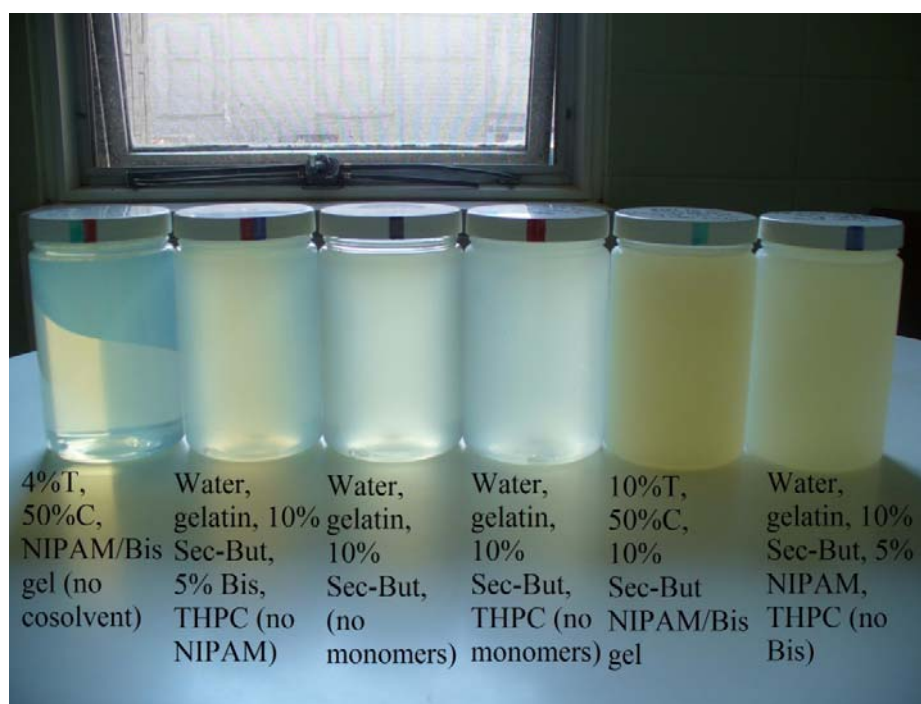


**Figure 3.4:** Photographs of gels containing Sec-Butanol prior to irradiation, showing that the clarity of the gels a) From left to right: i) 4%T, 50%C, NIPAM/Bis gel (no cosolvent); ii) Water, gelatin, 10% Sec-But, 5% Bis, THPC (no NIPAM) iii) Water, gelatin, 10% Sec-But, (no monomers); iv) Water, gelatin, 10% Sec-But, THPC (no monomers); v) 10%T, 50%C, 10% Sec-But NIPAM/Bis gel; vi) Water, gelatin, 10% Sec-But, 5% NIPAM, THPC (no Bis). All gels except iv) contained 10 mM THPC.

Figure 3.5a shows a 10%T 50%C 30% sec-butanol gel 48 hours after manufacture. It appears that most of the cosolvent, which is less dense than water, came out of the solution during cooling and

formed a separate layer at the top of the jar. This experiment further indicates the physical incompatibility of water and sec-butanol, especially when more than 10wt% of cosolvent is used. Sec-butanol also showed undesirable interactions with gelatin. As shown in Figure 3.5b, in a water/sec-butanol solution, gelatin formed a solid lump, which could not be readily dissolved, even at temperatures as high as 60 °C.

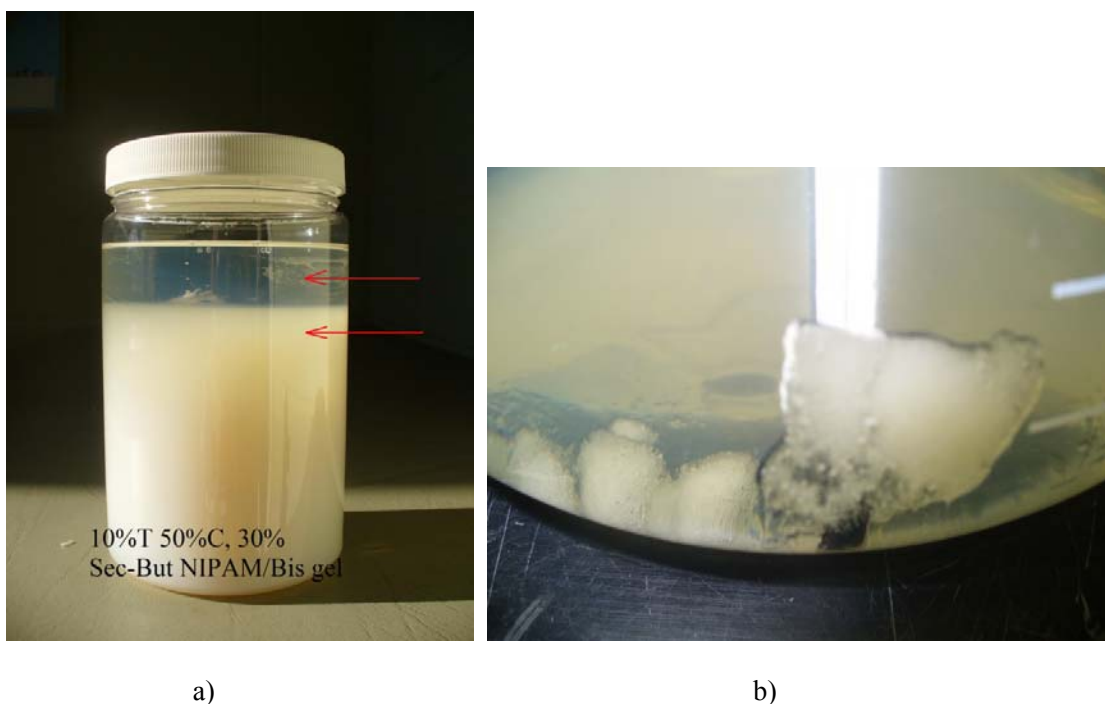


**Figure 3.5:** a) 10%T 50%C, 30% Sec-But NIPAM/Bis gel 48 hours after manufacturing. Notice that the solution separated into two distinct layers (arrows). b) Undissolved lumps formed when gelatin is soaked in an aqueous solution containing sec-butanol.

Since glycerol and isopropanol resulted in the clearest gels, these cosolvents were selected for further studies involving irradiation and imaging. A few gels containing n-propanol were also irradiated. Note that further study is required to optimize gel manufacturing procedures with these cosolvents. Although more Bis could be dissolved in gels containing large quantities of isopropanol (up to 30%) than gels containing glycerol, these gels tended to have more bubbles

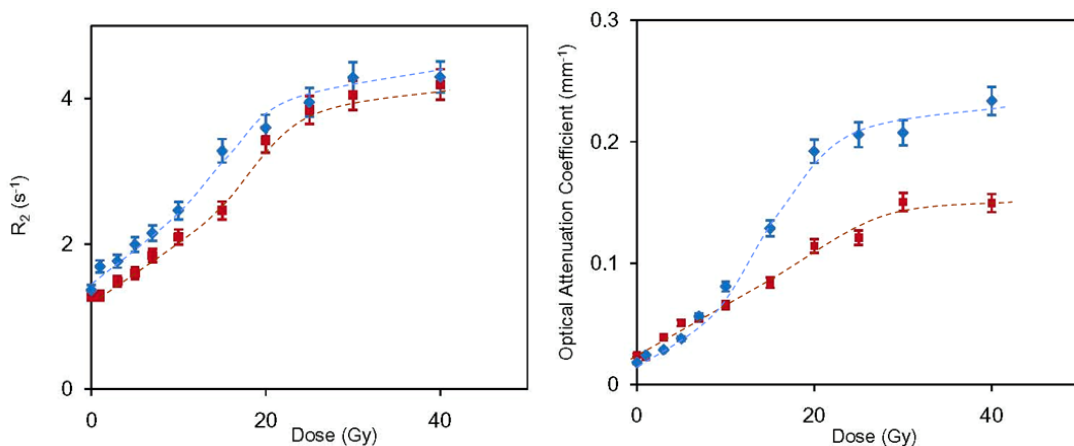


and problems with non-uniformities due to fast gelation, perhaps because gels with large quantities of cosolvent contain less water.

### 3.5.1.2 Irradiated Gels Containing Cosolvents

Figure 3.6a and 3.6b compare the NMR and optical dose responses, respectively, for a standard 6%T 50 %C dosimeter without cosolvent and the same dosimeter made using 30 wt% isopropanol. Note that in the dosimeters containing cosolvents, the mass of the water used in the recipe was reduced by the mass of cosolvent added.

The two NMR dose-response curves in Figure 3.6a are similar, indicating that the presence of the cosolvent had very little influence on the polymerization. It appears that the cosolvent increases the background  $R_2$ , at 0 Gy, which shifts the entire dose response curve upward slightly. Figure 3.6b shows that the isopropanol had a mild influence on the optical properties of the gel, possibly because the cosolvent influences the size and number of polymer particles that precipitate during polymerization.



a)

b)

**Figure 3.6:** Comparison of dose responses of a standard 6% T 50% C NIPAM/Bis dosimeter with no cosolvent (■) and a similar dosimeter containing 30 wt % isopropanol (◆). NMR responses are shown in a) and optical responses are shown in b). The gels contained 5 mMol THPC.

A 9:1 (by weight) water to co-solvent ratio was used to manufacture a series of gels containing glycerol, and 9:1 and 7:3 ratios were used to manufacture gels with isopropanol. In each case, the dosimeter with the new composition was compared to a standard cosolvent-free dosimeter (6%T, 50%C, with NIPAM monomer and Bis crosslinker), which was produced, irradiated, and analyzed at the same time. Figures 3.7, 3.8 and 3.9 show the overlaid  $R_2$ -dose response plots of the standard dosimeter and the dosimeters made with 10% glycerol, 10% isopropanol, and 30% isopropanol, respectively.

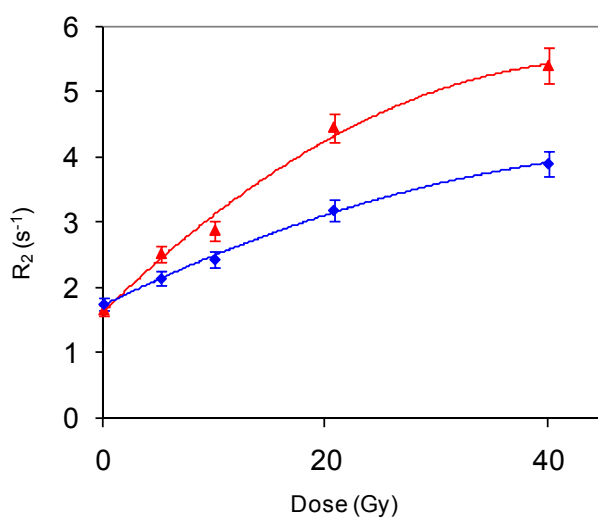


**Figure 3.7:** Dose response for an 8%T, 50%C dosimeter prepared using 10% glycerol (▲). A standard 6%T, 50%C dosimeter with no co-solvent (◆) is shown for comparison. The dosimeters contained 10 mM THPC.

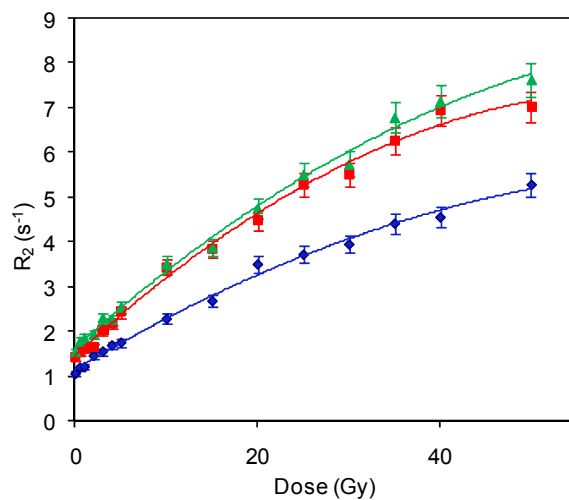


**Figure 3.8:** Comparison of dose responses for 10% T 50 %C NIPAM/Bis dosimeters prepared with different amounts of isopropanol co-solvent: 30% isopropanol (▲),10% isopropanol (■), no co-solvent (◆). The dosimeters contained 10 mM THPC.

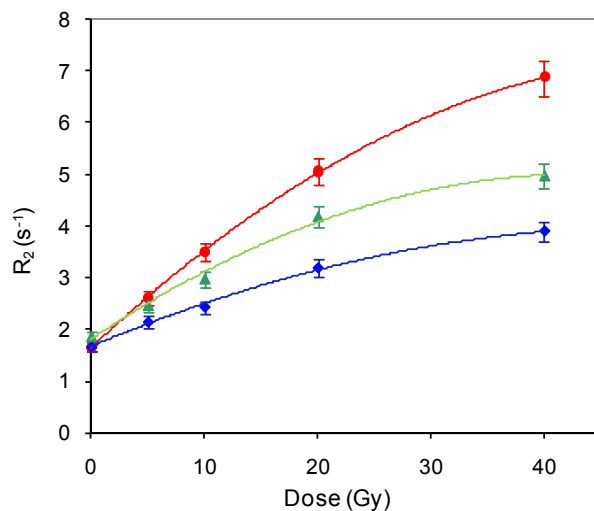


**Figure 3.9:** Comparison of dose-response of a 10% T, 50% C dosimeter containing 10% isopropanol (●) with an 8% T 50% C dosimeter containing 10% glycerol (▲). A standard 6%T, 50%C dosimeter with no co-solvent (◆) is shown for comparison. The dosimeters contained 10 mM THPC.

The results in Figures 3.7 to 3.9 reveal a substantial increase in the dose sensitivity compared to the standard dosimeter without cosolvent. The slope of the  $R_2$  vs. dose plots is greater when more Bis is added to (and dissolved in) the recipe. When a 10 %T, 50% C dosimeter is produced without co-solvent (diamonds in Figure 3.8), this recipe results in low dose sensitivity because a large portion of the crosslinker does not dissolve, and is unavailable for polymerization and crosslinking reactions. The dosimeters made with 10 and 30 wt% of isopropanol gave very similar dose responses, which suggests that using 10 wt% of isopropanol is enough to dissolve all of the Bis in the recipe.

Based on the results in Figures 3.7-3.9 and in Table 3.2, we elected to study isopropanol further as a possible cosolvent in polymer gel dosimeter recipes. Not only is the enhancement of solubility of Bis greater when using isopropanol instead of glycerol (see Table 3.2), but also the enhancement in dose sensitivity appears to be considerably higher than when glycerol is used (see Figure 3.9). Another advantage of using isopropanol instead of glycerol is that isopropanol is less viscous and easier to handle. A 10%T dosimeter with isopropanol was compared to a 8%T dosimeter with glycerol, because a dosimeter with %T greater than 8 cannot be produced with 10% glycerol due to precipitation of the monomers when the solution is cooled down to room temperature.

In order to be an effective calibration and verification tool for radiotherapy, good reproducibility of polymer gel dosimeters is essential. For this reason replicate dose response ( $R_2$ ) experiments were performed on different batches prepared on different days using identical manufacturing, irradiation and scanning procedures, so that we could confirm that the results are reproducible. Figure 3.10 shows the reproducibility of NMR responses of 10 %T 50%C dosimeters prepared using 30% isopropanol. The responses in Figure 3.10a indicate that considerable polymerization took place between 3 h and 20 h post irradiation, but that little

polymerization occurred after 20 h. Figure 3.10b shows results from three replicate batches 20 h after irradiation, indicating that the results are reproducible (within  $\pm 5\%$  error).

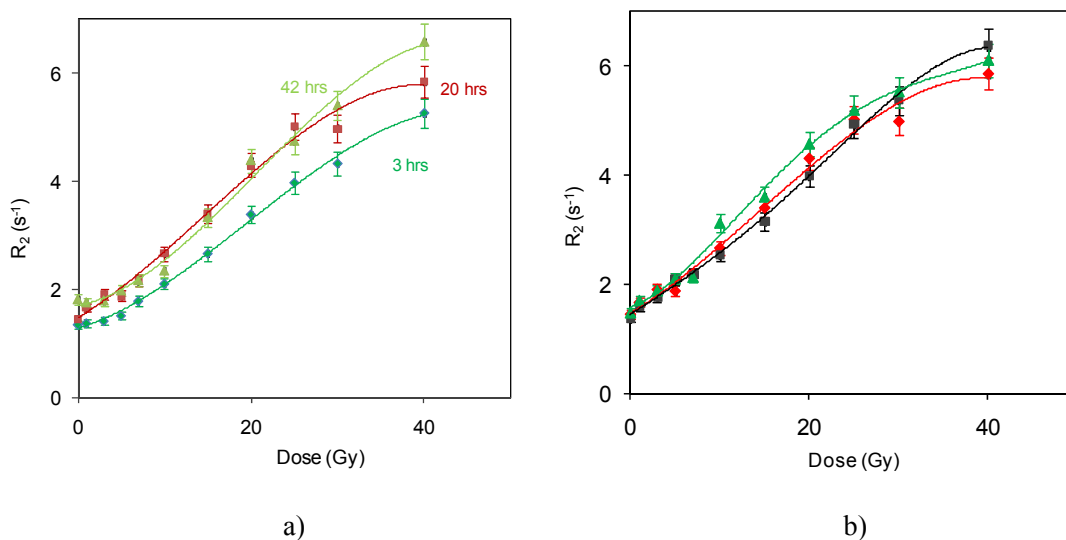


**Figure 3.10:** a) Influence of time on NMR dose response of 10%T, 50%C NIPAM/Bis dosimeters containing 30 wt% isopropanol 3 hours ( $\blacklozenge$ ) 20 hours ( $\blacksquare$ ) and 42 hours ( $\blacktriangle$ ) after irradiation; (b) Reproducibility dose response for three replicate batches of 10 %T 50 %C NIPAM/Bis dosimeters containing 30 wt% isopropanol 20 hours after irradiation. The dosimeters contained 10 mM THPC. Curves are added to guide the eye.

To investigate the influence of cosolvent type on dose sensitivity, a series of gels was produced in small vials using isopropanol and n-propanol. Figure 3.11 compares the  $R_2$  and optical responses of a standard 6 %T 50% C dosimeter with the responses of 10%T 50%C dosimeters prepared using isopropanol and n-propanol cosolvents. As expected, the 10 %T dosimeters with cosolvents produced greater dose sensitivities than the standard dosimeter, because more Bis was dissolved and available for crosslinking. The optical responses for the dosimeters produced using the two cosolvents were very similar. However, Figure 3.11a shows that the  $R_2$  dose sensitivity of the

dosimeter containing n-propanol was lower than that for the dosimeter containing isopropanol. This trend was reproducible using several batches of gels (results not shown). We are unsure why isopropanol produces a different  $R_2$  response than n-propanol. Perhaps the difference is related to the fact that isopropanol is a chain-transfer agent in NIPAM polymerization (Chang *et al* 2001) that may have an important influence on the molecular weight of the polymer that is produced.

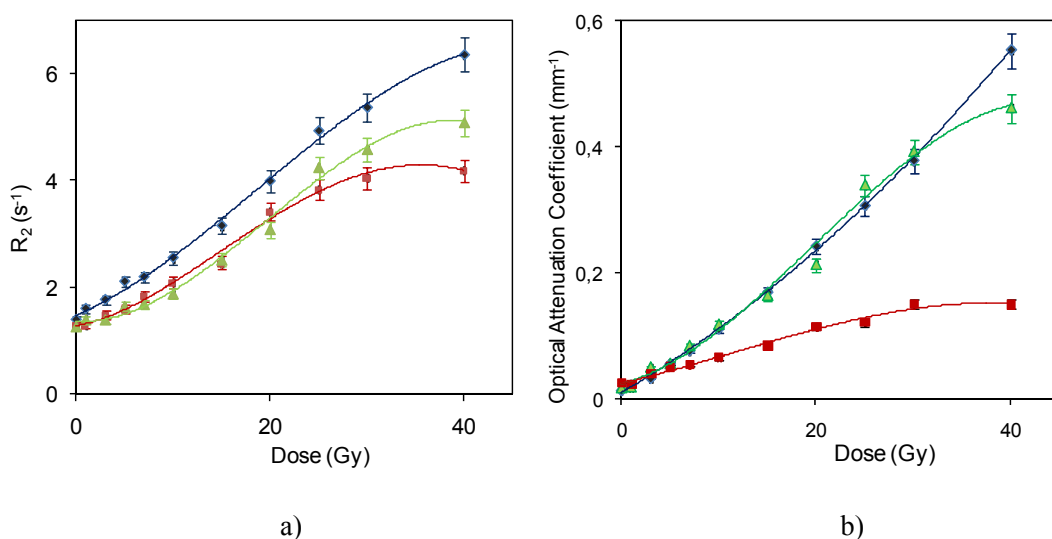


**Figure 3.11:** Comparison of dose responses for 10% T, 50 %C NIPAM/Bis dosimeter containing 30 wt% isopropanol (◆) and 30 wt % N-propanol (▲). The NMR a) and optical b) dose responses for a standard 6% T, 50 %C dosimeter without cosolvent (■) are shown for comparison. All dosimeters were prepared using 5 mM THPC.

We also tested the dosimeters containing isopropanol and glycerol using x-ray CT read-out, which relies on CT contrast due to density changes occurring in irradiated polymer gels. Figure 3.12 shows that 10%T 50 %C polymer gels containing isopropanol give larger responses than those without cosolvent, but are still less sensitive than traditional (anoxic) 6% T 50 %C polyacrylamide gels, whose data are shown as solid circles for comparison purposes.

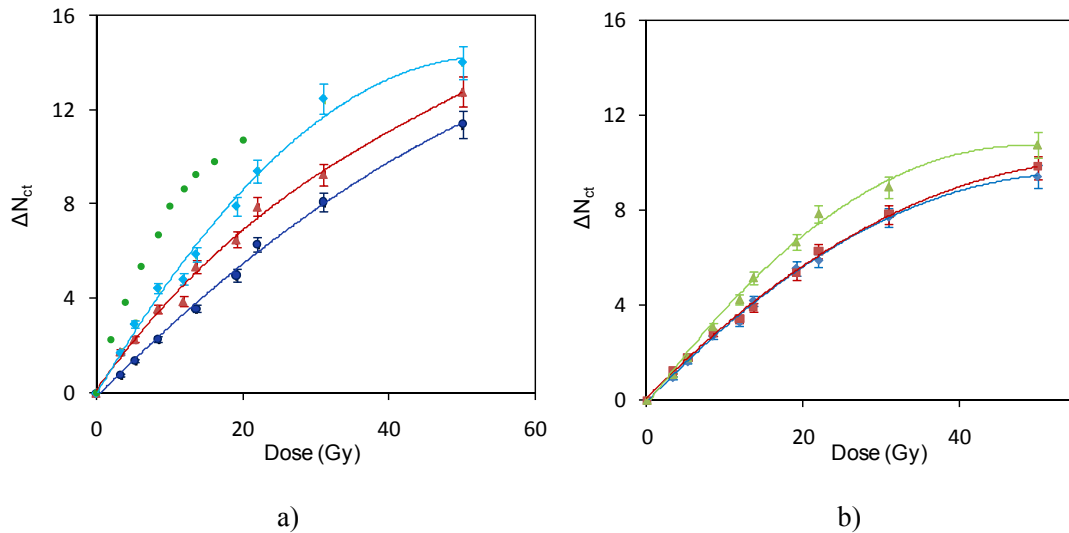


**Figure 3.12:** X-ray CT dose response curves for a) 10%T, 50%C NIPAM/Bis dosimeters containing 0 ( $\blacklozenge$ ), 10 ( $\blacktriangle$ ) and 30 ( $\blacklozenge$ ) wt% of isopropanol, and for b) 6% T, 50% C NIPAM/Bis dosimeters containing 0 ( $\blacklozenge$ ), 10 ( $\blacksquare$ ) and 30 ( $\blacktriangle$ ) wt% of glycerol. In Figure 3.12a the dose response for an anoxic PAG dosimeter (6% T 50% C) ( $\bullet$ ) is included for comparison. The dosimeters contained 5 mM THPC. Curves are added to guide the eye.

Optical CT (OptCT) is gaining favour for dosimeter readout because of the low cost of optical scanners (DeJean *et al* 2006a, DeJean *et al* 2006b). The opacity of polymer gel dosimeters increases with absorbed dose as indicated by the behaviour of the optical attenuation coefficient of uniformly irradiated dosimeters measured by spectrophotometer as shown in Figure 3.13.

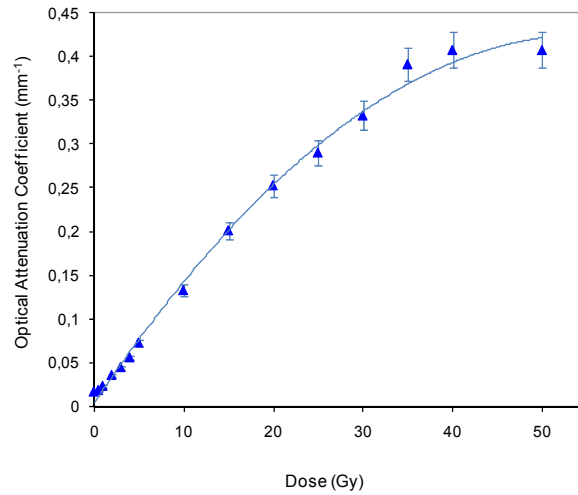


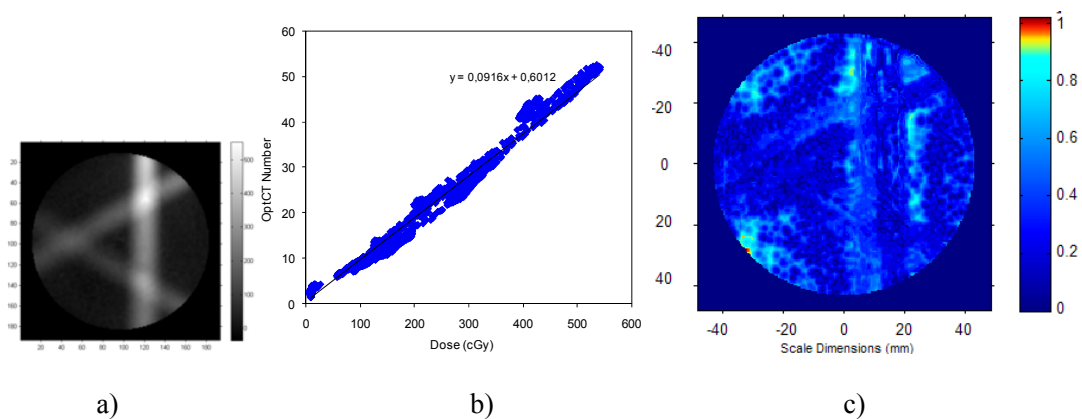
**Figure 3.13:** Optical dose-response for a uniformly irradiated 10% T 50% C NIPAM/Bis dosimeter containing 30% isopropanol. This is the same sample used to generate one of the replicate NMR dose-responses in Figure 3.8. The optical results were measured at 22 °C, 24 hours post irradiation. The dosimeter contained 10 mM THPC. Curve is added to guide the eye.

As indicated above, the NMR, x-ray CT and OptCT measurements of the systems under investigation on uniformly irradiated small samples all show well behaved dose response. Because the optical results obtained in vials using spatially uniform radiation were promising, further experiments were conducted using non-uniform radiation in 1L jars. This was to ensure that the dosimeters would also perform well in the situations in which they would be used clinically; that is, in large phantoms irradiated with spatially variable doses. To perform these measurements we used a nonuniform irradiation with a benchtop Cobalt tomotherapy irradiator along with 3-D cone beam OptCT imaging.

It has been shown that a 4%T 50%C dosimeter can provide reliable dosimetry for conformal dose delivery evaluation using OptCT readout (Olding *et al.* 2008). Figure 3.14 shows a plot of optical attenuation coefficient versus dose from a overlapping pencil beam calibration pattern (DeJean *et*



al 2006b) delivered to the 4%T 50%C dosimeter. This dosimeter has been developed to have high initial transparency and minimal gel irregularities while maintaining maximal dose sensitivity (Olding *et al* 2008). The pencil beam delivery was evaluated against the planned irradiation using Low's gamma function (Low and Dempsey 2003), which produces a colour-wash representation of the agreement between a planned distribution and the measurement.



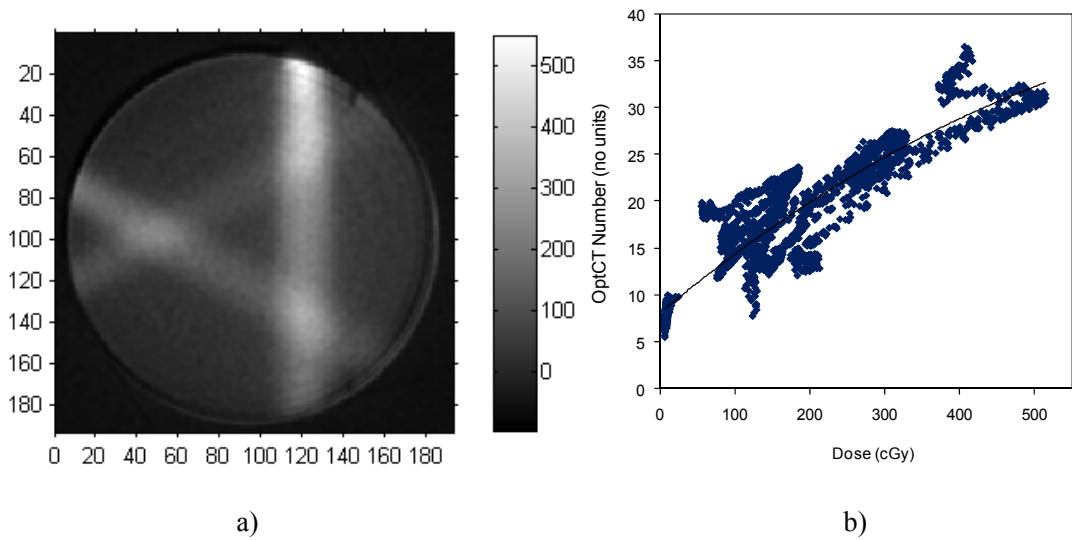
**Figure 3.14:** a) Reconstructed Opt CT image for the 4%T 50%C NIPAM/Bis dosimeter with no cosolvent. b) Raw optical dose response data for the 4%T 50%C NIPAM/Bis dosimeter calibration with no cosolvent. c) Gamma map of a 500 cGy treatment plan delivered to a 4% T 50% C NIPAM/Bis dosimeter containing no cosolvent for 3% 3mm criteria.

Figure 3.14c shows the gamma plot of a 500 cGy treatment irradiation. In this colour-wash the blue-green regions indicate dose agreement within 3% or 3mm (to a  $\gamma$  value of 1). The results show good agreement, with a few pixel failures near the dosimeter jar wall that are not significant to the dosimetry. In our experience with well defined dosimeters this particular radiation pattern consistently shows good results and, in fact, has become the calibration pattern in our 3-D dosimetry work.

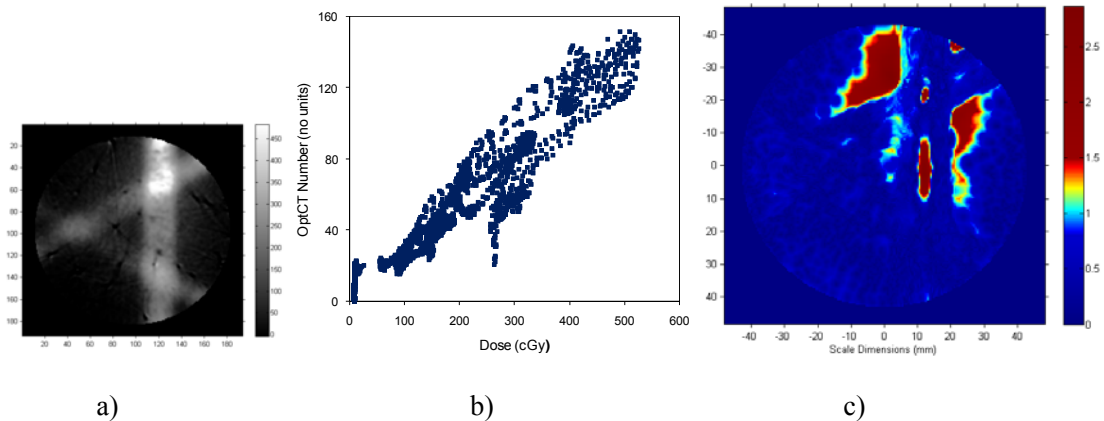
This 3-D spatial evaluation has been extended to the dosimeters with cosolvents under study. It was observed that the addition of the cosolvents isopropanol and glycerol produced dosimeters in small vials with good transparency prior to irradiation; these should be good candidates for OptCt. The spectrophotometer results shown in Figure 3.13 indicates, in particular, that the 30% isopropanol 10%T 50%C dosimeter might be suitable for 3-D imaging using OptCT. A similar 10%T 50%C dosimeter (not shown) containing only 10% isopropanol did not produce good optical results, due to initial cloudiness (attenuation coefficient =  $1.4 \text{ mm}^{-1}$  at 0 Gy).

Figure 3.15 shows the raw optical dose response data obtained from experiments involving the overlapping pencil beam calibration pattern for a dosimeter containing glycerol as a cosolvent. The resulting calibration plot of optical CT number vs. dose contains significant scatter primarily due to the irregular background and increased overall initial opacity of this gel dosimeter, as compared to the typical 4%T, 50%C dosimeter (recall Figure 3.14b).

Figure 3.16 shows raw dose response data obtained from experiments from a 10 %T 50 %C dosimeter with 30 % isopropanol as a cosolvent. The dose sensitivity for this high %T dosimeter is approximately three times that of the standard 4% T 50% C dosimeter without cosolvent in Figure 3.13. However, this gel set unevenly and had many small trapped air bubbles, which are seen as dark spots in Figure 16a. Of greater concern is the fact that there seems to be considerable polymer development outside of the high dose regions of the pencil beams (Figure 3.16b). This is clearly indicated in the Low's gamma function comparison in Figure 3.16c which shows significant dosimeter failure at the edges of the pencil beam, a result that is consistent with this conclusion. A possible explanation may be that isopropanol (and perhaps glycerol) is a chain transfer agent that leads to the formation of small radicals over time that can diffuse much more rapidly than long polymer chains.



**Figure 3.15:** a) Reconstructed Opt CT image for the 6%T 50%C NIPAM/Bis dosimeter containing 10% Glycerol. b) Raw optical dose response data for the 6%T 50%C NIPAM/Bis dosimeter containing 10% Glycerol, indicating that the calibration curves are unreliable.



**Figure 3.16** a) Reconstructed Opt CT image for the 10%T 50%C NIPAM/Bis dosimeter containing 30% isopropanol. b) Raw optical dose response data for the 10%T 50%C NIPAM/Bis dosimeter containing 30% isopropanol indicating that the calibration curves are unreliable. The presented in b) data is produced 2 hours post irradiation (■) and 20 hours post irradiation (■). Note that the points in b) correspond to the blue diamonds curve in Figure 3.20. c) Gamma map of a 500 cGy treatment plan delivered to a 10% T 50% C NIPAM/Bis dosimeter containing 30% IPA indicates regions of significant failure in the dosimetry for 3% 3mm criteria.

Olding *et al* (2008) have further determined from scattering gel phantom QA that the use of highly sensitive gel dosimeters can yield optical response in the dosimeter that is outside the linear performance range of the OptCT scanner. They showed that the overall dosimetry is improved by changing the polymer gel recipes from the 6% T 50%C dosimeters traditionally used with MRI to 4%T 50%C to restrict dosimeter behavior in a well-behaved region (Olding *et al* 2008). As a result, we do not recommend that high %T dosimeters using cosolvents should be used with cone-beam optical CT readout.

Experiments were also conducted to examine the long-term dose response of NIPAM/Bis gels containing isopropanol cosolvent. Figure 3.17 compares the optical dose response for a 4% T 50 %C dosimeter prepared using 12% isopropanol (Figure 3.17a) with that of a similar dosimeter without cosolvent (Figure 3.17b).

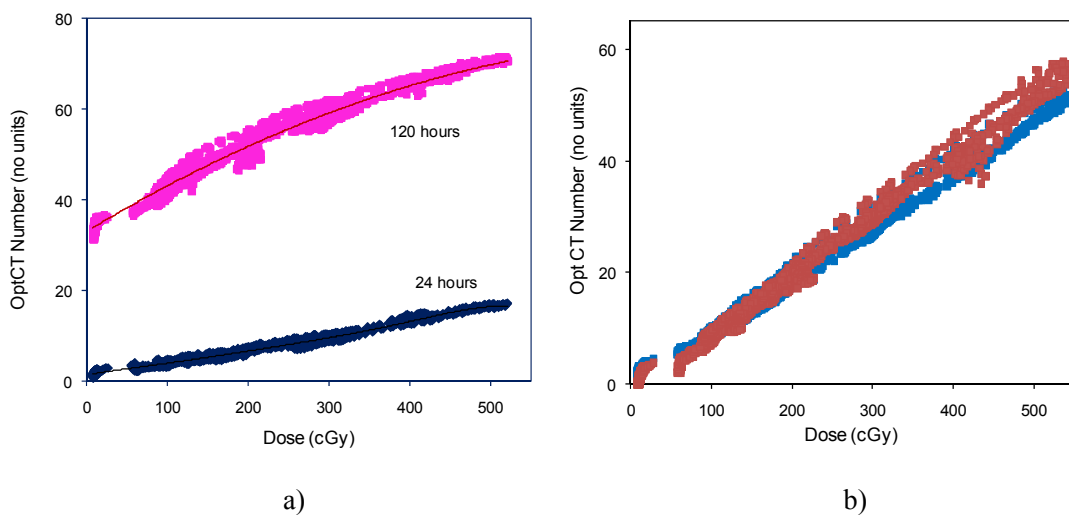


**Figure 3.17.** a) Raw optical dose response data for 4%T 50%C NIPAM/Bis dosimeter: a) with 12% isopropanol obtained 24 hours post irradiation (■) and 120 hours post irradiation (■) in a non-uniformly irradiated jar and b) without cosolvent obtained 24 hours post irradiation (■) and 4 months post irradiation (■) in a non-uniformly irradiated jar.

The optical response of the dosimeter containing 12% IPA obtained 120 hours post irradiation indicates that there is a significant shift in the dose response as the dosimeter continues to develop over time; whereas the dosimeter without cosolvent shows very little change in dose response when imaged 24 hours and 4 months after irradiation. The reasons for this change in dose response when isopropanol is present are not well understood.

Further experiments were conducted to examine the influence of isopropanol cosolvent on dose response. Figure 3.18 shows a plot of optical CT number versus dose for a reference 4%T 50%C dosimeter containing no cosolvent and a similar dosimeter containing 12% IPA.

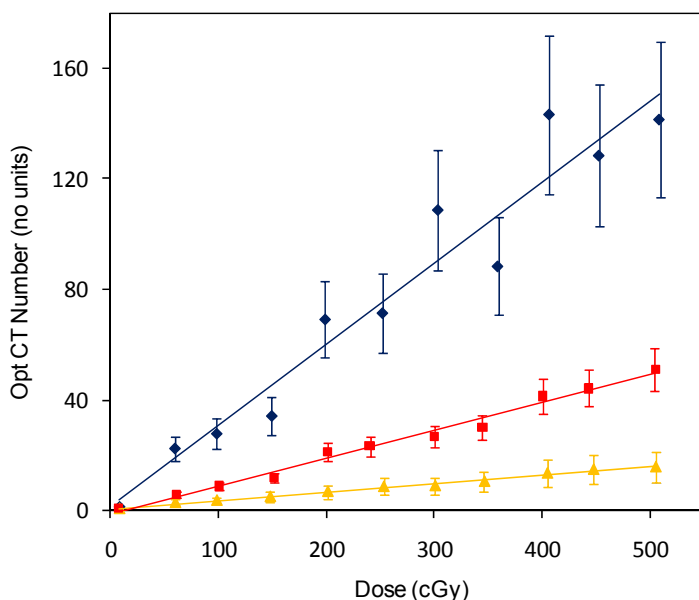


**Figure 3.18:** a) Optical data obtained from non-uniformly irradiated jars 24 hours post irradiation for: a reference 4%T 50%C dosimeter with no cosolvent (■), a 4%T 50%C dosimeter containing 12% isopropanol (▲), a 10%T 50%C dosimeter containing 30 wt% isopropanol (◆). Figure 3.18 also confirms that a 10%T 50%C dosimeter containing 30% IPA results in large optical dose sensitivity, which is approximately three times that of the 4 % T dosimeter without isopropanol. The larger dose sensitivity results from formation of additional crosslinked polymer. It seems that any reduction in dose sensitivity induced by the presence of the IPA is overcome by the effect of the additional polymer that forms.

The 4% T gel containing 12% IPA exhibits a lower optical dose response than the reference gel with no cosolvent. We are unsure of the cause of the lower dose response. Perhaps impurities in the cosolvent reduce the polymerization rate, or perhaps the cosolvent influences the size distribution of the polymer particles that precipitate, which, in turn, influences the optical response (as scattering is dependent both on the size and number of scattering particles).

### **3.6 Conclusions**

The solubility of bisacrylamide in polymer gel dosimeters can be increased substantially by adding cosolvents (glycerol, isopropanol, n-propanol or sec-butanol) to the dosimeter recipe. The increased levels of bisacrylamide (more than 5 wt %) that can be dissolved enable the manufacture of dosimeters with higher %T and %C, which result in higher NMR, optical and x-ray CT dose sensitivities than are possible using typical 6%T 50% C dosimeters produced without cosolvent. Unfortunately, it was difficult to dissolve gelatin in the recipes that were produced using two of the proposed cosolvents (N-propanol and sec-butanol) and the gels produced with these cosolvents were cloudy prior to irradiation and were deemed unacceptable for readout using optical techniques. Promising results were obtained from experiments using gels containing glycerol and isopropanol when spatially uniform radiation was delivered. For example, a normoxic 10 %T 50 %C dosimeter produced using 30 wt% isopropanol cosolvent produced x-ray CT dose response curves with a 53% higher dose sensitivity than a standard normoxic 6 %T 50 %C dosimeter without cosolvent. This high %T dosimeter had good optical clarity prior to irradiation, but did not produce reliable optical CT results for non-uniformly-irradiated gels. Further experiments are required to determine whether cosolvents can be used to manufacture

reliable gels with high dose sensitivity for readout using x-ray computed tomography. It will be important to test whether cosolvents influence the temporal stability of the x-ray CT response.

### **3.7 Acknowledgments**

Financial support for this work was provided by the Canada Institutes for Health Research (CIHR), the Natural Science and Engineering Research Council of Canada (NSERC), the Government of Ontario and Queen's University. The assistance of Oliver Holmes and medical physicists at the Cancer Center of South-eastern Ontario is greatly appreciated.

# Chapter 4

## Inhibition Effects: Kinetic Model Development

### 4.1 Chapter Overview

Using published and experimental data from polyacrylamide gel dosimeters, an existing kinetic model is extended to include the effects of oxygen and MEHQ contamination. Simulations are performed using the PREDICI<sup>®</sup> software package. Model predictions of vinyl bond conversion are presented to show the behaviour of the dosimeters with and without oxygen and MEHQ. Improved parameter estimates are reported for some of the model parameters and model predictions are compared with experimental gravimetric and calorimetric data to test the performance of the model.

The material presented in this chapter will be submitted to *Macromolecular Theory and Simulation* and appears in manuscript form.



# **Mathematical Modeling of PAG and NIPAM-Based Polymer Gel Dosimeters contaminated by oxygen and inhibitor.**

Valeria I Koeva<sup>1</sup>, Robert J Senden<sup>1</sup>, A H M Khadimul Imam<sup>1</sup>, L John Schreiner<sup>2,3</sup> and Kimberley B McAuley<sup>1\*</sup>

<sup>1</sup> Department of Chemical Engineering, Queen's University, Kingston, ON, Canada, K7L 3N6

<sup>2</sup> Cancer Centre of Southeastern Ontario, Kingston, ON, Canada, K7L 5P9

<sup>3</sup> Departments of Oncology and Physics, Queen's University, Kingston, ON, Canada, K7L 3N6

E-mail: [kim.mcauley@chee.queensu.ca](mailto:kim.mcauley@chee.queensu.ca)

Keywords: inhibition, modelling, parameter estimation, polymer gel dosimetry, radiation

## **4.2 Summary**

A mathematical model for crosslinking copolymerization of acrylamide or N-isopropyl acrylamide (NIPAM) in polymer gel dosimeters is extended to account for contamination by oxygen and the free-radical inhibitor monomethyl ether hydroquinone (MEHQ). This model improves basic understanding of interactions among oxygen, MEHQ and free-radical polymerization. These phenomena are important in “normoxic” polymer gel dosimeters that are prepared in the presence of oxygen rather than under an inert atmosphere. Experimental results

are presented that shed light on the influence of THPC (tetrakis (hydroxymethyl) phosphonium chloride), an oxygen scavenger that is added to normoxic dosimeters. It is concluded that present knowledge about THPC reaction mechanisms is insufficient to meaningfully include its influence in fundamental mathematical models. Improved estimates of model parameters are reported that result in a good match between model predictions and available data. The model predicts that oxygen causes a significant inhibition period, which increases in duration at higher levels of oxygen contamination, agreeing well with experimental results. The model also predicts that the presence of MEHQ has almost no influence on dosimeter response.

### **4.3. Introduction**

Polymer gel dosimetry is a technique used by medical physicists to verify spatial radiation dose distributions delivered by cancer radiotherapy equipment.<sup>[1]</sup> The most widely used dosimeter for verification of radiation dose distributions is the Polyacrylamide Gel (PAG) dosimeter. PAG dosimeters consist of acrylamide (Aam) and N,N'-methylene-bisacrylamide (Bis) crosslinker dissolved in an aqueous gelatin matrix. Upon irradiation of the dosimeter, water molecules dissociate into free radicals that can initiate polymerization and crosslinking.<sup>[2]</sup> The densely crosslinked polymer microgels<sup>[3]</sup> that are formed precipitate from the aqueous phase.<sup>[4]</sup> The crosslinked polymer particles, which are too large to diffuse through the gelatin matrix, provide a means for storing spatial information about the absorbed radiation dose. A photograph of a non-uniformly-irradiated PAG dosimeter is shown in Figure 4.1. More polymerization and crosslinking occurred in the white spiral and spherical regions where the radiation dose was high than in the transparent regions where the radiation dose was low. As shown in Figure 4.2, the amount of crosslinked polymer that forms increases with absorbed radiation dose. Note that

radiation doses are specified in units of Gray (Gy), where 1 Gy corresponds to 1 Joule of ionizing radiation delivered per kg of sample. Radiation-induced changes in several physical properties of the gel can be measured using a variety of different imaging techniques, e.g., using MRI (Magnetic Resonance Imaging)<sup>[5]</sup>, optical scanning<sup>[6]</sup> and x-ray computed tomography.<sup>[7]</sup>



**Figure 4.1:** Photograph of a non-uniformly irradiated polymer gel dosimeter.

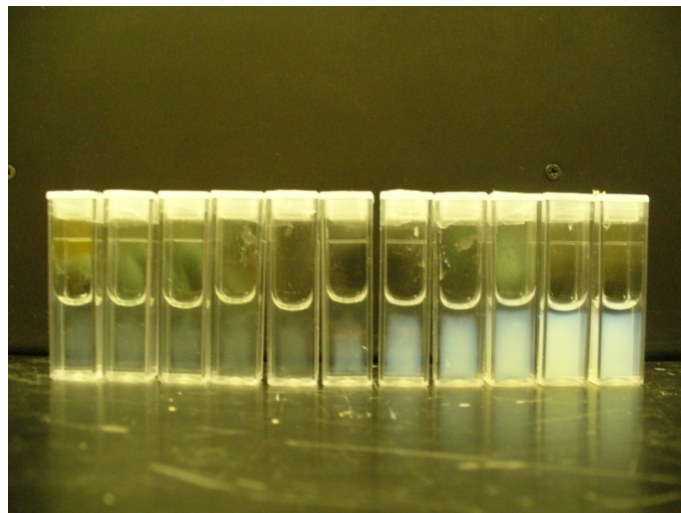


**Figure 4.2:** Photograph of uniformly irradiated polymer gel dosimeters. Radiation doses vary from 0 Gy for the vial at the left to 40 Gy for the vial at the right.

A typical composition of a PAG recipe is shown in Table 4.1.<sup>[8]</sup>

**Table 4.1:** Typical 6%T, 50%C Polymer Gel Dosimeter Recipe.

Monomer	Acrylamide (AAm) or N-isopropylacrylamide (NIPAM)	3 g
Crosslinker	N,N'-methylene-bisacrylamide (Bis)	3 g
Gelatin		5 g
Water		89 ml
Antioxidant	Tetrakis (hydroxymethyl) phosphonium chloride (THPC)	10 mMol

Unfortunately, Aam is a severe neurotoxin and suspected carcinogen.<sup>[9]</sup> Recently, Senden *et al* showed that Aam can be successfully replaced with NIPAM, thereby reducing the safety concerns associated with handling toxic chemicals in the clinical environment.<sup>[10]</sup> Polymer gel dosimeter recipes are usually referred to by the concentrations of monomers in the solution prior to irradiation. The specifications most commonly used are %T, the total mass percent of monomers (Aam or NIPAM plus Bis) in the gel system and %C, the mass percent of the monomer mixture that is crosslinker. The recipe in Table 4.1 with 3% AAm and 3% Bis is referred to as a 6 %T, 50 %C dosimeter. A typical calibration curve produced using a NIPAM-based dosimeter is shown in Figure 4.3 (filled diamonds), in which the NMR transverse relaxation rate ( $R_2$ ), which can be measured using MRI, is plotted against the radiation dose. Dose sensitivity is the slope of the initial linear portion of an  $R_2$  vs. dose plot. A large slope enables accurate dose calibration results.

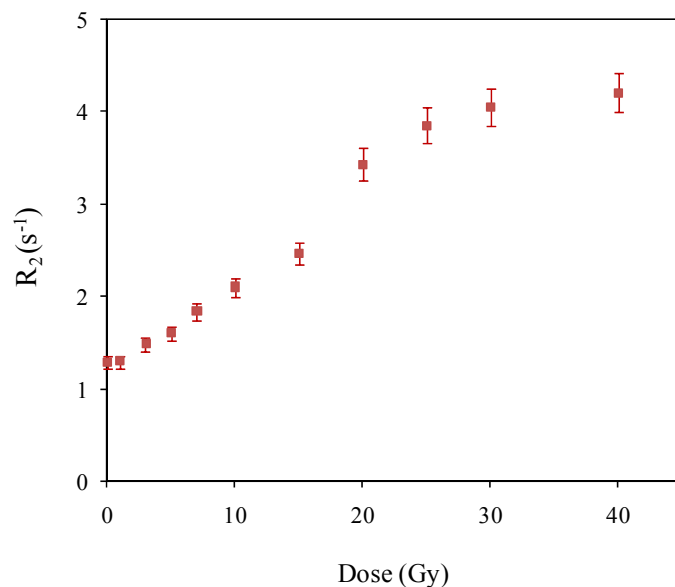
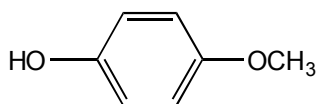


**Figure 4.3:** Dose-response curve of 6%T, 50%C NIPAM/Bis Dosimeter (■)

Commercial monomer-grade NIPAM and many other monomers (but not Aam) that have been used in polymer gel dosimeters<sup>[10]</sup> contain MEHQ inhibitor to prevent polymerization during shipping and storage.



monomethyl ether hydroquinone (MEHQ)

Monomers are usually used without removing MEHQ, but the effect of MEHQ on polymerization kinetics and dose response in polymer gel dosimeters has not been studied. Oxygen is also a well-known inhibitor of free-radical polymerization<sup>[11,12]</sup>, and is an important contaminant in all polymer gel dosimeters, unless special precautions have been taken to remove it.<sup>[2]</sup> Oxygen contamination has a significant effect on the performance of polymer gel dosimeters.<sup>[13,14,15]</sup>

Reactions between oxygen and free radicals are very fast, so that even small amounts of oxygen can consume enough radicals to significantly inhibit polymerization reactions. For example, when a dosimeter solution is initially in equilibrium with air, no appreciable polymerization is observed until more than 20 Gy of radiation has been absorbed.<sup>[15]</sup> The level of dissolved O<sub>2</sub> in polymer gel dosimeters can vary depending on manufacturing procedures and storage conditions prior to irradiation, resulting in variable dosimetry results. It is therefore important to reliably remove oxygen from polymer gel dosimeters. Traditionally this was done by bubbling the dosimeter solution with an inert gas,<sup>[16]</sup> but in recent years, oxygen scavengers have been used to remove the O<sub>2</sub> from normoxic dosimeters.<sup>[10,17,18,19,20,21]</sup> THPC is the preferred antioxidant due to its high reactivity in scavenging oxygen.<sup>[18]</sup> Current mathematical models that describe reaction kinetics in polymer gel dosimeters do not include the effects of oxygen or other inhibitors.<sup>[8,22]</sup> It would be beneficial to predict the behaviour of commonly-used normoxic dosimeters, by including reactions involving MEHQ, oxygen and THPC, so that simulations can be used for designing improved dosimeter recipes.

Our research group has developed dynamic mathematical models that describe the kinetic mechanisms of radiation-induced free-radical crosslinking copolymerization of Aam and Bis, using both spatially uniform and non-uniform radiation.<sup>[8,22]</sup> Although the models were developed to simulate dosimeters that use Aam, they are also useful for recipes that use NIPAM, since Aam and NIPAM should have similar reaction rates due to the similar chemical structures of their vinyl groups. Note, however that the phase partitioning behaviours (between the aqueous and polymer phases) of NIPAM and Aam may be quite different. The models can predict monomer conversion and the concentrations of crosslinks, unreacted pendant double bonds, and cyclized groups in the polymer gel, and also the associated temperature increase due to exothermic polymerization reactions. As shown in Table 4.2, the characteristic free-radical crosslinking

copolymerization steps included in the model are: radical generation by water radiolysis, initiation, propagation, cyclization, crosslinking, termination by disproportionation, chain transfer to monomers and chain transfer to gelatin. Phase separation and phase-volume changes due to polymer precipitation are also considered.<sup>[8,22]</sup> These models and the simpler model of DeDeene *et al*<sup>[23]</sup> have been particularly helpful in improving our understanding of temporal instability (due to long-lived radicals that participate in polymerization reactions long after irradiation ceases) and edge enhancement (due to diffusion of unreacted monomers from regions of high to low monomer concentration). Unfortunately, the models do not consider oxygen inhibition, inhibition by MEHQ, and the effects of oxygen scavengers like THPC. Recently, McAuley and Daneshvar<sup>[24]</sup> used the calorimetric data of Salomons *et al*<sup>[15]</sup> and the gravimetric data of Babic and Schreiner<sup>[25]</sup> to estimate some of the poorly known parameters in the models. In this article, we extend the model to include the effects of oxygen inhibition, so that additional calorimetric data from experiments with oxygen inhibition can be used to further improve the parameter estimates. We demonstrate that the model with the updated parameter values (see Table 4.4) provides a good quantitative match to the experimental data, and we also extend the models to including MEHQ inhibition mechanisms. As described below, too little is currently known about the influence of THPC to realistically include its oxygen scavenging reactions and many side-reactions in the model.

#### **4.4. Influence of THPC on Polymer Gel Dosimeters**

Ideally, the antioxidant used in polymer gel dosimeters would scavenge oxygen, without reacting with other gel components to influence the dose response of the dosimeter. However, this is not the case, in PAG dosimeters that contain THPC. Due to side reactions involving THPC, normoxic

PAG dosimeters with THPC have a lower dose-response than traditional PAG dosimeters, which were originally produced without oxygen and THPC.<sup>[20]</sup> Jirasek *et al* showed that THPC can react with gelatin prior to irradiation, and suggested that THPC reacts with amine groups on the gelatin strands.<sup>[21]</sup>

To investigate the influence of THPC on polymer gel dosimeters, Senden prepared and analyzed several PAG dosimeters with and without THPC, gelatin, monomers and oxygen contamination as shown in Table 4.3.<sup>[26]</sup> The polymer gel dosimeters were manufactured inside a fume hood under a normal oxygen atmosphere. Gelatin (300 Bloom Type A) was allowed to swell in 80% of the de-ionized water for 10 minutes at room temperature, before heating to 50 °C. While stirring continuously, the crosslinker was dissolved, requiring around 10 minutes. After the gelatin-crosslinker mixture was cooled to approximately 35-40 °C the monomer (acrylamide) was added. A solution of the antioxidant (THPC) was prepared with the remaining 20% of the water, and added to the solution. The resulting solution was transferred into test tubes, which were filled to a height of 2 cm and then capped. The caps were wrapped with sealing film to prevent additional oxygen from entering the samples.

Senden did not irradiate any of the dosimeter samples, but left them at room temperature for three weeks and observed their behaviour over time. The samples were wrapped with aluminum foil to prevent polymerization induced by light. During the preparation of some of the polymer gel samples Senden observed that the solutions became faintly cloudy upon the addition of THPC antioxidant.<sup>[26]</sup> He suggested that the cloudiness might be caused by reactions between THPC and gelatin, or may be due to polymerization, which occurred in the absence of irradiation. Slight fogging of polymer gel dosimeters prior to irradiation has also been observed with methacrylic-acid-based polymer gel dosimeters (MAGIC gels) that use ascorbic acid as an oxygen scavenger<sup>[17,18]</sup> and with NIPAM-based dosimeters containing THPC (See Chapter 3).<sup>[27]</sup>



**Table 4.3:** Optical observations for a variety of unirradiated 6 %T 50% C PAG recipes. The symbol X indicates that a particular component was present. Recipes with gelatin contained 5 wt% gelatin and those with THPC contained 10 mM THPC. The dosimeter that was purged with N<sub>2</sub> was oxygen-free. No radiation, except stray light, was applied to any of the dosimeters so that side reactions could be investigated.<sup>[26]</sup> Samples were wrapped with aluminum foil to prevent polymerization reactions initiated by light and placed in the refrigerator to solidify.

	Gelatin	AAM/Bis	THPC	N <sub>2</sub> purge	Observations
1			X		Clear liquid solution up to 3 weeks
2		X			Clear liquid solution up to 3 weeks
3	X				Clear gelled solution up to 3 weeks
4	X	X			Clear gelled solution up to 3 weeks
5	X		X		Clear gelled solution up to 3 weeks
6	X	X	X		Faintly cloudy gelled solution. Cloudiness increased over time.
7		X	X		Liquid solution increasingly cloudy. White flocs visible within 3-4 days.
8		X	X	X	Liquid solution increasingly cloudy (but much less than solution 7). No white flocs visible within 3-4 days.

Senden reported that aqueous solutions containing only gelatin and THPC remained clear (solution 5 in Table 4.3), indicating that reactions between THPC and the gelatin matrix do not seem to be the cause of the cloudiness that was observed in unirradiated polymer gel dosimeters by Jirasek *et al*<sup>[21,26]</sup> All of the solutions containing the monomers and THPC (solutions 6, 7 and 8) were faintly cloudy immediately after preparation. The cloudiness appeared to increase over

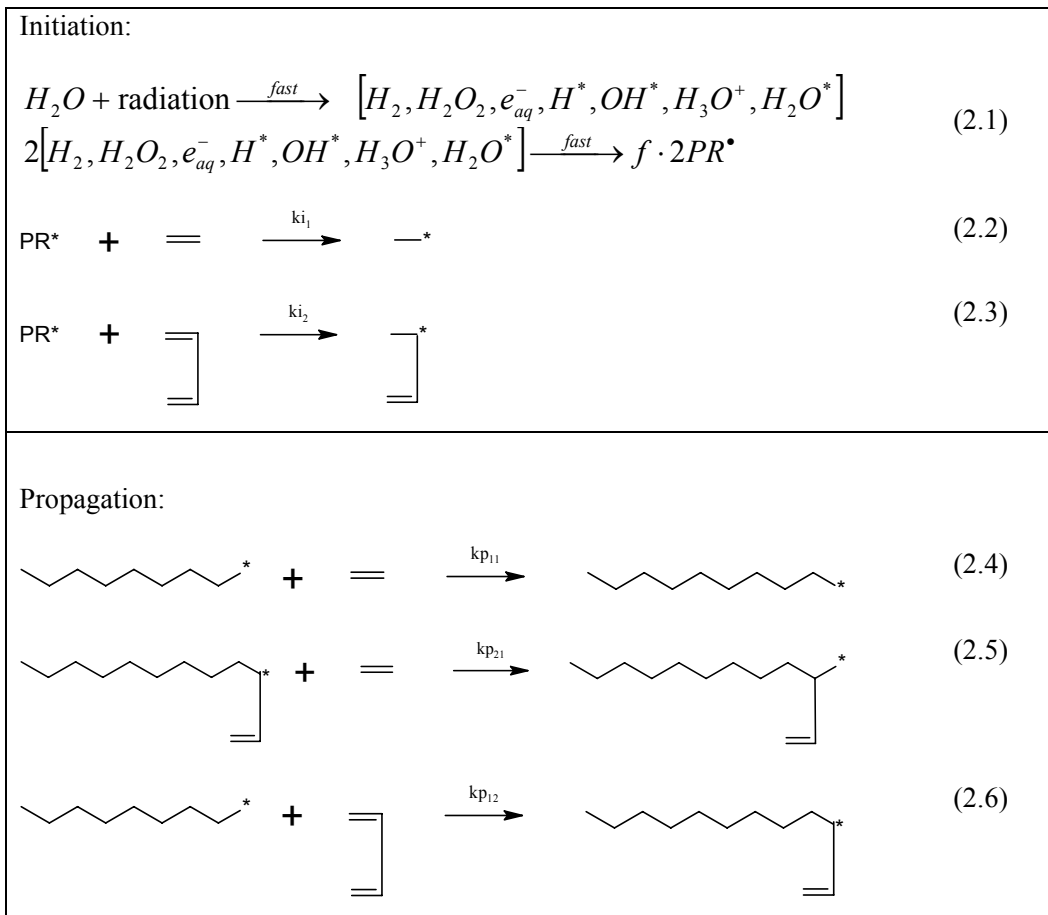
time, and white particles (flocks) developed in these unirradiated solutions, suggesting that some free radicals are being produced by reactions involving THPC. Note that Venning *et al* added small quantities of hydroquinone (a free-radical inhibitor) to reduce undesired prepolymerization in their PAG dosimeters containing THPC.<sup>[19]</sup>

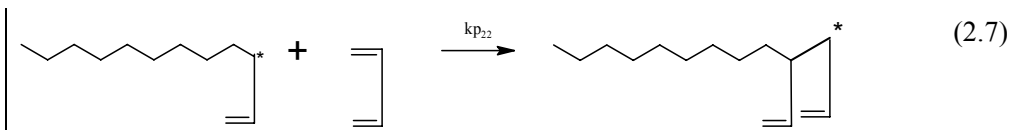
Jirasek *et al* showed that substantial quantities of THPC can be consumed by impurities in the water used in dosimeter recipes, so that it is important to use very pure distilled and deionized water for dosimeter preparation.<sup>[21]</sup> Some researchers have used 10mM THPC<sup>[10,28]</sup> in their dosimeter recipes, but it is becoming common to use 5 mM THPC<sup>[19,21,29,30]</sup> because dose sensitivity decreases with increasing THPC concentration<sup>[21]</sup>. Developing a better understanding of THPC side reactions will be essential before the effects of THCP can be reliably included in mathematical models. As such, the current modeling work focuses on extending the model of Fuxman *et al.* to include the influence of oxygen and MEHQ, but not the effects of THPC.

## 4.5. Previous Kinetic Model

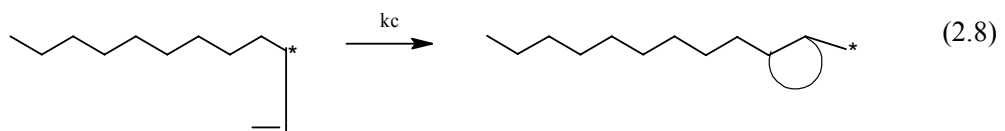
The mathematical modeling efforts described in the current article are based on a previous kinetic model for uniformly irradiated PAG dosimeters developed by Fuxman *et al*<sup>[8]</sup> using PREDICI<sup>®</sup> (Computing in Technology, GmbH). Note that the scheme in Table 4.2 is somewhat simplified compared with the actual model equations because Table 4.2 does not show the precipitation of polymer chains and the growth in volume of the polymer phase over time, which are accounted for in Fuxman's model. Fuxman *et al* assumed that a polymer molecule precipitates from the aqueous phase as soon as a single crosslink is formed, and that the reactions in Table 4.2 occur at different rates in the aqueous and polymer phases, due to different reactant concentrations and diffusivities.

**Table 4.2:** Simplified reaction scheme in the aqueous phase in a PAG dosimeter. The scheme is illustrated using cartoons:  $\equiv$  represents Aam monomer;  $\boxed{\equiv}$  represents Bis,  $\sim$  is a polymer chain that can have a radical (\*) on either an Aam or Bis end unit. Reaction (1) indicates that many different products are generated by water radiolysis. The efficiency factor,  $f$ , accounts for the fact that only a fraction of the radical pairs generated by radiolysis can diffuse out of the cage to initiate polymerization. Reactions analogous to (9-11) involving polymer chains with a terminal Bis are included in the model, but are not shown to save space. The model also assumes that polymer chains with a single crosslink precipitate to form a separate phase and that polymerization and crosslinking reactions continue in the precipitated microgels. Details are presented by Fuxman *et al.*<sup>[8,22]</sup>

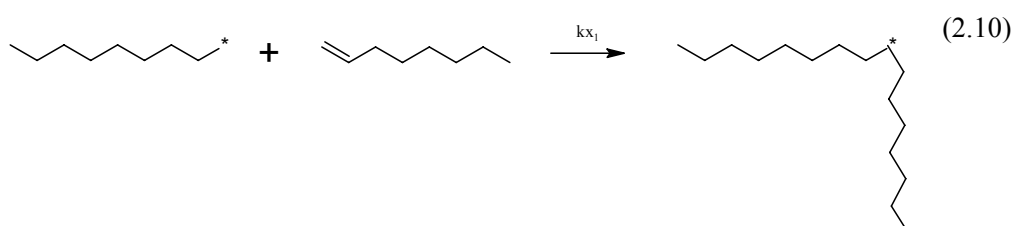
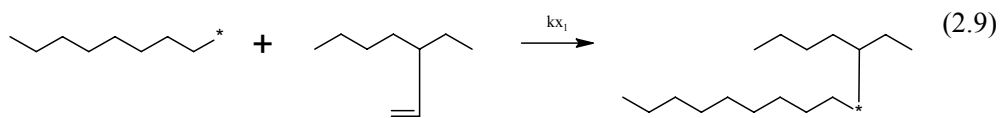




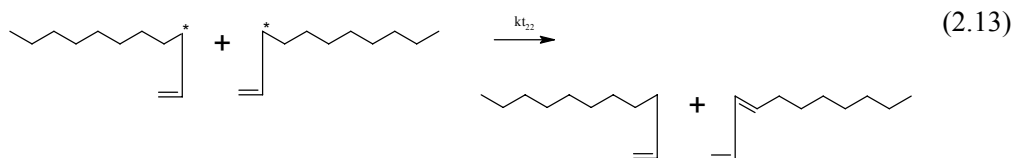
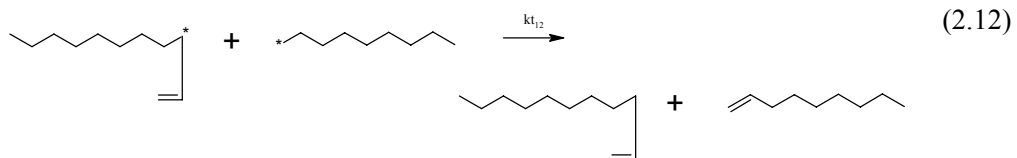
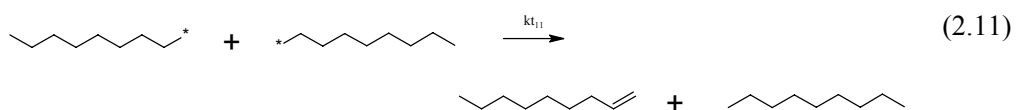
Primary cyclization:



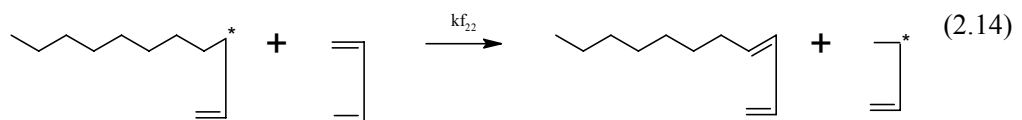
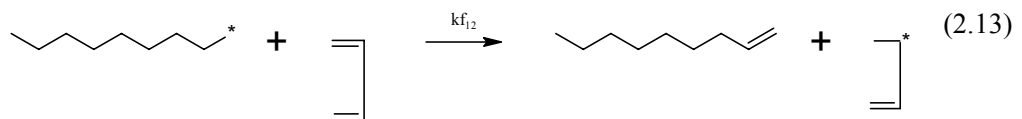
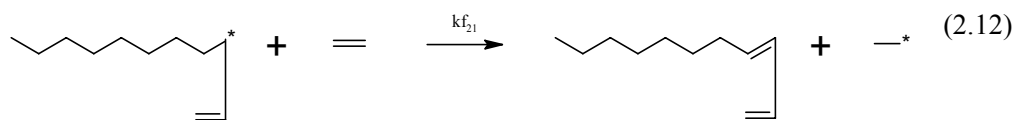
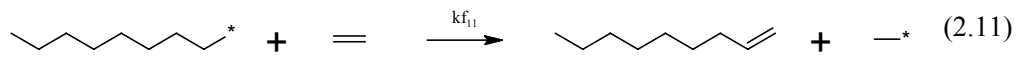
Crosslinking, branching:



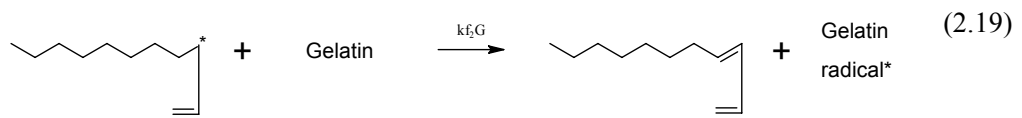
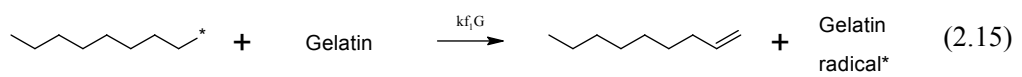
Termination by disproportionation:



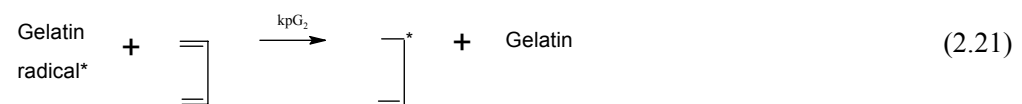
Transfer to monomer:



Transfer to gelatin:



Re-initiation:



Fuxman *et al* simplified the water radiolysis mechanism by assuming a single type of primary radical ( $PR^\bullet$ ). Direct ionization of monomers and other gel components was neglected because of the high water content of gel dosimeters (approximately 90 wt%). Fuxman *et al* assumed that a fraction ( $f$ ) of the primary radicals is able to diffuse out of the solvent cage to initiate polymerization reactions (steps (2.1)-(2.3) in Table 4.2). Subsequent reaction steps were described using a terminal model. Polymer chains with the radical on a bisacrylamide unit were assumed to be less reactive (by a factor  $\nu$ ) due to steric effects of the unreacted pendant vinyl group. The vinyl groups on AAm and Bis were assumed to have equal reactivities.<sup>[31]</sup>

Although both monomers undergo propagation (steps (2.4)-(2.7)), only the incorporation of Bis into the polymer chains can lead to cyclization and crosslinking reactions. Primary cyclization occurs when chains with the radical on a bisacrylamide unit react with the pendant vinyl group from the same bisacrylamide unit. The resulting cyclized radicals (step (2.8)) were assumed to have the same reactivity as radicals on an acrylamide end unit. Pendant double bonds (PDBs) that do not undergo primary cyclization can lead to crosslinks by reacting with radicals on other polymer chains (steps (2.9)-(2.10)). Terminal double bonds were assumed to have the same reactivity as PDBs. The growing radicals can terminate by disproportionation<sup>[32]</sup>, or by transfer of the radical to a monomer or to gelatin (steps (2.11)-(2.13) and (2.14)-(2.19), respectively). Values for some of the parameters used by Fuxman *et al* were available from the literature (e.g., kinetic parameters for water radiolysis<sup>[33]</sup> and parameters for acrylamide polymerization<sup>[34]</sup>; see Table 4.4). However, some parameter values were poorly known, including the initiation efficiency  $f$  and parameters related to chain transfer to gelatin. Fuxman *et al* <sup>[8,22]</sup> adjusted a few of these poorly-known parameters to obtain a good match with the calorimetric data.<sup>[15]</sup> Subsequently, Babic and Schreiner performed gravimetric experiments on PAG dosimeters without gelatin, in which the mass of polymer produced was measured for a

variety of recipes and radiation doses.<sup>[25]</sup> Unfortunately, the model, with Fuxman's parameter values, gives poor predictions of these recent data. To remedy this problem, McAuley and Daneshvar<sup>[24]</sup> estimated 6 of the 12 poorly known parameters in Fuxman's model using the available calorimetric<sup>[15]</sup> and gravimetric data<sup>[25]</sup> and the least-squares parameter-estimation routine in Predici. The six parameters estimated were  $k_{pg}$ ,  $k_{fg}$ ,  $k_c$ ,  $\theta$ ,  $\Phi_{H_2O}$ ,  $\Phi_M$ . Unfortunately, all twelve poorly-known parameters cannot be estimated because the available data lack sufficient information and because the effects of some model parameters are highly correlated with the effects of others. McAuley and Daneshvar used an estimability analysis algorithm<sup>[35]</sup> to rank the parameters from most estimable to least estimable and determined that good predictions could be obtained by estimating the top six parameters and by leaving the remaining parameters at Fuxman's values.

In the current article, the mechanism described by Fuxman *et al* is extended in Section 3 to include oxygen and MEHQ inhibition reactions. Three additional parameters ( $k_{c_{s1}}$ ,  $k_{p_{11}}$ ,  $k_i$ ) related to oxygen inhibition appear in the extended model. These parameters have been added to the estimability analysis of McAuley and Daneshvar. The new ranking, which uses information from the gravimetric experiments<sup>[25]</sup> and the calorimetric experiments with and without oxygen contamination<sup>[15]</sup>, indicates that the six parameters estimated by McAuley and Daneshvar and two new parameters ( $k_{c_{s1}}$ ,  $k_{p_{11}}$ ) can be estimated from the available data. Unfortunately, there are no available gravimetric or calorimetric data for dosimeters containing MEHQ, so MEHQ-related parameters could not be estimated. Values for the re-estimated parameters are shown in **bold** in Table 4.4.

**Table 4.4:** Parameters used in Polymer Gel Dosimeter Simulations. The parameters that are in **bold** are new values estimated from experimental data.<sup>[15,25]</sup> The remaining values were used by Fuxman *et al.*<sup>[8,22]</sup> or are from the literature.

Parameter	Value	Description	Units	Source
a) Model parameters for simulations without oxygen and MEHQ				
$k_{ini_1}$	$\approx 1 \times 10^{10}$	Initiation rate constant for reaction between primary radical and monomer.	$l \text{ mol}^{-1} \text{ s}^{-1}$ 1	[33]
$k_{p_{11}}^0$	$1.65 \times 10^6 \exp(-2743/RT)$	Propagation rate coefficient in the absence of diffusion control.	$l \text{ mol}^{-1} \text{ s}^{-1}$ 1	[34]
<b><math>k_{pg}</math></b>	<b>3.676E-03</b>	Propagation of gelatin-centred radicals	$L \text{ mol}^{-1} \text{ s}^{-1}$ 1	
$k_{f_{11}}^0$	$9.55 \times 10^6 \exp(-10438/RT)$	Rate coefficient for transfer reaction between a macroradical and monomer.	$l \text{ mol}^{-1} \text{ s}^{-1}$ 1	[34]
$k_{fg}$	<b>0.02825</b>	Chain transfer to gelatin	$L \text{ mol}^{-1} \text{ s}^{-1}$ 1	
$k_{t_{11}}^0$	$(1532 \exp(-741/RT))^2$	Bimolecular termination rate coefficient in the absence of diffusion control.	$l \text{ mol}^{-1} \text{ s}^{-1}$ 1	[34]
$k_c$	<b>1.1495E+04</b>	Primary cyclization	$\text{s}^{-1}$	
$k_{p_{11}}^0/k_{p_{12}}^0$	0.5		-	[31]
$k_{p_{22}}^0/k_{p_{21}}^0$	2		-	[31]
$\theta$	<b>0.929993</b>	Fraction of gelatin-centred radicals that can propagate		
$\sigma_{M_1}$	$5.02 \times 10^{-8}$	Lennard-Jones diameter of acrylamide monomer.	cm	[55,56]



$\sigma_{M_2}$	$6.42 \times 10^{-8}$	Lennard-Jones diameter of bisacrylamide monomer.	cm	[55,56]
$a_1$	$1.54 \times 10^{-8}$	Mean distance travelled by a radical when an acrylamide monomer unit is added.	cm	[57]
$D_{M_1}$	$4 \times 10^{-6}$	Diffusivity in the water phase of acrylamide monomer.	$\text{cm}^2 \text{s}^{-1}$	[8]
$D_{H_2O^{aq}}$	$1.5 \times 10^{-5}$	Diffusivity in the water phase of water.	$\text{cm}^2 \text{s}^{-1}$	[8]
$C_p$	4184	Heat capacity of the PAG gel system.	$\text{Jkg}^{-1}\text{K}^{-1}$	[15]
$-\Delta H_R$	81500	Enthalpy of the reaction.	$\text{Jmol}^{-1}$	[34]
$k_{cond}^{20^\circ\text{C}}$	$5.98 \times 10^{-3}$	Thermal conductivity in the PAG gel dosimeter at 20°C.	$\text{Jcm}^{-1}\text{K}^{-1}$ $\text{s}^{-1}$	[8]
$h$	$5 \times 10^{-3}$	Heat transfer coefficient for heat transfer from the PAG to the surrounding environment.	$\text{Jcm}^{-2}\text{K}^{-1}$ $\text{s}^{-1}$	[15]
$G(\epsilon_{aq+H\cdot+OH\cdot})$	$6.27 \times 10^{-7}$	Chemical yield of $H\cdot$ , $\epsilon_{aq}^-$ or $OH\cdot$	$\text{molJ}^{-1}$	[8]
$\Phi_{PDB}$	0.1	Fraction of pendant vinyl groups in polymer phase that can crosslink with aqueous-phase radicals.	-	[22]
$\Phi_{H_2O}$	<b>0.6817</b>	Partition coefficient for water between polymer and aqueous phases	$\frac{\text{mol/L}_{pol}}{\text{mol/L}_{aq}}$	
$\Phi_M$	<b>0.0881</b>	Partition coefficient for monomers between polymer and aqueous phases	$\frac{\text{mol/L}_{pol}}{\text{mol/L}_{aq}}$	
$f$	0.5	Radical efficiency in aqueous phase.	-	[22]
$D_{M_1}$	1.0E-11	Diffusivity of acrylamide in polymer phase.	$\text{cm}^2 \text{s}^{-1}$	[8]
$D_{M_2}$	$3/4 D_{M_1}$	Diffusivity of bisacrylamide in polymer phase.	$\text{cm}^2 \text{s}^{-1}$	[8]
$k_{X_1}^0$	$k_{P_{11}}^0$	Rate constant for reaction between a macroradical bearing the active radical on a acrylamide unit and unreacted double bond.	$1 \text{ mol}^{-1}\text{s}^{-1}$ 1	[22]

$D_{PRW}$	$10D_{M1}^*$	Dead primary radicals in the aqueous phase.	$\text{cm}^2 \text{s}^{-1}$	[22]
$D_{S1}^*$	Varied from $D_{M1}^*$ to 0	Dead polymer chain bearing the active radical on an acrylamide unit.	$\text{cm}^2 \text{s}^{-1}$	[22]
$D_{S2}^*$	$D_{S1}^*$	Dead polymer chain bearing the active radical on a bisacrylamide unit.	$\text{cm}^2 \text{s}^{-1}$	[22]
$a_2$	$2a_1$	Mean distance travelled by a radical when a bisacrylamide monomer unit is added.	cm	[8]
$\Phi_G$	1	Ratio of the concentration of gelatin in the polymer phase over its concentration in aqueous phase.	-	[8]
$\nu$	2	Ratio of reactivity of radicals with terminal acrylamide to radicals with bisacrylamide	-	[8]
b) Parameters for Reactions Involving Oxygen and MEHQ				
$k_{p13}$	<b>2.04E+08</b>	Rate constant for inhibition reaction between oxygen and a polymer radical on an acrylamide unit	$\text{M}^{-1}\text{s}^{-1}$	
$k_{p23}$	$k_{p13}/\nu$	Rate constant for inhibition reaction between oxygen and a polymer radical on a bisacrylamide unit	$\text{M}^{-1}\text{s}^{-1}$	[8]
$k_{p51}$	$\frac{k_{p11}}{2000}$	Rate constant for re-initiation of a peroxy radical with acrylamide monomer	$\text{M}^{-1}\text{s}^{-1}$	[49]
$k_{p52}$	$2k_{p51}$	Rate constant for re-initiation of a peroxy radical with bisacrylamide monomer	$\text{M}^{-1}\text{s}^{-1}$	[8]
$k_{t33}$	$k_{p51} * 10^7$	Rate constant for termination reaction between a polymer radical bearing the active radical on a peroxy unit and a polymer radical bearing the active radical on a peroxy unit	$\text{M}^{-1}\text{s}^{-1}$	[51]
$k_{t31}$	<b>2.382E+03</b>	Rate constant for termination reaction between a polymer radical bearing the active radical on a peroxy unit and a polymer radical bearing the active radical on an acrylamide unit	$\text{M}^{-1}\text{s}^{-1}$	
$k_{t52}$	$k_{t31}/\nu$	Rate constant for termination reaction between a polymer radical bearing the active radical on a	$\text{M}^{-1}\text{s}^{-1}$	[8]

		peroxy unit and a polymer radical bearing the active radical on a bisacrylamide unit		
$k_{f_{21}}$	$k_{f_{21}}/2000$	Rate constant for chain transfer reaction of a polymer radical bearing the active radical on a peroxy unit to acrylamide monomer	$M^{-1}s^{-1}$	[49]
$k_{f_{12}}$	$2k_{f_{21}}$	Rate constant for chain transfer reaction of a polymer radical bearing the active radical on a peroxy unit to bisacrylamide monomer	$M^{-1}s^{-1}$	[8]
$k_{f_{3G}}$	$k_{f_{1G}}/2000$	Rate constant for chain transfer reaction of a polymer radical bearing the active radical on a peroxy unit to gelatin	$M^{-1}s^{-1}$	[49]
$k_{inh,MEHQ_1}$	$2.7E-05 (k_{p_{21}})$	Rate constant for the MEHQ-alone inhibition in case we have acrylamide unit at the end of the polymer chain.	$M^{-1}s^{-1}$	[48,54]
$k_{inh,MEHQ_2}$	$2.7E-05 (k_{p_{21}})$	Rate constant for the MEHQ-alone inhibition in case we have bisacrylamide unit at the end of the polymer chain.	$M^{-1}s^{-1}$	[48,54]
$k_{inh,MEHQ_3}$	$200 (k_{p_{21}})$	Rate constant determining the synergistic inhibition effect of oxygen and MEHQ.	$M^{-1}s^{-1}$	[48,54]
$k_{inh,MEHQ_4}$	$(10^4)k_{t_{33}}$	Rate coefficient describing the inhibition of the peroxy radicals by MEHQ radicals.	$M^{-1}s^{-1}$	[48,54]

Using these revised parameter values, good predictions of gravimetric data and calorimetric are obtained. When the model with the new parameter values is used to simulate dosimeter behaviour for a variety of different dose rates and recipes (i.e., different values of %C, %T and %gelatin), predictions (not shown) are consistent with trends that have been observed experimentally <sup>[36,37,38,39,40]</sup>. A detailed summary of these trends is provided by Fuxman et al. in Table 7 of their article.<sup>[8]</sup> Figure 4.4 shows a comparison of the predicted and measured temperature predictions from calorimetric experiments with and without oxygen contamination.

Using the extended model and improved parameter values, it is now possible to simulate the behaviour of PAG and related NIPAM-based dosimeters that have been contaminated with oxygen and MEHQ. In the future, it will be important to include reactions involving THPC or other oxygen scavengers, so that the behaviour of normoxic polymer gel dosimeters can be simulated.

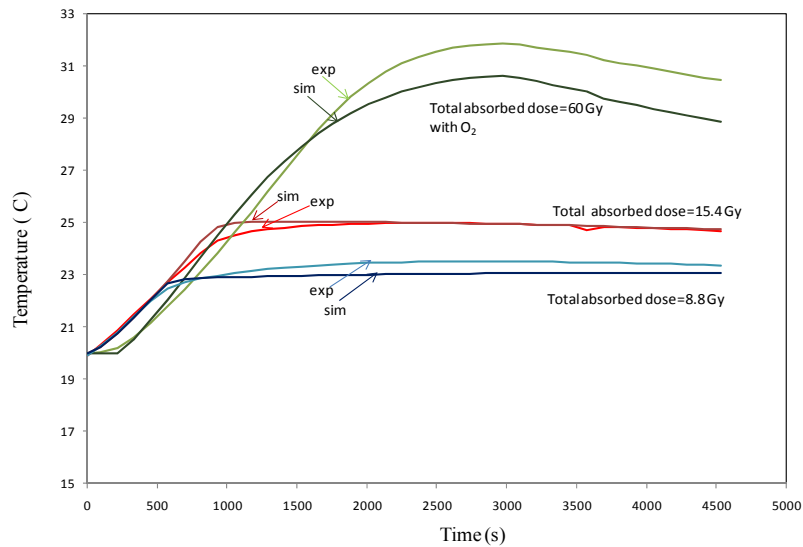


**Figure 4.4:** Comparison of the simulated and experimental calorimetric data<sup>[15]</sup> used in the parameters estimation. The samples containing O<sub>2</sub> were irradiated at a dose rate of 1.25 Gy/min to a total dose of 60 Gy and those without O<sub>2</sub> were irradiated at a dose rate of 1.1 Gy/min to a total dose of 15.4 Gy and 8.8 Gy, respectively.

## 4.6. Extension of Mathematical Model to Include Oxygen and MEHQ Inhibition

### 4.6.1 Modeling of oxygen inhibition

We assume that oxygen inhibition takes place primarily in the aqueous phase, since the formation of the polymer phase is observed only after the inhibition period ends.<sup>[15]</sup> Oxygen can scavenge

initiating (primary) radicals as well as propagating (polymer) radicals in polymer gel dosimeters. A similar oxygen inhibition scheme has been used in models for the photopolymerization of acrylates.<sup>[41,42]</sup>

#### **4.6.1.1 Scavenging of primary radicals**

Upon irradiation, the primary radicals produced by water radiolysis (Table 4.2) can react with the monomers AAm and Bis, as well as with any dissolved oxygen. The superoxide anion radicals ( $O_2^{\bullet -}$ ) and perhydroxyl radicals ( $HO_2^{\bullet}$ ) that form in the reactions with oxygen are unreactive toward most organic compounds and are therefore not expected to initiate polymerization.<sup>[33,43,44]</sup>

The rate constants for the initiation reactions between primary radicals and monomer are of the same order of magnitude ( $\sim 10^{10} \text{ M}^{-1}\text{s}^{-1}$ ) as the rate constants for radical scavenging reactions between primary radicals and oxygen. However, the total initial monomer concentration ( $[M_i] = 0.61 \text{ M}$ ) is much larger than the concentration of dissolved oxygen in air-saturated water at room temperature ( $[O_2] \approx 2.5 \times 10^{-4} \text{ M}$ ). This large difference in the concentrations (approximately a factor of 2500 initially) suggests that relatively few primary radicals will be scavenged by oxygen, but instead propagate to form short polymer radicals. Hence, the main oxygen inhibition mechanism must be the scavenging of these short propagating radicals and the formation of relatively stable organic peroxy radicals (see next section).

#### **4.6.1.2 Scavenging of propagating radicals by oxygen**

Figure 4.5 shows that there is a competition between monomers and oxygen for propagating radicals. However, radical scavenging by  $O_2$  is so fast ( $\sim 5 \times 10^8 \text{ M}^{-1}\text{s}^{-1}$ )<sup>[42,45]</sup> compared to propagation ( $\sim 1.5 \times 10^4 \text{ M}^{-1}\text{s}^{-1}$  for AAm)<sup>[34]</sup> that the oxygen inhibition reactions are initially much

faster than chain propagation even though  $[O_2] \ll [M_i]$ . A very small amount of propagation will still occur, but the polymerization cannot develop until the oxygen concentration declines. For example, using the above rate constants and typical concentrations in a polymer gel dosimeter, the rates of oxygen scavenging and propagation finally become equal (i.e.,  $k[O_2] \approx k_p[M_i]$ ) when  $[O_2]$  has decreased to less than  $2 \times 10^{-5}$  M (approximately 7-8% of the oxygen concentration for a dosimeter saturated with air). The effects of oxygen inhibition have been observed experimentally as an induction period (See Figure 4.6). The length of the induction period is dependent on the level of oxygen.<sup>[15]</sup>

The mechanism in Table 4.5 shows that peroxy radicals can react in three different ways: by re-initiation, bimolecular termination and hydrogen abstraction.

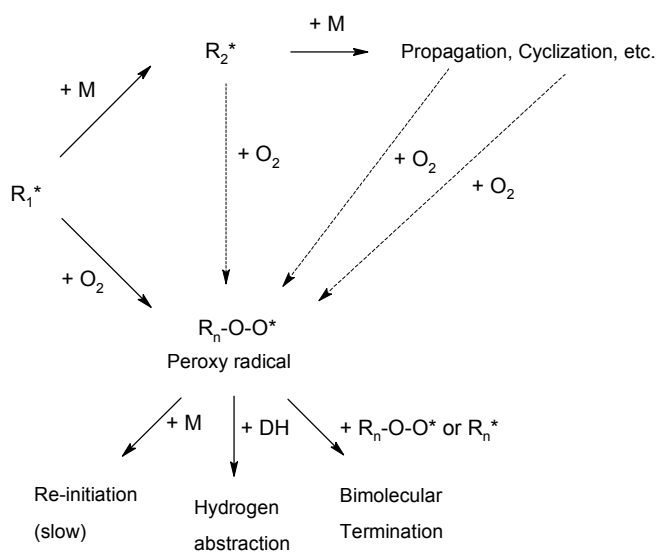


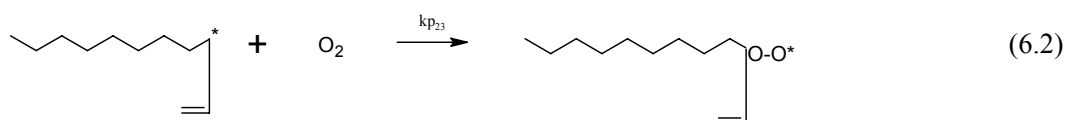
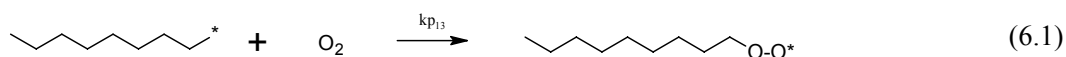
**Figure 4.5:** Reaction mechanism of oxygen inhibition by scavenging of propagating radicals, where  $R_n^*$  is a propagating chain of length  $n$  with a monomer ( $M$ ) end unit,  $R_n-O-O^*$  is a propagating chain of length  $n$  with a peroxy end unit, and  $DH$  is a hydrogen donor (e.g. monomer).<sup>[46]</sup>

Since no visible polymer is produced in the presence of oxygen, the peroxy radicals must be relatively slow to re-initiate propagation. The relative stability of peroxy radicals and slow re-initiation is the key to oxygen inhibition. Most peroxy radicals will undergo rapid bimolecular termination, or will abstract protons from other molecules, e.g. monomers or gelatin.<sup>[46]</sup> The radicals that form by hydrogen abstraction can again be scavenged by oxygen to produce new peroxy radicals (chain oxidation process). The products of bimolecular termination reactions are mostly inactive at low temperatures. Decker and Jenkins used a similar mechanism to describe O<sub>2</sub> inhibition in the photopolymerization of multi-acrylates.<sup>[42]</sup>

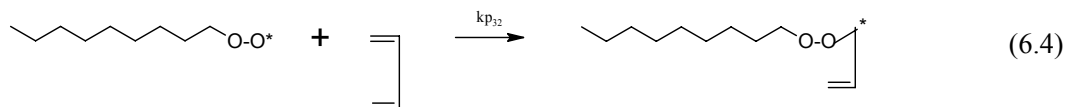
The general mechanism for scavenging of propagating radicals by oxygen and MEHQ was transformed into a kinetic reaction scheme (Table 4.5), which is included along with the reactions in Table 4.2 in our extended polymer gel dosimeter model. Accompanying reaction equations and rate constants can be found in Table 4.6.

**Table 4.5:** Proposed simplified reaction scheme for oxygen inhibition by scavenging of propagating radicals using cartoons: acrylamide monomer ( $\text{=}$ ), bisacrylamide monomer ( $\text{=}$ ), AAm/Bis co-polymer chain ( $\text{---}$ ) that can have a radical ( $\text{*}$ ) on either an acrylamide, bisacrylamide or peroxy end unit. Q\* is a MEHQ radical, and Q is a dead species. This mechanism is shown in Table 4.6 using the notation of Fuxman *et al.*<sup>[8,22]</sup>

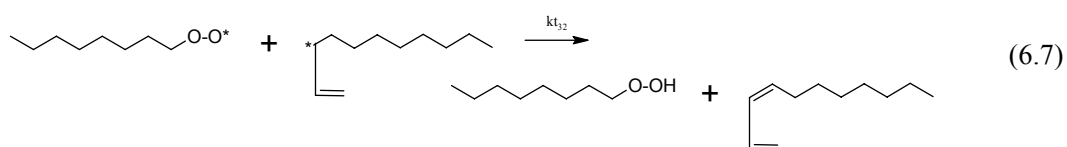
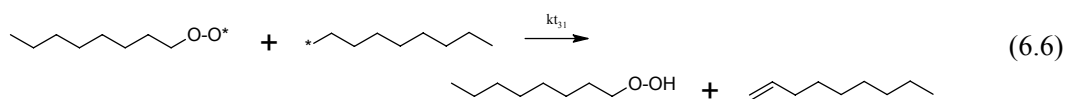
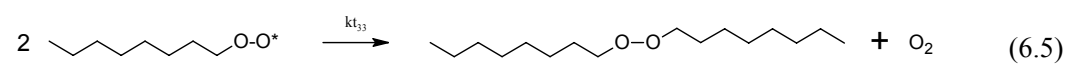
Propagation with oxygen (i.e. inhibition):



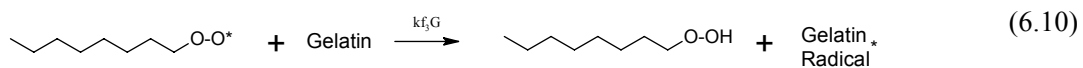
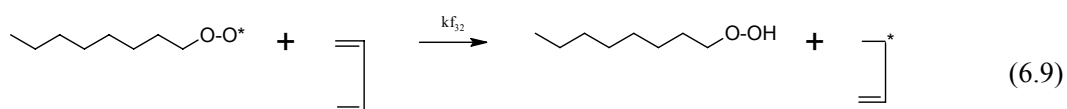
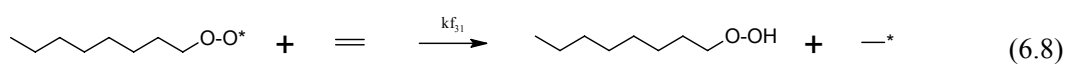
Re-initiation:



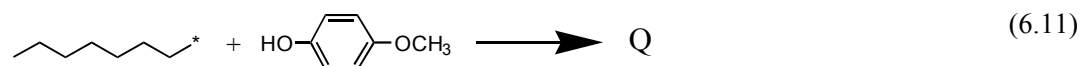
Bimolecular termination:



Chain transfer to monomer and gelatin:



MEHQ inhibition





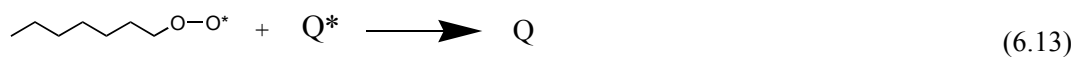
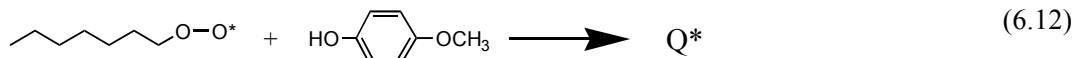


**Table 4.6:** Proposed reaction scheme for oxygen inhibition by scavenging of propagating radicals and for reactions involving MEHQ, where  $S_{i,n}$  is a short chain radical of length  $n$  with acrylamide ( $i = 1$ ), bisacrylamide ( $i = 2$ ) or peroxy ( $i = 3$ ) radical end unit, dead polyperoxides ( $D_{3,n}$ ) and peroxy acids ( $D_{4,n}$ ).  $Q^*$  is a MEHQ radical, and  $Q$  is a dead species. These reaction equations are added to the original PAG dosimeter model of Fuxman *et al* (2003).<sup>[8]</sup> The oxygen reactions are assumed to happen only in the aqueous phase.

Propagation with oxygen (i.e. inhibition):



Re-initiation:



Bimolecular termination:



Chain transfer to monomer and gelatin:



MEHQ inhibition



Growing chains with the radical on AAm ( $S_{1,n}$ ) or on Bis ( $S_{2,n}$ ) monomer units are scavenged by oxygen, producing relatively stable peroxy radicals ( $S_{3,n}$ ) (steps (6.1)-(6.2)). Decker and Jenkins and Andrzejewska *et al* reported rate constants for oxygen scavenging of polymer radicals on the order of  $10^8$ - $10^9 \text{ M}^{-1}\text{s}^{-1}$ .<sup>[42,45]</sup> This approximate value is in agreement with very high ratios of oxygen inhibition rate constants to propagation rate constants mentioned e.g. by Batch and Macosko and Cutié *et al* <sup>[47,48]</sup> The peroxy radicals are slow to re-initiate polymerization (steps (6.3)-(6.4)). Anseth *et al.* reported kinetic constants for methyl methacrylate, indicating that the polymer radicals (i.e. propagation) are approximately  $2 \times 10^3$  times more reactive towards monomer than peroxy radicals.<sup>[49]</sup> Re-initiation rate constants for acrylamide and bisacrylamide, required for simulations in this article, were calculated using the propagation rate constant and the ratio  $k_p/k_{\text{re-initiation}} = 2 \times 10^3$ . It was assumed that Bis is twice as reactive as AAm because of its second vinyl group.<sup>[8]</sup>

Peroxy radicals can combine rapidly in bimolecular termination reactions with other peroxy radicals or with propagating chains (steps (6.5)-(6.7)).<sup>[46,50]</sup> Since rate constants for the termination reactions of peroxy radicals in AAm/Bis systems are not available in the literature, they were approximated using data reported for (meth)acrylate polymerization. Kerber and Serini determined the rate constants for the re-initiation of peroxy radicals ( $k_{p31}$ ) and bimolecular termination of two peroxy radicals ( $k_{t33}$ ) for different free-radical polymerization systems in the presence of oxygen at 20 °C.<sup>[51]</sup> For methyl methacrylate the ratio  $k_{t33}/k_{p31}$  is approximately  $10^7$ , which has been used in the current polymer gel dosimeter model. This value is in agreement with approximate rate constants for (meth)acrylate systems mentioned by Andrzejewska *et al*<sup>[45]</sup> It is assumed that bimolecular termination occurs by disproportionation.<sup>[32]</sup>

The transfer of peroxy radicals occurs when they abstract hydrogen from monomer or gelatin molecules (steps (6.8)-(6.10)). The newly formed radicals can then re-initiate polymerization, or they can be scavenged by oxygen, forming new peroxy radicals. Kinetic constants for the transfer reactions are assumed to be proportional to the re-initiation rate constants (i.e., it is assumed that in chain transfer, peroxy radicals are also  $2 \times 10^3$  times less reactive than propagating chains).

The polyperoxides (R-O-O-R,  $D_{3,n}$ ) and peroxy acids (R-O-OH,  $D_{4,n}$ ) that form in bimolecular termination and chain transfer reactions can decompose upon exposure to heat or light, and form radicals that re-initiate polymerization.<sup>[46]</sup> It is anticipated that irradiation of polymer gel dosimeters may also break the O-O bond to form additional radicals. However, these reactions are not included in the current model because the number of radicals formed in this manner will be much smaller than the number formed by water radiolysis (due to very high water concentrations).

## 4.6.2 Modeling of MEHQ inhibition

Commercial monomer-grade NIPAM contains about 500 ppm monomethyl ether hydroquinone (MEHQ), which is an inhibitor for free radical polymerization. NIPAM and other monomers are used in polymer gel dosimeters without removing MEHQ, so it is important to better understand the effect of MEHQ on dosimeter behaviour. Phenolic inhibitors, such as MEHQ, require oxygen to function well<sup>[52]</sup>, so that in a totally oxygen-free environment, MEHQ is a less effective free-radical inhibitor than when oxygen is present. Several studies have focused on the role of oxygen and MEHQ and their synergistic interactions. Cutié *et al* have shown that when MEHQ is added to acrylic acid polymerization systems, the rate of polymerization decreases but does not stop, indicating that MEHQ, by itself, is a retarder.<sup>[48]</sup> Cutié *et al* also showed that when both MEHQ and oxygen are present, MEHQ can react with peroxy radicals to form very stable radicals that can participate in termination reactions, but not propagation reactions. Without MEHQ, some peroxy radicals eventually propagate with monomer, producing polymer chains with peroxy groups along the backbone.<sup>[53]</sup> MEHQ inhibits the formation and growth of polymer chains, reduces the consumption rate of oxygen, and enhances the inhibition by oxygen.

Since rate constants for inhibition reactions of MEHQ in AAm/Bis or NIPAM/Bis systems are not available in the literature, we approximated them using data reported for acrylic acid polymerization.<sup>[48,54]</sup> Reactions involving oxygen and MEHQ inhibition are shown using cartoons in Table 4.5 and using the notation of Fuxman *et al* in Table 4.6. We use ratios of kinetic rate constants determined by Cutie et al. for acrylic acid polymerization to make the following assumptions: i) the inhibition rate constants for reaction between polymeric radicals with terminal Aam and Bis units and MEHQ are  $k_{inh,MEHQ1}=2.7 \times 10^{-5}k_{p11}$  and  $k_{inh,MEHQ2}=2.7 \times 10^{-5}k_{p21}$ , respectively; ii) the synergistic inhibition rate constant for reaction between a peroxy radical and MEHQ is  $k_{inh,MEHQ3} = 200 k_{p31}$  where  $k_{p31}$  is the rate constant for propagation of peroxy radicals;

iii) the rate constant for termination between peroxy and MEHQ radicals is  $k_{\text{inh,MEHQ},4} = (10^4)k_{t33}$  where  $k_{t33}$  is the rate constant for bimolecular termination of two peroxy radicals.<sup>[51]</sup>

PREDICI<sup>®</sup> software was used to simulate the influences of MEHQ and oxygen using the reaction scheme shown in Tables 4.5 and 4.6, along with the original reactions shown in Table 4.2 (see Appendix C for input file). Peroxy radicals are relatively stable, but can react very quickly with MEHQ to form a more stable radical Q\* (step (6.12) in Table 4.6). Step (6.12) is the reaction that accounts for the synergistic inhibition effects between oxygen and MEHQ. Peroxy radicals can combine rapidly in bimolecular termination reactions with the Q\* radical. The products of the disproportionation reaction are oxygen molecules, which can further inhibit the polymerization, and dead MEHQ radicals (step 6.13 in Table 4.6). In their model for MEHQ-inhibited polymerization of acrylic acid, Li and Schork assumed that the Q\* radicals cannot undergo any reactions except for termination with peroxy radicals, and we adopt a similar assumption.

## 4.7. Results and Discussion

### 4.7.1. Simulations with oxygen inhibition

Figure 4.6 shows the predicted conversion of vinyl groups with different initial levels of oxygen in PAG dosimeters that are irradiated to a dose of 20 Gy at a dose rate of 1 Gy/min. An induction period in which no polymerization occurs is clearly observed in all of the simulated runs with oxygen; there is no appreciable conversion of the vinyl groups until nearly all of the oxygen is consumed. The length of the predicted induction period decreases when the amount of dissolved oxygen is decreased. These simulation results agree with experimental observations.<sup>[15]</sup>

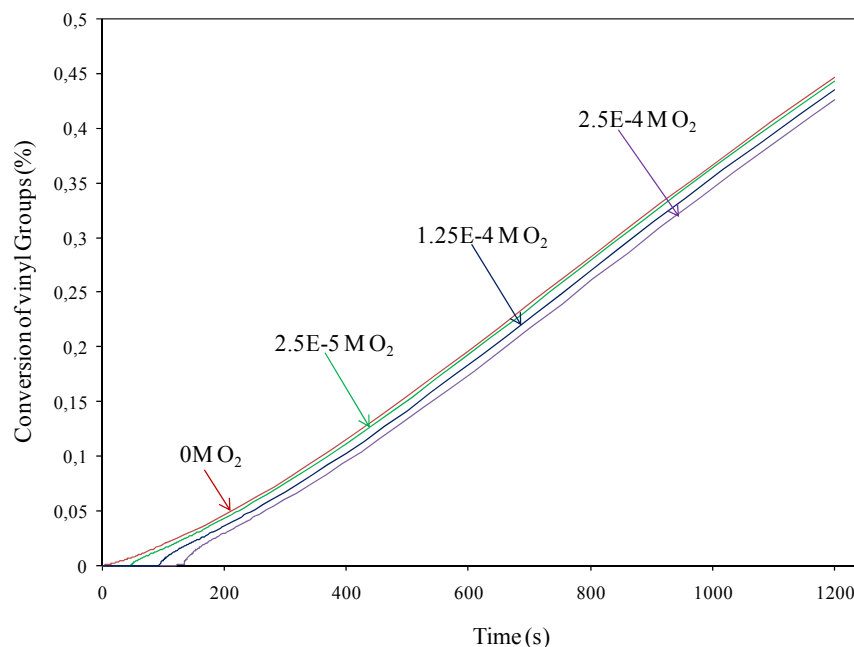


**Figure 4.6:** Simulation results showing the conversion of vinyl groups in PAG dosimeters with different initial concentrations of oxygen. The 6 %T, 50 % C dosimeters were irradiated at a dose rate of 1 Gy/min to a total dose of 20 Gy. The concentration of O<sub>2</sub> in a dosimeter in equilibrium with air is  $2.5 \times 10^{-4}$  M.

#### 4.7.2. Simulation of MEHQ inhibition

Figure 4.7 shows the conversion of vinyl groups over time in dosimeters containing either oxygen or MEHQ, or both. Curves b) and c) show simulation results for an oxygen concentration of  $2.5 \times 10^{-5}$  M, which is 10% of the concentration of O<sub>2</sub> in equilibrium with air (which is  $2.5 \times 10^{-4}$  M). Note that 15 ppm of MEHQ in the final recipe corresponds to an MEHQ level of 500 ppm in the monomer, which is a typical amount in commercial NIPAM. The dosimeters simulated in Figure 4.7 were irradiated at a dose rate of 1 Gy/min.

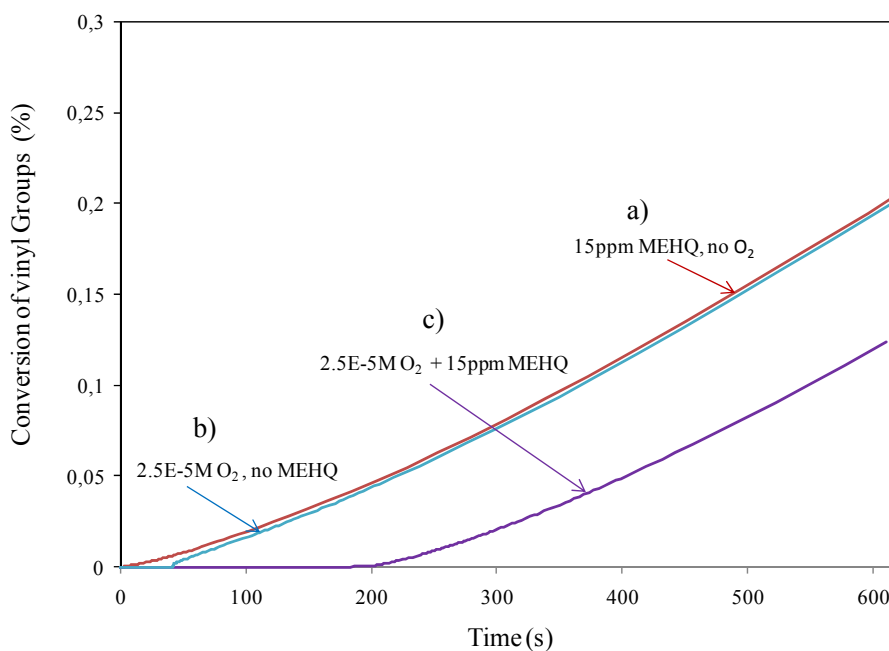


**Figure 4.7:** Simulation results comparing the vinyl group conversion over time in dosimeters with and without oxygen and MEHQ contamination. The concentration of  $O_2$  in a dosimeter in equilibrium with air is  $2.5 \times 10^{-4}$  M. Curves b) and c) with oxygen were obtained using one tenth of this concentration. The simulated 6%T 50 %C dosimeters were irradiated at a dose rate of 1 Gy/min to a total dose of 10 Gy.

Comparison of curves b) and c) in Figure 7 shows that there is an appreciable change in the length of the induction period when MEHQ is added to an oxygen-contaminated dosimeter. The synergistic inhibition effect of oxygen and MEHQ becomes stronger with the increase in the concentration of oxygen. In the case when the concentration of  $O_2$  in the dosimeter is in equilibrium with air ( $2.5 \times 10^{-4}$  M) and 15 ppm MEHQ is present, no appreciable polymerization is observed up to a total absorbed dose of 20 Gy (results not shown). The results in Figure 4.7 demonstrate that MEHQ has no appreciable effect on the polymerization in the absence of oxygen, but it plays a significant role as an inhibitor when oxygen is present.

The simulation results in Figures 4.7 show that MEHQ contamination resulting from typical levels used in commercial-grade NIPAM have no appreciable influence on the rate of polymer formation in polymer gel dosimeters when all of the oxygen is scavenged from the system. Unfortunately, even very small amounts of oxygen will enhance the inhibition effect of MEHQ to a point where no polymer is formed. As a result, scientists who manufacture and use polymer gel dosimeters should not take any steps to remove the MEHQ. Oxygen removal, however, is very important to achieve reliable dosimeter results.

## **4.8. Conclusions**

Reaction mechanisms for inhibition by oxygen and MEHQ were incorporated into a previous kinetic model for polyacrylamide gel dosimeters. Several important model parameters were estimated using gravimetric and calorimetric data, with and without oxygen contamination. Predictions from the model with the improved parameter values provide a good quantitative match to the experimental data. The oxygen inhibition observed in polymer gel dosimeters was successfully modeled based on the scavenging of propagating polymer radicals and the formation of relatively stable peroxy radicals. The model predicts an increase in the induction period with increasing levels of oxygen contamination, but also predicts significant influence of MEHQ for typical levels of MEHQ in commercial NIPAM monomer, when its effect is enhanced by the presence of oxygen in the system. As a result, it is recommended that dosimeter users should ensure that all oxygen is either removed or chemically scavenged from their dosimeter phantoms, but MEHQ removal is not required. The extended model developed in this article is an important step toward predicting the behaviour of normoxic polymer gel dosimeters. Better understanding



of the many chemical reactions involving the oxygen scavenger THPC is required before its influence can be included in models in a meaningful way.

## **4.9. Acknowledgments**

Funding for this work was provided by Natural Science and Engineering Research Council (NSERC), the Canada Institutes of Health Research (CIHR), the Ontario Consortium of Image Guided Surgery and Therapy (OCITS), and Queen's University.

## 4.10. References in Chapter 4

- [1] *J. Phys.: Conf. Ser.*— 3<sup>rd</sup> **2004**, 4<sup>th</sup> **2006** and 5<sup>th</sup> **2008** International Conference on Radiotherapy Gel Dosimetry.
- [2] M. J. Maryanski, R. J. Schulz, G. S. Ibbott, J. C. Gatenby, J. Xie, D. Horton and J. C. Gore, **1994b**, ‘Magnetic resonance imaging of radiation dose distributions using a polymer-gel dosimeter’, *Phys. Med. Biol.* **39** 1437-55.
- [3] F. Teymour and J. D. Campbell, **1994**, ‘Analysis of the dynamics of gelation in polymerization reactors using the “numerical fractionation” technique’, *Macromolecules* **27**, 2460–2469.
- [4] K. B. McAuley, **2004**, ‘The chemistry and physics of polyacrylamide gel dosimeters: why they do and don’t work’, *Journal of Physics: Conference Series* **3**: 29-33.
- [5] J. C. Gore, Y. S. Kang and R. J. Schulz, **1984**, ‘Measurement of radiation dose distributions by nuclear magnetic resonance (NMR) imaging’, *Phys. Med. Biol.* **29** 1189-97.
- [6] M. J. Maryanski, Y. Z. Zastavker and J. C. Gore, **1996a**, ‘Radiation dose distributions in three dimensions from tomographic optical density scanning of polymer gels: II. Optical properties of the BANG polymer gel’, *Phys. Med. Biol.* **41** 2705-17.
- [7] M. Hilts, C. Audet, C. Duzenli and A. Jirasek, **2000**, ‘Polymer gel dosimetry using x-ray computed tomography: a feasibility study’, *Phys. Med. Biol.* **44** 2559-71.
- [8] A. M. Fuxman, K. B. McAuley and L. J. Schreiner, **2003**, ‘Modeling of free-radical crosslinking copolymerization of acrylamide and N,N’-methylenebis(acrylamide) for radiation dosimetry’, *Macromol. Theory Simul.* **12** 647-62.
- [9] G. S. Ibbott, **2004**, ‘Applications of gel dosimetry’, *J. Phys.: Conf. Ser.* **3**, 58-77.

- [10] R. J. Senden, P. De Jean, K. B. McAuley and L. J. Schreiner, **2006**, 'Polymer gel dosimeters with reduced toxicity: a preliminary investigation of the NMR and optical dose-response using different monomers', *Phys. Med. Biol.* **51** 3301-14
- [11] A. Rudin **1982** 'The elements of polymer science and engineering', *Academic Press*, New York.
- [12] G. Odian **1991** 'Principles of polymerization' *3<sup>rd</sup> ed* John Wiley & Sons, New York.
- [13] S. J. Hepworth, M. O. Leach and S. J. Doran, **1999**, 'Dynamics of polymerization in polyacrylamide gel (PAG) dosimeters: (II) modelling oxygen diffusion', *Phys. Med. Biol.* **44** 1875-84.
- [14] M. McJury, M. Oldham, M. O. Leach and S. Webb, **1999**, 'Dynamics of polymerization in polyacrylamide gel (PAG) dosimeters: (I) ageing and long-term stability', *Phys. Med. Biol.* **44** 1863-73.
- [15] G. J. Salomons, Y. S. Park, K. B. McAuley and L. J. Schreiner, **2002**, 'Temperature increases associated with polymerization of irradiated PAG dosimeters', *Phys. Med. Biol.* **47** 1435-48.
- [16] C. Baldock, R. P. Burford, N. Billingham, G. S. Wagner, S. Patval, R. D. Badawi, and S. F. Keevil, **1998**, 'Experimental procedure for the manufacture and calibration of polyacrylamide gel (PAG) for magnetic resonance imaging (MRI) radiation dosimetry', *Phys. Med. Biol.* **43** 695-702
- [17] P. M. Fong, D. C. Keil, M. D. Does and J. C. Gore, **2001**, 'Polymer gels for magnetic resonance imaging of radiation dose distributions at normal room atmosphere', *Phys. Med. Biol.* **46** 3105-13.

- [18] Y. De Deene, C. Hurley, A. Venning, K. Vergote, M. Mather, B. J. Healy and C. Baldock, **2002b**, 'A basic study of some normoxic polymer gel dosimeters', *Phys. Med. Biol.* **47** 3441-63.
- [19] A. J. Venning, B. Hill, S. Brindha, B. J. Healy and C. Baldock, **2005**, 'Investigation of the PAGAT polymer gel dosimeter using magnetic resonance imaging', *Phys. Med. Biol.* **50** 3875-88.
- [20] Y. De Deene, K. Vergote, C. Claeys and C. De Wagter, **2006**, 'The fundamental radiation properties of normoxic polymer gel dosimeters: a comparison between a methacrylic acid based gel and acrylamide based gels', *Phys. Med. Biol.* **51** 653-73.
- [21] A. Jirasek, M. Hilts, C. Shaw and P. Baxter, **2006**, 'Investigation of tetrakis hydroxymethyl phosphonium chloride as an antioxidant for use in x-ray computed tomography polyacrylamide gel dosimetry', *Phys. Med. Biol.* **51** 1891-1906.
- [22] A. M. Fuxman, K. B. McAuley and L. J. Schreiner, **2005**, 'Modelling of polyacrylamide gel dosimeters with spatially non-uniform radiation dose distributions', *Chem. Eng. Sci.* **60** 1277-93.
- [23] Y. De Deene, **2004**, 'Essential characteristics of polymer gel dosimeters', *J. of Phys.* **3** 34-57.
- [24] K.B. McAuley and S. Daneshvar, **2006**, 'Parameter Estimation and Estimability Analysis in a Polymer Gel Dosimetry Model', *Jacque Cartier Conference on Modelling, Monitoring and Control of Polymer Properties, ESCPE*, Lyon, France, Dec. 2007.
- [25] S. Babic and L. J. Schreiner, **2006**, 'An NMR relaxometry and gravimetric study of gelatin-free aqueous polyacrylamide dosimeters', *Phys. Med. Biol.* **51**, 4171-4187.
- [26] R. J. Senden, **2006**, '*Polymer gel dosimeters with reduced toxicity and enhanced performance*' M.Sc. Thesis, Queen's University.

- [27] V. I. Koeva, T. Olding, A. Jirasek, K. B. McAuley and L.J. Schreiner, **2008b**, ‘Preliminary investigation of the NMR, optical and x-ray CT dose-response of polymer gel dosimeters that use cosolvents to increase crosslinker levels’ *Submitted to Phys. Med. Biol.*
- [28] A. J. Venning, S. Brindha, B. Hill, and C. Baldock, **2004**, ‘Preliminary study of a normoxic PAG gel dosimeter with tetrakis (hydroxymethyl) phosphonium chloride as an antioxidant’, *Journal of Physics: Conference Series* **3**, 155–158.
- [29] Y. De Deene, G. Pittomvils and S. Visalatchi, 2007, ‘The influence of cooling rate on the accuracy of normoxic polymer gel dosimeters’, *Phys. Med. Biol.* **52**, 2719–2728.
- [30] A. Karlsson, H. Gustavsson, S Månsson, K. B. McAuley and S Å Bäck, 2007, ‘Dose integration characteristics in normoxic polymer gel dosimetry investigated using sequential beam irradiation’, *Phys. Med. Biol.* **51**, 4697–4706.
- [31] H. Tobita and A. E. Hamielec, **1990**, ‘Crosslinking kinetics in polyacrylamide networks’, *Polymer* **31** 1546-52.
- [32] T. Ishige and A. E. Hamielec, **1979**, ‘Solution polymerization of acrylamide to high conversion’, *J. Appl. Polym. Sci.* **17** 1479-1506.
- [33] J. W. T. Spinks and R. J. Woods, **1976**, ‘An Introduction to Radiation Chemistry’ *2<sup>nd</sup> ed* John Wiley & Sons, New York.
- [34] J. Hernandez-Barajas and J. D. Hunkeler, **1997**, ‘Inverse-emulsion polymerization of acrylamide using block copolymeric surfactants: mechanism, kinetics, and modeling’, *Polymer* **38**(2) 437-447.
- [35] B. Kou, K. B. McAuley, C. C. Hsu, D. V. Bacon and K. Z. Yao, **2005**, ‘Mathematical Model and Parameter Estimation for Gas-Phase Ethylene Homopolymerization with Supported Metallocene Catalyst’, *Ind. Eng. Chem. Res.* **44**, 2428-2442.

- [36] M. J. Maryanski, C. Audet and J. C. Gore, **1997**, 'Effects of crosslinking and temperature on the dose response of a BANG polymer gel dosimeter', *Phys. Med. Biol.* **42**, 303-11.
- [37] M. Lepage, A. K. Whittaker, L. Rintoul, and C. Baldock, **2001a**, '<sup>13</sup>C-NMR, <sup>1</sup>H-NMR, and FT-Raman study of radiation-induced modifications in radiation dosimetry polymer gels', *J. Appl. Polym. Sci.* **79**, 1572-81.
- [38] A. I. Jirasek and C. Duzenli, **2001**, 'Effects of crosslinker fraction in polymer gel dosimeters using FT Raman spectroscopy', *Phys. Med. Biol.* **46**, 1949-61.
- [39] M. Lepage, A. K. Whittaker, L. Rintoul, S. Å. J. Bäck, and C. Baldock, **2001b**, 'The relationship between radiation-induced chemical processes and transverse relaxation times in polymer gel dosimeters', *Phys. Med. Biol.* **46**, 1061-74.
- [40] C. Audet, **1995**, 'NMR-dose response studies of gels used for 3-D MRI radiation dosimetry', PhD Thesis, McGill University.
- [41] A. K. O'Brien and C. N. Bowman, **2006**, 'Modeling the effect of oxygen on photopolymerization kinetics' *Macromol. Theory Simul.* **15** 176-82.
- [42] C. Decker and A. D. Jenkins, **1985**, 'Kinetic approach of O<sub>2</sub> inhibition in ultraviolet- and laser-induced polymerizations' *Macromolecules* **18** 1241-4.
- [43] J. H. O'Donnell and D. F. Sangster, **1970**, 'Principles of radiation chemistry' *American Elsevier Publishing Company Inc*, New York.
- [44] A. J. Swallow, **1973**, 'Radiation Chemistry' *Longman Group Limited*, London.
- [45] E. Andrzejewska, M. B. Bogacki, M. A. Andrzejewski and M. Janaszczyk, **2003**, 'Termination mechanism during the photo-induced radical cross-linking polymerization in the presence and absence of oxygen' *Phys. Chem. Chem. Phys.* **5** 2635-42.
- [46] K. Kishore, V. Gayathri and K. Ravindran, **1981**, 'Formation and degradation of polymeric peroxides' *J. Macromol. Sci. Chem.* **A16 (8)** 1359-83.

- [47] G. L. Batch and C. W. Macosko, **1990**, 'Oxygen inhibition in differential scanning calorimetry of free-radical polymerization' *Thermochim. Acta* **166** 185-98.
- [48] S. S. Cutié, D. E. Henton, C. Powell, R. E. Reim, P. B. Smith and T. L. Staples, **1997**, 'The effects of MEHQ on the polymerization of acrylic acid in the preparation of superabsorbent gels' *J. Appl. Polym. Sci.* **64** 577-89.
- [49] K. S. Anseth, S. M. Newman and C. N. Bowman, **1995**, 'Polymeric dental composites: properties and reaction behavior of multimethacrylate dental restorations' *Adv. Polym. Sci.* **122** 177-217.
- [50] M. H. George and A. Ghosh, **1978**, 'Effect of oxygen on the radical polymerization of acrylamide in ethanol and water' *J. Polym. Sci. Polym. Chem. Ed.* **16** 981-95.
- [51] R. Kerber and V. Serini, **1970**, 'Bestimmung der wachstums- und abbruchskonstanten bei der copolymerisation von styrol,  $\alpha$ -methylstyrol und methylmethacrylat mit molekularem sauerstoff' *Makromolekul. Chem.* **140** 1-19.
- [52] L. B. Levy, **1985**, 'Inhibition of acrylic acid polymerization by phenothiazine and para-methoxyphenol' *J. Polym. Sci. Polym. Chem.* **23**, 1505-1515.
- [53] J. J. Kurland, **1980**, 'Quantitative aspects of synergistic inhibition of oxygen and para-methoxyphenol in acrylic-acid polymerization' *J. Polym. Sci. Polym. Chem.* **18**, 1139-1145.
- [54] R. Li and F. Joseph Schork, **2006**, 'Modeling of the Inhibition Mechanism of Acrylic Acid Polymerization' *Ind.Eng. Chem. Res.* **45**, 3001-3008.
- [55] G. T Russell, D. H. Napper and R. G. Gilbert, **1988**, 'Termination in free-radical polymerizing systems at high conversion', *Macromolecules* **21**, 2133-40.
- [56] R. C. Reis, J. M. Prausnitz and B. E. Poling, 'The Properties of Gases and Liquids', McGraw-Hill, New York **1987**.

[57] R. A. Orwoll, Y. S. Chong, in: Polymer Data Handbook, J. E. Mark, Ed., Oxford University Press, Oxford **1999**.



# Chapter 5

## Conclusions and Recommendations

### 5.1. Conclusions

In this thesis (Chapter 2), new polymer gel dosimeter recipes were investigated using CEAMBLOOM 3240 as an alternative gelling agent, ascorbic acid and  $[\text{Cu}^{2+}]$  as alternative oxygen-scavenging system and several new potential crosslinkers. Although the gels produced using CEAMBLOOM 3240 instead of gelatin set very quickly, they resulted in very low dose sensitivity. As a result, CEAMBLOOM 3240, with its current additives, is an ineffective gelling agent for use in polymer gel dosimetry applications.

Tetrakis (hydroxymethyl) phosphonium chloride (THPC) oxygen scavenger is a toxic liquid, and an alternative scavenging system, Ascorbic acid and  $\text{Cu}^{2+}$ , would be preferred because the components are less toxic than THPC and they are available as solids, which could be incorporated into prepackaged polymer-gel powder packets. Radiation dose-response curves and visual observations revealed that no precipitated polymer was formed when this alternative oxygen scavenger was used. In addition, the alternative oxygen-scavenging system resulted in very poor gel stiffness. Some of the gels became liquid at room temperature. It is not clear why this alternative oxygen-scavenging system works well for polymethacrylic acid dosimeters, but not NIPAM-based dosimeters.

The suitability and the performance of crosslinkers in polymer gel dosimetry are influenced by many factors, such as toxicity, primary cyclization reactions and water solubility.

Ten candidates for replacing N,N'-methylene-bisacrylamide, the crosslinker that is currently used in polymer gel dosimeter recipes, were tested. Unfortunately, the polymer gel dosimeters prepared with the 9 of the candidate crosslinkers did not show a better sensitivity results than the standard dosimeter recipe using N,N'-methylene-bisacrylamide. Only N,N'-ethylene-bisacrylamide produced results that are similar to those obtained using N,N'-methylene-bisacrylamide crosslinker, but N,N'-ethylene-bisacrylamide is not recommended because it is considerably more expensive than N,N'-methylene-bisacrylamide.

Chapter 3 describes how the solubility of bisacrylamide can be increased substantially by adding either glycerol, isopropanol or n-propanol (as cosolvent) to the dosimeter recipe. Dosimeters produced using isopropanol cosolvent and up to 5% N,N'-methylene-bisacrylamide by weight were shown to produce  $R_2$  vs. dose response curves with significantly higher dose sensitivity than the standard polymer gel dosimeter recipe containing 3% N,N'-methylene-bisacrylamide. For example, a normoxic 10 %T 50 %C dosimeter produced using 30 wt% isopropanol cosolvent produced x-ray CT dose response curves with a 53% higher dose sensitivity than a standard normoxic 6 %T 50 %C dosimeter without cosolvent. This high %T dosimeter had good optical clarity prior to irradiation. More thorough research, involving spatially non-uniform radiation doses, was conducted to confirm the suitability of the proposed dosimeter recipes for read-out using OptCT. Unfortunately, this high %T dosimeter did not produce reliable optical CT results for non-uniformly-irradiated gels and the resulting plots of optical CT number vs. dose contained significant scatter, presumably due to stray light arising from multiple scatter and cone-beam-scanner artefacts (Olding *et al*, 2008). Some of the gels made with isopropanol appeared to set unevenly and had many small trapped air bubbles when cooled. Another concern is that the polymer seems to have formed (or migrated) outside of the zones corresponding to the delivered radiation. Note that lower %T NIPAM-based gels produced

without cosolvent (4 %T 50 %C gels) have recently been used effectively for optical CT readout by members of our research group (Olding *et al*, 2008). Although these gels have lower dose sensitivity than standard 6% T 50 %C gels and than the 10%T gels with cosolvents reported in this thesis, they result in more-accurate optical CT responses due to less problems with stray light and multiple scattering. Nevertheless, the optical CT results in this thesis confirm that NIPAB-based gels produced with cosolvents can record spatially non-uniform radiation dose distributions, suggesting that these gels may be effective for x-ray CT, where stray light and scattering is not an issue.

Dosimeters containing 12 wt% isopropanol show a significant change in OptCT response between 1 day and 5 days after irradiation, whereas dosimeters without isopropanol had a very little change in dose response curves. It will be important to test whether cosolvents influence the temporal stability of the x-ray CT response.

The dosimeters containing isopropanol and glycerol were also tested using x-ray CT read-out. 10%T 50 %C polymer gels containing isopropanol give larger responses than those without cosolvent, but are still less sensitive than traditional (anoxic) 6% T 50 %C polyacrylamide gels. Note that no attempts have been made yet to optimize the recipes for NIPAM-based gels made with cosolvents, so that the highest possible dose sensitivity and dose resolution (Baldock *et al* 1998) can be obtained for x-ray CT readout.

In Chapter 4 the oxygen inhibition observed in PAG and NIPAM-based polymer gel dosimeters was successfully modeled based on the scavenging of propagating polymer radicals by oxygen, and the formation of relatively stable peroxy radicals. The model predictions agree well with experimental findings of Salomons *et al* (2002). Salomons *et al* observed that the duration of the induction period, in which no polymerization occurs, increases with higher levels of oxygen. The simulations predict the same behaviour. The dynamic kinetic model for PAG and NIPAM-

based polymer gel dosimeters was also extended to include MEHQ in the oxygen-inhibition mechanism, because MEHQ is present as an inhibitor in NIPAM monomer. The extended model, which uses MEHQ kinetics proposed by Li *et al.* (2006) was used to simulate the synergistic inhibition effects of MEHQ and oxygen on free radical polymerization in uniformly irradiated PAG or NIPAM dosimeters. Simulations show that the addition of MEHQ to the recipe has little influence on the amount of polymer formed (and on the dose response) when there is no oxygen present. When significant amounts of oxygen are present in the gel, the inhibition effect of oxygen is enhanced by the MEHQ and almost no polymerization is observed when up to 20 Gy of radiation is delivered when the amount of oxygen is in equilibrium with air. In this case MEHQ has important influence on the polymerization rate. MEHQ is only effective in preventing polymerization when oxygen is not scavenged from the system and for this reason we do not recommend that MEHQ is removed during manufacturing of polymer gels.

## **5.2 Recommendations**

The following recommendations are made for future research on polymer gel dosimeters with improved recipes:

- Carrageenan-based gelling agents should be tested again if gelling agents without additives (or with lower levels of additives) become commercially available, because the poor radiation-dose response observed in this thesis may result from the citric acid and potassium chloride additives rather than from the carrageenan.
- Further experiments are required to determine whether cosolvents can be used to manufacture reliable gels with high dose sensitivity, high dose resolution and high spatial resolution for

readout using x-ray computed tomography. It will be important to conduct a thorough study aimed at optimizing a NIPAM-based recipe that is suitable for x-ray CT readout. Higher dose sensitivity might be obtained by: reducing the gelatin concentration, reducing the THPC concentration, changing the NIPAM to Bis ratio (%C), increasing the total monomer concentration (%T) and selecting the appropriate level of cosolvent and cosolvent concentration. Note that recent experimental results from our collaborators indicate that glycerol cosolvent can influence dose response, even if no additional Bis is included in the recipe (Jirasek *et al*, 2008). Mechanisms for this type of behaviour are not understood and require further study.

- Since optical CT readout can be performed effectively with low %T gels, no additional resources should be spent on developing high %T gels with cosolvents for optical CT applications, unless new and different scanners are developed.
- When investigating new crosslinkers, Senden (2006) ruled out many commercially-available crosslinkers, because they were liquids at room temperature that were stabilized with inhibitors to prevent polymerization during shipping and storage. The most common inhibitor used is MEHQ. In Chapter 4, simulations using the extended model show that 500 ppm (the amount used to stabilize NIPAM) does not lead to significant retardation of the polymerization process when oxygen is not present in the system. We recommend that the list of potential crosslinkers should be reconsidered, so that more effective crosslinkers (containing MEHQ) can be tested. MEHQ removal from dosimeter recipes is not recommended.
- Current polymer gel dosimeter recipes include THPC to scavenge oxygen. THPC also participates in many side reactions. As more becomes known about the kinetics of these reactions, the model should be extended to include reactions with THPC.

# Bibliography:

[www.chemicaland21.com](http://www.chemicaland21.com)

*J. Phys.: Conf. Ser.*— 3<sup>rd</sup> **2004**, 4<sup>th</sup> **2006** and 5<sup>th</sup> **2008** International Conference on Radiotherapy Gel Dosimetry.

Andrzejewska, E., M. B. Bogacki, M. A. Andrzejewski, and M. Janaszczyk (2003), 'Termination mechanism during the photo-induced radical cross-linking polymerization in the presence and absence of oxygen', *Phys. Chem. Chem. Phys.* **5**, 2635-42.

Anseth, K. S., S. M. Newman, and C. N. Bowman (1995), 'Polymeric dental composites: properties and reaction behavior of multimethacrylate dental restorations', *Adv. Polym. Sci.* **122**, 177-217.

Audet C. (1995), 'NMR-dose response studies of gels used for 3-D MRI radiation dosimetry', PhD Thesis, McGill University.

Babic, S. (2004), *Nuclear Magnetic Resonance relaxometry studies of an Aqueous Polyacrylamide dosimeter*, M.Sc. Thesis, Queen's University.

Babic, S., and L. J. Schreiner (2006), 'An NMR relaxometry and gravimetric study of gelatin-free aqueous polyacrylamide dosimeters', *Phys. Med. Biol.* **51**, 4171–4187

Baldock, C., R.P. Burford, N. Billingham, G. S. Wagner, S. Patval, R.D. Badawi, and S.F. Keevil (1998), 'Experimental procedure for the manufacture and calibration of polyacrylamide gel (PAG) for magnetic resonance imaging (MRI) radiation dosimetry', *Phys. Med. Biol.* **43**, 695-702

Batch, G. L., and C. W. Macosko (1990), 'Oxygen inhibition in differential scanning calorimetry of free-radical polymerization', *Thermochim. Acta* **166**, 185-98.

- Bussche, E. V., Y. De Deene, K. Vergote and C. De Wagter (2004) ‘Alternative gelling agents for normoxic gels: a stability study’ *Journal of Physics: Conference Series* **3**, 168–171
- Chang Y., Mumick P.S., Worldwide K.C. (2001) “Process for synthesizing temperature-responsive N-isopropylacrylamide polymers” *United States Patent*, Patent # US 6 268 449 B1.
- Cutié, S. S., D. E. Henton, C. Powell, R. E. Reim, P. B. Smith, and T. L. Staples (1997), ‘The effects of MEHQ on the polymerization of acrylic acid in the preparation of superabsorbent gels’, *J. Appl. Polym. Sci.* **64**, 577-89.
- DeJean, P. D., R. J. Senden, K. B. McAuley, M. Rogers, and L.J. Schreiner (2006), ‘Initial experience with a commercial cone beam optical CT unit for polymer gel dosimetry I: Optical dosimetry issues’ *Journal of Physics: Conference Series* **56**, 179–182
- DeJean, P. D., R. J. Senden, K. B. McAuley, M. Rogers, and L. J. Schreiner (2006), ‘Initial experience with a commercial cone beam optical CT unit for polymer gel dosimetry II: Clinical potential’ *Journal of Physics: Conference Series* **56**, 183-186
- Decker, C., and A. D. Jenkins (1985), ‘Kinetic approach of O<sub>2</sub> inhibition in ultraviolet- and laser-induced polymerizations’, *Macromolecules* **18**, 1241-4.
- De Deene Y, Venning A, Hurley C, Healy B and Baldock C (2002a) ‘Dose-response stability and integrity of the dose distribution of various polymer dosimeters’ *Phys. Med. Biol.* **47** 2459–70
- De Deene, Y., C. Hurley, A. Venning, K. Vergote, M. Mather, B. J. Healy, and C. Baldock (2002b) ‘A basic study of some normoxic polymer gel dosimeters’, *Phys. Med. Biol.* **47**, 3441-63.
- De Deene, Y. (2004), ‘Essential characteristics of polymer gel dosimeters’, *J. Phys.: Conf. Ser.* **3**, 34-57.

- De Deene, Y., K. Vergote, C. Claeys, and C. De Wagter (2006), 'The fundamental radiation properties of normoxic polymer gel dosimeters: a comparison between a methacrylic acid based gel and acrylamide based gels', *Phys. Med. Biol.* **51**, 653-73.
- De Deene Y, G Pittomvils and S Visalatchi (2007) 'The influence of cooling rate on the accuracy of normoxic polymer gel dosimeters' *Phys. Med. Biol.* **52**, 2719–2728
- De Deene Y (2008) 'Review of quantitative MRI principles for gel dosimetry' Dosgel 2008 Crete, Greece
- Digenis G. A. , T. B. Gold and V. P. Shah (2006), 'Cross-linking of gelatin capsules and its relevance to their in vitro-in vivo performance', *J. Pharm. Sci.* **83**, Issue 7, 915 - 921
- Fong, P. M., D. C. Keil, M. D. Does, and J. C. Gore (2001), 'Polymer gels for magnetic resonance imaging of radiation dose distributions at normal room atmosphere', *Phys. Med. Biol.* **46**, 3105-13.
- Fuxman, A. M., K. B. McAuley, and L. J. Schreiner (2003), 'Modeling of free-radical crosslinking copolymerization of acrylamide and N,N'-methylenebis(acrylamide) for radiation dosimetry', *Macromol. Theory Simul.* **12**, 647-62.
- Fuxman, A. M., K. B. McAuley, and L. J. Schreiner (2005), 'Modelling of polyacrylamide gel dosimeters with spatially non-uniform radiation dose distributions', *Chem. Eng. Sci.* **60**, 1277-93.
- Garcia, E., D.Martino, D.Esteno, G. Meira, and J. Warner (2006), 'Copolymerization of vinylbenzyl thymine and vinylphenylsulfonic salt. Mathematical modeling and characterization of the obtained water-soluble polymers', *World Polymer Congress – Macro, 41<sup>st</sup> Int. Symp. Macromol. Proc. (Rio De Janeiro, Brazil)*.
- George, M. H., and A. Ghosh (1978), 'Effect of oxygen on the radical polymerization of acrylamide in ethanol and water', *J. Polym. Sci. Polym. Chem. Ed.* **16**, 981-95.



- Gopalan, A., P. Venuvanalingam, S. P. Manickam, K. Venkatarao, and N.R. Subbaratnam (1982), 'Kinetics of polymerization of N,N'-methylenebisacrylamde initiated by  $\text{KmnO}_4\text{H}_2\text{C}_2\text{O}_4$  redox system', *Eur. Polym. J.* **18**, 531-4.
- Gore, J. C., Y. S. Kang, and R. J. Schulz (1984), 'Measurement of radiation dose distributions by nuclear magnetic resonance (NMR) imaging', *Phys. Med. Biol.* **29**, 1189-97.
- Haraldsson, P., A. Karlsson, E. Wieslander, H. Gustavsson and S. A. J. Back (2006) Dose response evaluation of low-density Normoxic polymer gel dosimeter using MRI *Phis. Med. Biol.* **51** 919-928
- Hayashi I Sh, M Yoshioka, Sh Usui I, K Haneda and T Tominaga (2008) 'The role of gelatin in a methacrylic acid based gel dosimeter' Dosgel 2008 Crete, Greece
- Hepworth, S. J., M. O. Leach, and S. J. Doran (1999), 'Dynamics of polymerization in polyacrylamide gel (PAG) dosimeters: (II) modelling oxygen diffusion', *Phys. Med. Biol.* **44**, 1875-84.
- Hernandez-Barajas J. and J. D. Hunkeler (1997), 'Inverse-emulsion polymerization of acrylamide using block copolymeric surfactants: mechanism, kinetics, and modeling', *Polymer* **38**(2) 437-447.
- Hilts, M., C. Audet, C. Duzenli, and A. Jirasek (2000), 'Polymer gel dosimetry using x-ray computed tomography: a feasibility study', *Phys. Med. Biol.* **44**, 2559-71.
- Hurley, C. A., A. Venning and C Baldock (2005) A study of nomoxic polymer gel dosimeter comprising methacrylic acid, gelatin and tetrakis (hydroxymethyl) phosphonium chloride (MAGAT) *Appl. Rad. Isotopes* **63** 443-456
- Ibbott, G. S. (2004), 'Applications of gel dosimetry', *J. Phys.: Conf. Ser.* **3**, 58-77.
- Ishige, T., and A. E. Hamielec (1979), 'Solution polymerization of acrylamide to high conversion', *J. Appl. Polym. Sci.* **17**, 1479-1506.

- Jirasek A and Duzenli C (2001) Effects of crosslinker fraction in polymer gel dosimeters using FT Raman spectroscopy *Phys. Med. Biol.* **46** 1949-1961
- Jirasek A., M. Hilts, C. Shaw, and P. Baxter (2006), 'Investigation of tetrakis hydroxymethyl phosphonium chloride as an antioxidant for use in x-ray computed tomography polyacrylamide gel dosimetry', *Phys. Med. Biol.* **51**, 1891-1906.
- Jirasek A., M. Hilts, A. Berman, and K. B. McAuley (2008), 'Effects of bis-acrylamide co-solvent on the rate and form of polymer gel dose response', *Submitted to Phys. Med. Biol.*
- Karlsson A., H. Gustavsson, S. Månsson, K. B. McAuley and S. Å. J Bäck , (2007). Dose integration characteristics in normoxic polymer gel dosimetry investigated using sequential beam irradiation. *Phys. Med. Biol.* **52**, 4697-4706.
- Kennan, R.P., K.A. Richardson, J. Zhong, M.J. Maryanski, and J. C. Gore. (1996) 'The effect of cross-link density and chemical exchange on magnetization transfer in polyacrylamide gels', *Journal of Magnetic Resonance, Series B.* **110**, 267-277
- Kerber, R., and V. Serini (1970), 'Bestimmung der wachstums- und abbruchskonstanten bei der copolymerisation von styrol,  $\alpha$ -methylstyrol und methylnmethacrylat mit molekularem sauerstoff', *Makromolekul. Chem.* **140**, 1-19.
- Kishore, K., V. Gayathri, and K. Ravindran (1981), 'Formation and degradation of polymeric peroxides', *J. Macromol. Sci. Chem.* **A16** (8), 1359-83.
- Koeva V.I., E.S. Csaszar, R.J. Senden, K.B. McAuley, L.J. Schreiner (2008) 'Polymer gel dosimeters with increased solubility: a preliminary investigation of the NMR and optical dose-response using different crosslinkers and co-solvents', *Macromol. Symp.* **261**, 157-166.
- Koeva V.K., (2008) 'Improved recipes for Polymer Gel Dosimeters containing N-Isopropylacrylamide', M.Sc. Thesis, Queen's University.

- Kou B., K. B. McAuley, C. C. Hsu, D. V. Bacon and K. Z. Yao, **2005**, ‘Mathematical Model and Parameter Estimation for Gas-Phase Ethylene Homopolymerization with Supported Metallocene Catalyst’, *Ind. Eng. Chem. Res.* **44**, 2428-2442.
- Kurland, J. J. (1980), ‘Quantitative aspects of synergistic inhibition of oxygen and p-methoxyphenol in acrylic acid polymerization’, *J. Polym. Sci. Polym. Chem. Ed.* **18**, 1139-45.
- Laustsen K. (2006) ‘Getting closer to Gelatine’ *Food Market and Techn.* Issue **5/2006**  
[www.ceamsa.com](http://www.ceamsa.com) Products Copyright © 20002 CEAMSA Compañia Española de Algas Marinas, S.A.
- Lepage, M., A. K. Whittaker, L. Rintoul, S. Å. J. Bäck, and C. Baldock (2001b), ‘The relationship between radiation-induced chemical processes and transverse relaxation times in polymer gel dosimeters’, *Phys. Med. Biol.* **46**, 1061-74.
- Lepage, M., A. K. Whittaker, L. Rintoul, S. Å. J. Bäck, and C. Baldock (2001d), ‘Modelling of post-irradiation events in polymer gel dosimeters’, *Phys. Med. Biol.* **46**, 2827-39.
- Levy, L. B. (1985), ‘Inhibition of acrylic acid polymerization by phenothiazine and p-methoxyphenol’, *J. Polym. Sci. Polym. Chem. Ed.* **23**, 1505-15.
- Li R. and F. Joseph Schork (2006), ‘Modeling of the Inhibition Mechanism of Acrylic Acid Polymerization’ *Ind.Eng. Chem. Res.* **45**, 3001-3008.
- Low D. A., and J. F. Dempsey (2003) ‘Evaluation of the gamma dose distribution comparison method’, *Medical Physics*, **30** (9), 2455-2464.
- Luci, J.J., H.M. Whitney, J.C. Gore (2007) ‘Optimization of MAGIC gel formulation for three-dimensional radiation therapy dosimetry’, *Phys. Med. Biol.* **52**, N241-N248.
- Maryanski, M. J., J. C. Gore, R. P. Kennan, and R. J. Schulz (1993), ‘NMR relaxation enhancement in gels polymerized and cross-linked by ionizing radiation: a new approach to 3D dosimetry by MRI’, *Magn. Reson. Imaging* **11**, 253-8.

- Maryanski, M. J., R. J. Schulz, G. S. Ibbott, J. C. Gatenby, J. Xie, D. Horton, and J. C. Gore (1994b), 'Magnetic resonance imaging of radiation dose distributions using a polymer-gel dosimeter', *Phys. Med. Biol.* **39**, 1437-55.
- Maryanski, M. J., Y. Z. Zastavker, and J. C. Gore (1996a), 'Radiation dose distributions in three dimensions from tomographic optical density scanning of polymer gels: II. Optical properties of the BANG polymer gel', *Phys. Med. Biol.* **41**, 2705-17.
- Maryanski, M.J., C Audet, and J.C. Gore. (1997). Effects of crosslinking and temperature on the dose response of a BANG polymer gel dosimeter. *Phys. Med. Biol.* **42**, 303-311.
- McAuley, K. B. (2004) 'The chemistry and physics of polyacrylamide gel dosimeters: why they do and don't work', *Journal of Physics, Conference Series* **3**: 29-33.
- McAuley K.B. and S. Daneshvar (2006), 'Parameter Estimation and Estimability Analysis in a Polymer Gel Dosimetry Model', *Jacque Cartier Conference on Modelling, Monitoring and Control of Polymer Properties, ESCPE*, Lyon, France, Dec. 2007.
- McJury, M., M. Oldham, M. O. Leach, and S. Webb (1999), 'Dynamics of polymerization in polyacrylamide gel (PAG) dosimeters: (I) ageing and long-term stability', *Phys. Med. Biol.* **44**, 1863-73.
- Naghash, H. J., and O. Okay (1996), 'Formation and structure of polyacrylamide gels', *J. Appl. Polym.Sci.* **60**, 971-9.
- O'Brien, A. K., and C. N. Bowman (2006), 'Modeling the effect of oxygen on photopolymerization kinetics', *Macromol. Theory Simul.* **15**, 176-82.
- Odian, G. (1991), *Principles of polymerization*, 3<sup>rd</sup> ed., John Wiley & Sons, New York.
- O'Donnell J. H. and D. F. Sangster (1970), 'Principles of radiation chemistry' *American Elsevier Publishing Company Inc*, New York.

- Oldham, M., J. H. Siewerdsen, A. Shetty, D. A. Jaffray (2001), 'High resolution gel-dosimetry by optical-CT and MR scanning', *Med. Phys.* **28**, 1436-45.
- Olding T., O. Holmes, L. J. Schreiner (2008) Scatter Corrections for Cone Beam Optical CT. *DosGel 2008 Conference*, Crete, Greece. *Journal of Physics: Conference Series*
- R. A. Orwoll, Y. S. Chong, in: *Polymer Data Handbook*, J. E. Mark, Ed., Oxford University Press, Oxford (1999).
- Papagianis P, Pantelis E, Georgiou E, Karaiskos P, Angelopoulos A, Sakelliou, Stiliaris S, Baltas D and Seimenis I (2006) 'Polymer gel dosimetry for the Tg-43 dosimetric characterization of a new 125I Interstitial brachytherapy seed ', *Phys. Med. Biol.* **51**, 2101-2111.
- Reeves, W. and Guthrie J. D. (1956) 'Intermediate for flame resistant polymers: reactions of tetrakis(hydroxymethyl)phosphonium chloride' *Indust. Eng. Chem.* **48**, 64-67
- R. C. Reis, J. M. Prausnitz and B. E. Poling (1987), 'The Properties of Gases and Liquids', McGraw-Hill, New York.
- Rudin, A. (1982), *The elements of polymer science and engineering*, Academic Press, New York.
- Russell, G. T., D. H. Napper, and R. G. Gilbert (1988), 'Termination in free-radical polymerizing systems at high conversion', *Macromolecules* **21**, 2133-40.
- Salomons, G. J., Y. S. Park, K. B. McAuley, and L. J. Schreiner (2002), Temperature increases associated with polymerization of irradiated PAG dosimeters *Phys. Med. Biol.* **47**, 1435-48.
- Schreiner LJ (2006) 'Dosimetry in modern radiation therapy', *Journal of Physics: Conference Series* **56**, 1-13.
- Schreiner L J (2008) 'NMR mechanisms in gel dosimetry' *Dosgel 2008 Crete, Greece*
- Senden R. J. (2006), '*Polymer gel dosimeters with reduced toxicity and enhanced performance*' M.Sc. Thesis, Queen's University.

- Senden, R. J., P. D. Jean, K. B. McAuley, and L. J. Schreiner. (2006). 'Polymer gel dosimeters with reduced toxicity: a preliminary investigation of the NMR and optical dose–response using different monomers', *Physics in Medicine and Biology*. **51**, 3301-3314.
- Spinks, J. W. T., and R. J. Woods (1976), *An Introduction to Radiation Chemistry*, 2<sup>nd</sup> ed., John Wiley & Sons, New York.
- Statistics Canada (2006), *Cancer Incidence in Canada*. Statistics Canada Catalogue no. 82-231-XIE-2006001. Ottawa: Minister of Industry.
- Swallow, A. J. (1973), *Radiation Chemistry*, Longman Group Limited, London.
- Teymour, F., Campbell, J.D., (1994) 'Analysis of the dynamics of gelation in polymerization reactors using the "numerical fractionation" technique', *Macromolecules*. **27**, 2460–2469.
- Tobita, H., and A. E. Hamielec (1990), 'Crosslinking kinetics in polyacrylamide networks', *Polymer* **31**, 1546-52.
- Venning, A. J., S. Brindha, B. Hill, and C. Baldock (2004), 'Preliminary study of a normoxic PAG gel dosimeter with tetrakis (hydroxymethyl) phosphonium chloride as an anti-oxidant', *J. Phys.: Conf. Ser.* **3**, 155-58.
- Venning, A. J., B. Hill, S. Brindha, B. J. Healy, and C. Baldock (2005), 'Investigation of the PAGAT polymer gel dosimeter using magnetic resonance imaging', *Phys. Med. Biol.* **50**, 3875-88.
- Vergote, K., Y. De Deene, E. Vanden Bussche, and C. De Wagter (2004), 'On the relation between the spatial dose integrity and the temporal instability of polymer gel dosimeters', *Phys. Med. Biol.* **49**, 4507-22.

# **Appendix A: Problems and Recommendations during gel manufacturing**

The different problems encountered during gel manufacturing and useful tips to deal with them are included in this appendix. Most of the changes to the manufacturing procedure were introduced when 1L gels were produced. Cloudiness, bubble formation, and gelation of the solution during manufacturing were some of the challenges that had to be overcome.

## **A.1 Cloudiness**

The heated water-NIPAM mixture goes cloudy with a fine colloidal suspended precipitate at around 35 °C. (It doesn't happen at 32 °C or below). For this reason use the following procedure for gel preparation:

### **Solution A**

- i. Add 60% of the DI water to flask.
- ii. Add 50 g gelatin. Swell for 10 minutes at RT, heat to 50 °C.
- iii. Add the bisacrylamide. Hold at 50 °C until dissolved.
- iv. Cool to 35 °C. Add NIPAM mixture and stir for 1 min. Pour the solution into the 1L jar before refrigerating.

### **Solution B**

- i. Add DI water with room temperature to a separate container.
- ii. Add NIPAM and stir, holding until NIPAM is dissolved.

- iii. Add THPC and let sit for 5 minutes.

The temperature of the final mixture should not exceed 32 °C.

## **A.2 Bubbles and undesired viscosity**

- i. For the reasons stated above we did not want to go over 32 °C when NIPAM is present in the solution. On the other hand, we had to be very careful because we did not want the temperature of the solution to go below 32 °C because this caused a premature gelation. The gelatine starts to set and solid chunks of the gel precipitate at the bottom of the flask. The uniformity of the gel is affected due to uneven gelation, which leads to poor dose response results.
- ii. When cosolvents (i.e. isopropanol) were used to increase the solubility of Bis in gel dosimeters we had an additional problem namely bubble formation during refrigeration. We are not completely sure what is this phenomenon due to, but one of the possibilities might be that a significant portion of air is trapped in the cosolvent and cannot escape the solution during the setting of the gel. My suggestions will be:
  - a. Leave the jar at room temperature for 1 hour before refrigerating.
  - b. Perform degasification of the cosolvent before using it.



## Appendix B: Experimental Procedures

This appendix includes a more practical step-by-step approach of the experimental procedures, in addition to the information provided throughout this thesis. The following procedures were used in the general preparation (Baldock *et al.*, 1998; De Deene *et al.*, 2002b), irradiation (Babic, 2004) and NMR scanning (Babic, 2004) of the polymer gel dosimeters in this thesis. Changes to the procedures of Babic (2004) include the use of a cooling system to maintain sample temperatures lower than 27 °C inside the NMR spectrometer.

### B.1 Gel Preparation

- i. Always prepare the gel in the fume hood and take adequate personal safety measures (i.e. goggles, gloves, lab coat, et cetera).
- ii. Swell the gelatin in about 80% of the water for 10 minutes at room temperature. Don't stir.
- iii. Use a magnetic heater/stirrer plate to heat the gelatin solution to approximately 50 °C, and stir continuously until a clear solution is obtained. Cover to minimize the evaporation of water.
- iv. Cool down the gelatin solution to 35-40 °C and add the crosslinker if it is easily soluble. Or, in case of Bis, keep the temperature at 50 °C until most has dissolved, and then let the solution cool to 35-40 °C.
- v. Add the monomer at 35-40 °C, and stir until all of the co-monomer is dissolved (usually about 15 minutes in total).
- vi. Mix the THPC solution with the rest of the water. Add it to the gel-monomer mixture last at approximately 35 °C.
- vii. Transfer gel solution into test tubes using a syringe. Cap the tubes with rubber septa.

- viii. Replace the air above the gel inside the test tubes with nitrogen using two needles (one IN, and one OUT) and N<sub>2</sub> supply from the cylinder.
- ix. Wrap parafilm around the rubber septa, and aluminium foil around the test tube to prevent polymerization reactions initiated by light.
- x. Place the samples in the fridge to solidify.

## **B.2 Irradiation**

- i. See the research staff of the Cancer Center of Southeastern Ontario to obtain more details, and permission to operate the MDS Nordion T-780 Cobalt-60 unit. Training and a safety course are required.
- ii. Place the test tube(s) in the correct position of the water tank.
- iii. Irradiate the samples for the time required using a 10x10 cm<sup>2</sup> field. Halfway through, the samples should be rotated 180° to avoid a dose gradient over the diameter of the test tubes.
- iv. Store irradiated samples in the fume hood at room temperature until imaging.

## **B.3 NMR relaxometry**

- i. Read the operating manual of the Maran 20/35 bench top NMR spectrometer (located at the Cancer Center of Southeastern Ontario) to gain an understanding of the equipment.
- ii. Set the correct parameter values for polymer gel samples. The following parameter settings have been used in this thesis, according to information obtained from the operating manual, equipment guidelines (Bouchard, personal communication and PowerPoint slides with the operating manual), and Babic (2004, and personal communication):

FID (Free Induction Decay)	CPMG (Carr-Purcell-Meiboom-Gill) pulse sequence
P90: run .autop90	P90, P180: run .autop90
Dead1: 15.0 us *	Dead1: 15.0 us *
Dead2: 20 us *	Dead2: 20 us *
SF: 25.3 MHz *	SF: 25.3 MHz *
O1: run .autoO1	O1: run .autoO1
FW: 10 <sup>6</sup> Hz *	FW: 10 <sup>6</sup> Hz *
DW: 1.0 us *	DW: 1.0 us *
SI: 1024 *	SI: 1 * (Bouchard)
NS: 4 *	NS: 4 * (Bouchard)
RG: run .autoRG	RG: run .autoRG
RD: 10 <sup>6</sup> us *	RD: 15 x 10 <sup>6</sup> us
PH1: 0213 *	Tau: 500 us (Babic, 2004)
PH2: 0213 *	Nech: 8000 (Babic, 2004)
DS: 0 *	PH1: 0213, PH2: 0213, PH3: 1122 *
RFAO: 100% *	DS: 0 *
	RFAO: 100% *

\* indicates parameter settings obtained from the operating manual that should not be changed.

- iii. Run FID (Free Induction Decay) with mineral oil to set the P90 (90° Pulse) and RG (Receiver Gain) using the automated scripts. Keep P90 and RG values constant in order to compare data sets. Set the offset (O1) before each series of T2 measurements.
  - a. *LOAD FID*
  - b. *.autoO1* (3x)
  - c. *.autoP90*
  - d. *.autoRG*

- iv. Place a glass dewar inside the NMR, and a polymer gel sample inside the dewar. Run the CPMG (Carr-Purcell-Meiboom-Gill) pulse sequence to determine the sample  $T_2$  at a certain time post-irradiation.
- a. *LOAD CPMG*
  - b. *.autoO1*
  - c. *GO*
  - d. *T2*
- v. If required, use air to cool the samples while inside the NMR (the optimal operating temperature of the magnet is 27 °C, but a lower temperature (e.g. 21 °C) gives higher  $R_2$  values and dose-sensitivities). The air can be maintained at a constant temperature, by passing it through copper tubing inside the cooler/heater filled with water at the required temperature. In addition, a water bath should be used to equilibrate the temperature of the samples before and in between measurements. A glass dewar is used to isolate the samples from the higher NMR temperature when inside the NMR.

## Appendix C: PREDICI<sup>®</sup> Input File

The reaction scheme developed by Fuxman *et al.* (2003) for radiation-induced polymerization, including the extension proposed in this thesis for synergistic oxygen-MEHQ inhibition (Table 4.5-Table 4.6), was implemented in the software package PREDICI<sup>®</sup> Version 6.37.4 (Computing in Technology, GmbH). The differential balance equations were generated and solved by PREDICI<sup>®</sup> using the input file shown below.

## Information

Polyacrylamide gel dosimeter: Two-phase model

Accuracy 1.0000e-02

Library: library.lib

Only moment computing

Units: kg l s K

Reactors: 1

Type Operation: CSTR semi-batch

Copolymerisation by composition

Volume contraction

Reactionsteps 125

## Water\_Phase

### Initiation

$y' = f(\text{GenerationofPR.fun}(y))$ , ODE-System (Generation\_of\_Primary\_Radicals)

$\text{PR}^* + \text{PR}^* \rightarrow \text{eff}(\text{eff.fun}) * (\text{I}^* + \text{I}^*)$ ,  $\text{ki}(\text{eff.fun})$ , Elementalreaction2

$\text{I}^* + \text{M1} \rightarrow \text{P1w}(1) + \text{C1}$ ,  $\text{ki1}$ , Initiation(anion)

$\text{I}^* + \text{M2} \rightarrow \text{P2w}(1) + \text{C2}$ ,  $\text{ki2}$ , Initiation(anion)

### Propagation.

$\text{P1w}(s) + \text{M1} \rightarrow \text{P1w}(s+1) + \text{C1}$ ,  $\text{kp11}$ , Propagation(copolymer) (Propagation\_of\_acrylamide)

$\text{P1w}(s) + \text{M2} \rightarrow \text{P2w}(s+1) + \text{C2}$ ,  $\text{kp12}(\text{kp12.fun})$ , Propagation(copolymer) (Propagation\_of\_bis(acrylamide))

$\text{P1w}(s) + \text{O2} \rightarrow \text{P3w}(s+1) + \text{C3}$ ,  $\text{kp13}$ , Propagation(copolymer) (Formation\_of\_peroxy\_radical)

**$\text{P1w}(s) + \text{MEHQ} \rightarrow \text{Q}(s)$ ,  $\text{k\_inh\_MEHQ1}$ , Change (Inhibition\_of\_[~AAM]\_polymer\_pieces)**

$\text{P2w}(s) + \text{M1} \rightarrow \text{P1w}(s+1) + \text{C1}$ ,  $\text{kp21}(\text{kp21.fun})$ , Propagation(copolymer) (Propagation\_of\_acrylamide)

$\text{P2w}(s) + \text{M2} \rightarrow \text{P2w}(s+1) + \text{C2}$ ,  $\text{kp22}(\text{kp22.fun})$ , Propagation(copolymer) (Propagation\_of\_bis(acrylamide))

$\text{P2w}(s) + \text{O2} \rightarrow \text{P3w}(s+1) + \text{C3}$ ,  $\text{kp23}(\text{kp23.fun})$ , Propagation(copolymer) (Formation\_of\_peroxy\_radical)

**$\text{P2w}(s) + \text{MEHQ} \rightarrow \text{Q}(s)$ ,  $\text{k\_inh\_MEHQ2}$ , Change (Inhibition\_of\_[~Bis]\_polymer\_pieces)**

$y' = f(\text{PDBbypropagation.fun}(y))$ , ODE-System (Generation\_of\_double\_bonds\_("PDB")\_by\_propagation\_reactions)

### Cyclization.

$\text{P2w}(s) \rightarrow \text{P1w}(s) + \text{C}$ ,  $\text{kc}$ , Change (Cyclization)

### Crosslinking.

$\text{P1w}(s) + \text{PDBeffw} \rightarrow \text{S}(s)$ ,  $\text{kx1}(\text{kx1.fun})$ , Change (Crosslinking)

$\text{P2w}(s) + \text{PDBeffw} \rightarrow \text{T}(s) + \text{PDBeffw}$ ,  $\text{kx2}(\text{kx2.fun})$ , Change (Crosslinking)

$\text{P1w}(s) + \text{PDBacc} \rightarrow \text{S}(s)$ ,  $\text{kx1}(\text{kx1.fun})$ , Change (Crosslinking)

$\text{P2w}(s) + \text{PDBacc} \rightarrow \text{T}(s) + \text{PDBeffw}$ ,  $\text{kx2}(\text{kx2.fun})$ , Change (Crosslinking)

### Transfer to monomer

$\text{P1w}(s) + \text{M1} \rightarrow \text{Dw}(s) + \text{P1w}(1)$ ,  $\text{kf11}$ , Transfer(copolymer) (Transfer\_to\_monomer)

$\text{P1w}(s) + \text{M2} \rightarrow \text{Dw}(s) + \text{P2w}(1)$ ,  $\text{kf12}(\text{kf12.fun})$ , Transfer(copolymer) (Transfer\_to\_monomer)

$\text{P2w}(s) + \text{M1} \rightarrow \text{Dw}(s) + \text{P1w}(1)$ ,  $\text{kf21}(\text{kf21.fun})$ , Transfer(copolymer) (Transfer\_to\_monomer)

$\text{P2w}(s) + \text{M2} \rightarrow \text{Dw}(s) + \text{P2w}(1)$ ,  $\text{kf22}(\text{kf22.fun})$ , Transfer(copolymer) (Transfer\_to\_monomer)

$\text{P3w}(s) + \text{M1} \rightarrow \text{D4w}(s) + \text{P1w}(1)$ ,  $\text{kf31}(\text{kf31.fun})$ , Transfer(copolymer) (Transfer\_to\_monomer)

$\text{P3w}(s) + \text{M2} \rightarrow \text{D4w}(s) + \text{P2w}(1)$ ,  $\text{kf32}(\text{kf32.fun})$ , Transfer(copolymer) (Transfer\_to\_monomer)

**$\text{P3w}(s) + \text{MEHQ} \rightarrow \text{Q}^*(s)$ ,  $\text{k\_inh\_MEHQ\_3}$ , Change (Inhibition\_of\_peroxy\_radicals\_by\_MEHQ)**

$y' = f(\text{TDBbytransfermonomer.fun}(y))$ , ODE-System

(Generation\_of\_terminal\_double\_bonds\_("TDB")\_by\_transfer\_reactions\_to\_monomer)

$y' = f(\text{PDBbytransfermonomer.fun}(y))$ , ODE-System

(Generation\_of\_pendant\_double\_bonds\_("PDB")\_by\_transfer\_reactions\_to\_monomer)

### Termination

$P1w(s) + P1w(r) \rightarrow Dw(s+r)$  ,  $k0(ktss.fun)$  , Combination(copolymer)  
 $P1w(s) + P1w(r) \rightarrow Dw(s) + Dw(r)$  ,  $ktss(ktss.fun)$  , Combination(copolymer) (Termination)  
 $P1w(s) + P2w(r) \rightarrow Dw(s+r)$  ,  $k0(ktss12.fun)$  , Combination(copolymer)  
 $P1w(s) + P2w(r) \rightarrow Dw(s) + Dw(r)$  ,  $ktss(ktss12.fun)$  , Combination(copolymer) (Termination)  
 $P2w(s) + P2w(r) \rightarrow Dw(s+r)$  ,  $k0(ktss22.fun)$  , Combination(copolymer)  
 $P2w(s) + P2w(r) \rightarrow Dw(s) + Dw(r)$  ,  $ktss(ktss22.fun)$  , Combination(copolymer) (Termination)  
 $P3w(s) + P3w(r) \rightarrow D3w(s+r) + O2$  ,  $kt33(kt33.fun)$  , Combination(copolymer)  
 $P3w(s) + P3w(r) \rightarrow D3w(s) + D3w(r) + 2O2$  ,  $k0(kt33.fun)$  , Combination(copolymer) (Termination\_of\_peroxy\_radical)  
 $P3w(s) + P1w(r) \rightarrow Dw(s+r)$  ,  $k0$  , Combination(copolymer)  
 $P3w(s) + P1w(r) \rightarrow Dw(s) + Dw(r)$  ,  $kt31$  , Combination(copolymer) (Termination\_of\_peroxy\_radical\_dispro)  
 $P3w(s) + P2w(r) \rightarrow Dw(s+r)$  ,  $k0(kt32.fun)$  , Combination(copolymer)  
 $P3w(s) + P2w(r) \rightarrow Dw(s) + Dw(r)$  ,  $kt32(kt32.fun)$  , Combination(copolymer) (Termination\_of\_peroxy\_radical\_dispro)  
 **$P3w(s) + Q^*(r) \rightarrow Q(s+r) + O2$  ,  $k_{inh\_MEHQ\_4}$  , Combination(copolymer)**  
 **$P3w(s) + Q^*(r) \rightarrow Q(s) + Q(r) + 2O2, 0$  , Combination(copolymer)**  
**Inhibition\_of\_peroxy\_radicals\_by\_a\_MEHQ\_radical**  
 $y' = f(TDBbytermination.fun(y))$  , ODE-System  
(Generation\_of\_terminal\_double\_bonds("TDB")\_by\_termination\_in\_water-phase)  
 $y' = f(PDBbytermination.fun(y))$  , ODE-System (Generation\_of\_double\_bonds("PDB")\_by\_termination\_in\_water-phase)

Transfer to gelatin

$P1w(s) + Gelatin \rightarrow Dw(s)$  ,  $kfGelatin$  , Change (Transfer\_to\_gelatin)  
 $P2w(s) + Gelatin \rightarrow Dw(s)$  ,  $kfGelatin2chem(kfGelatin2chem.fun)$  , Change (Transfer\_to\_gelatin)  
 $P3w(s) + Gelatin \rightarrow D4w(s)$  ,  $kf3Gelatin(kf3Gelatin.fun)$  , Change (Transfer\_to\_gelatin)  
 $y' = f(Transfertogelatinaqueous.fun(y))$  , ODE-System (Transfer\_to\_gelatin\_(aqueous\_phase))  
 $y' = f(PDBbytransferGelatin.fun(y))$  , ODE-System  
(Generation\_of\_double\_bonds("PDB")\_by\_transfer\_to\_gelatin\_in\_water-phase)

Re-Initiation

$Gelatinrad + M1 \rightarrow P1w(1) + C1$  ,  $kpG$  , Initiation(anion) (Re-initiation)  
 $Gelatinrad + M2 \rightarrow P2w(1) + C2$  ,  $kpG(kpG2.fun)$  , Initiation(anion) (Re-initiation)  
 $P3w(s) + M1 \rightarrow P1w(s+1) + C1$  ,  $kp31(kp31.fun)$  , Propagation(copolymer) (Reinitiation\_of\_peroxy\_radical)  
 $P3w(s) + M2 \rightarrow P2w(s+1) + C2$  ,  $kp32(kp32.fun)$  , Propagation(copolymer) (Reinitiation\_of\_peroxy\_radical)  
 $y' = f(Gelatinbyre-initiation.fun(y))$  , ODE-System (Generation\_of\_Gelatin\_by\_Re-initiation)

Change from TDB to PDB

$TDBw \rightarrow PDBeffw$  ,  $kinf$  , Elementalreaction (Change\_of\_characteristic\_of\_TDB)  
Equilibrium between phases  
 $y' = f(equilibriumM1.fun(y))$  , ODE-System (Partition\_Equilibrium\_for\_Acrylamide)  
 $y' = f(equilibriumM2.fun(y))$  , ODE-System (Partition\_Equilibrium\_for\_Bis(acrylamide))  
 $y' = f(equilibriumwater.fun(y))$  , ODE-System (Partition\_Equilibrium\_for\_Water)  
 $y' = f(equilibriumGelatin.fun(y))$  , ODE-System (Partition\_Equilibrium\_for\_Gelatin)  
 $y' = f(equilibriumPDB.fun(y))$  , ODE-System (Partition\_Equilibrium\_for\_PDB\_)  
Phase-Transfer  
 $S(s) \rightarrow U(s)$  ,  $kinf$  , Change (Precipitation)  
 $T(s) \rightarrow V(s)$  ,  $kinf$  , Change (Precipitation)  
 $U(s) \rightarrow Prpfake(s) + RL1pf$  ,  $kinf$  , Change (Precipitation)  
 $V(s) \rightarrow Prpfake(s) + RL1pf$  ,  $kinf$  , Change (Precipitation)  
 $y' = f(transferofPDB.fun(y))$  , ODE-System (Transfer\_between\_phases\_of\_PDB)  
 $y' = f(transferofC.fun(y))$  , ODE-System (Transfer\_between\_phases\_of\_Cyclized\_units)  
 $y' = f(transferofX.fun(y))$  , ODE-System (Transfer\_between\_phases\_of\_Crosslink\_units)

## Polymer\_Phase

### Short\_Radicals

Initiation.

$y' = f(GenerationofPRpolymer.fun(y))$  , ODE-System (Generation\_of\_Primary\_Radicals\_in\_Polymer\_Phase)  
 $PRp + PRp \rightarrow eff*(I^*p + I^*p)$  ,  $ki$  , Elementalreaction2

$I^*p + M1p \rightarrow P1p(1) + C1p$  ,  $ki1$  , Initiation(anion) (Initiation)  
 $I^*p + M2p \rightarrow P2p(1) + C2p$  ,  $ki2$  , Initiation(anion) (Initiation)

Propagation..

$P1p(s) + M1p \rightarrow P1p(s+1) + C1p$  ,  $kp11(kp11S.fun)$  , Propagation(copolymer) (Propagation\_of\_acrylamide)  
 $P1p(s) + M2p \rightarrow P2p(s+1) + C2p$  ,  $kp12(kp12S.fun)$  , Propagation(copolymer) (Propagation\_of\_acrylamide)  
 $P2p(s) + M1p \rightarrow P1p(s+1) + C1p$  ,  $kp21(kp21S.fun)$  , Propagation(copolymer) (Propagation\_of\_bisacrylamide)  
 $P2p(s) + M2p \rightarrow P2p(s+1) + C2p$  ,  $kp22(kp22S.fun)$  , Propagation(copolymer) (Propagation\_of\_bisacrylamide)  
 $y' = f(PDBbypropagationpolymer.fun(y))$ , ODE-System  
 (Generation\_of\_double\_bonds\_("PDB")\_by\_propagation\_reactions)

Cyclization..

$P2p(s) \rightarrow P1p(s) + Cp$  ,  $kc$  , Change (Cyclization)

Crosslinking..

$P1p(s) + PDBeffp \rightarrow XX(s) + RL1pf$  ,  $kx1(kx1S.fun)$  , Change (Crosslinking)  
 $P2p(s) + PDBeffp \rightarrow YY(s) + RL1pf$  ,  $kx2(kx2S.fun)$  , Change (Crosslinking)  
 $y' = f(Xbycrosslinking.fun(y))$  , ODE-System (Crosslink\_Units)  
 $y' = f(PDBbycrosslinkingpolymerS.fun(y))$  , ODE-System (PDB\_by\_crosslinking\_in\_polymer\_phase\_(short\_radicals))

Transfer to monomer.

$P1p(s) + M1p \rightarrow Dp(s) + P1p(1)$  ,  $kf11(kf11S.fun)$  , Transfer(copolymer) (Transfer\_to\_monomer)  
 $P1p(s) + M2p \rightarrow Dp(s) + P2p(1)$  ,  $kf12(kf12S.fun)$  , Transfer(copolymer) (Transfer\_to\_monomer)  
 $P2p(s) + M1p \rightarrow Dp(s) + P1p(1)$  ,  $kf21(kf21S.fun)$  , Transfer(copolymer) (Transfer\_to\_monomer)  
 $P2p(s) + M2p \rightarrow Dp(s) + P2p(1)$  ,  $kf22(kf22S.fun)$  , Transfer(copolymer) (Transfer\_to\_monomer)  
 $y' = f(TDBbytransfermonomerpolymerS.fun(y))$ , ODE-System  
 (Generation\_of\_terminal\_double\_bonds\_("TDB")\_by\_transfer\_reactions\_to\_monomer\_in\_polymer\_phase\_..  
 $y' = f(PDBbytransfermonomerpolymerS.fun(y))$ , ODE-System  
 (Generation\_of\_pendant\_double\_bonds\_("PDB")\_by\_transfer\_reactions\_to\_monomer\_in\_polymer\_phase\_(s..

Termination..

$P1p(s) + P1p(r) \rightarrow Dp(s+r)$  ,  $k0(ktss(p).fun)$  , Combination(copolymer)  
 $P1p(s) + P1p(r) \rightarrow Dp(s) + Dp(r)$  ,  $ktss(ktss(p).fun)$  , Combination(copolymer) (Termination)  
 $P1p(s) + P2p(r) \rightarrow Dp(s+r)$  ,  $k0(ktss12(p).fun)$  , Combination(copolymer)  
 $P1p(s) + P2p(r) \rightarrow Dp(s) + Dp(r)$  ,  $ktss(ktss12(p).fun)$  , Combination(copolymer) (Termination)  
 $P2p(s) + P2p(r) \rightarrow Dp(s+r)$  ,  $k0(ktss22(p).fun)$  , Combination(copolymer)  
 $P2p(s) + P2p(r) \rightarrow Dp(s) + Dp(r)$  ,  $ktss(ktss22(p).fun)$  , Combination(copolymer) (Termination)  
 $y' = f(TDBbyterminationpolymerS.fun(y))$ , ODE-System (TDB\_by\_termination\_in\_the\_polymer\_phase\_(short\_radicals))  
 $y' = f(PDBbyterminationpolymerS.fun(y))$ , ODE-System  
 (PDB\_by\_termination\_in\_the\_polymer\_phase\_(short\_radicals))

Transfer to gelatin.

$P1p(s) + Gelatinp \rightarrow Dp(s)$  ,  $kfGelatin(kfGelatin1S.fun)$  , Change (Transfer\_to\_gelatin)  
 $P2p(s) + Gelatinp \rightarrow Dp(s)$  ,  $kfGelatin(kfGelatin2S.fun)$  , Change (Transfer\_to\_gelatin)  
 $y' = f(transfertogelatinpolymershorts.fun(y))$  , ODE-System (Transfer\_to\_gelatin\_(polymer\_short))

Long\_Radicals

Propagation

$k1RL1p^k1 + k1M1p^k1 \leftrightarrow k1RL1p^k1 + k1D1,p^k1$ ,  $kp11, k0(kp11L.fun)$ , Kinetic  
 (Propagation\_of\_acrylamide\_monomer\_)  
 $k1RL1p^k1 + k1M2p^k1 \leftrightarrow k1RL2p^k1 + k1D2,p^k1$ ,  $kp12, k0(kp12L.fun)$ , Kinetic  
 (Propagation\_of\_bis(acrylamide)\_monomer\_)  
 $k1RL2p^k1 + k1M1p^k1 \leftrightarrow k1RL1p^k1 + k1PDBeffp^k1 + k1D1,p^k1$ ,  $kp21, k0(kp21L.fun)$ , Kinetic  
 (Propagation\_of\_acrylamide\_monomer\_)  
 $k1RL2p^k1 + k1M2p^k1 \leftrightarrow k1RL2p^k1 + k1PDBeffp^k1 + k1D2,p^k1$ ,  $kp22, k0(kp22L.fun)$ , Kinetic  
 (Propagation\_of\_acrylamide\_monomer\_)  
 $k1RL1pf^k1 + k1M1p^k1 \leftrightarrow k1RL1p^k1 + k1D1,p^k1$ ,  $kp21, k0(kp21L.fun)$ , Kinetic  
 (Propagation\_of\_acrylamide\_monomer\_(fake))



$k_1 RL1p^k1 + k_1 M2p^k1 \rightleftharpoons k_1 RL2p^k1 + k_1 D2p^k1$ ,  $kp22, k0(kp22L.fun)$ , Kinetic  
(Propagation\_of\_bis(acrylamide)\_monomer\_(fake))

Cyclization

$RL2p \rightarrow RL1p + Cp$ ,  $kc$ , Elementalreaction (Cyclization)

Crosslinking

$RL1p + PDBeffp \rightarrow RL1pf + Xp$ ,  $kx1(kx1L.fun)$ , Elementalreaction (Crosslinking)

$RL2p + PDBeffp \rightarrow RL1pf + Xp$ ,  $kx2(kx2L.fun)$ , Elementalreaction (Crosslinking)

$y' = f(PDBbycrosslinkingpolymerL.fun(y))$ , ODE-System (PDB\_by\_crosslinking\_in\_polymer\_phase\_(long\_radicals))

Transfer to Monomer

$RL1p + M1p \rightarrow P1p(1) + Dp$ ,  $kf11(kf11L.fun)$ , Initiation(anion) (Transfer\_to\_Monomer)

$RL1p + M2p \rightarrow P2p(1) + Dp$ ,  $kf12(kf12L.fun)$ , Initiation(anion) (Transfer\_to\_Monomer)

$RL2p + M1p \rightarrow P1p(1) + Dp$ ,  $kf21(kf21L.fun)$ , Initiation(anion) (Transfer\_to\_Monomer)

$RL2p + M2p \rightarrow P2p(1) + Dp$ ,  $kf22(kf22L.fun)$ , Initiation(anion) (Transfer\_to\_Monomer)

$y' = f(TDBbytransfermonomerpolymerL.fun(y))$ , ODE-System

(Generation\_of\_terminal\_double\_bonds("TDB")\_by\_transfer\_reactions\_to\_monomer\_in\_polymer\_phase\_..)

$y' = f(PDBbytransfermonomerpolymerL.fun(y))$ , ODE-System

(Generation\_of\_pendant\_double\_bonds("PDB")\_by\_transfer\_reactions\_to\_monomer\_in\_polymer\_phase\_(l..))

Transfer to Gelatin

$y' = f(Trabsfertogelatin.fun(y))$ , ODE-System (Trannsfer\_to\_gelatin\_(polymer\_phase))

$y' = f(PDBbytransfertomonomerpolymer.fun(y))$ , ODE-System (PDB\_by\_transfer\_to\_gelatin\_in\_the\_polymer\_phase)

Re-Initiation.

$Gelatinprad + M1p \rightarrow RL1p + D1p$ ,  $kpG(kpG1L.fun)$ , Elementalreaction (Re-initiation)

$Gelatinprad + M2p \rightarrow RL2p + D2p$ ,  $kpG(kpG2L.fun)$ , Elementalreaction (Re-initiation)

$y' = f(Gelatininpolymerbyre-initiation.fun(y))$ , ODE-System (Generation\_of\_Gelatin\_by\_Re-initiation\_in\_polymer\_phase)

Termination.

$RL1p + RL1p \rightarrow k_1(ktl.fun)*(Dp + Dp)$ ,  $ktl(ktl.fun)$ , Elementalreaction2 (Termination)

$RL1p + RL2p \rightarrow TDBp + Dp$ ,  $ktl(ktl2.fun)$ , Elementalreaction (Termination)

$RL2p + RL2p \rightarrow k_1(ktl22.fun)*(Dp + Dp)$ ,  $ktl(ktl22.fun)$ , Elementalreaction2 (Termination)

$y' = f(PDBpolymerbytermination.fun(y))$ , ODE-System

(Generation\_of\_double\_bonds("PDB")\_by\_termination\_in\_polymer-phase)

$y' = f(TDBpolymerbytermination.fun(y))$ , ODE-System

(Generation\_of\_terminal\_double\_bonds("TDB")\_by\_termination\_in\_polymer-phase)

Change of characteristic in polymer phase

$TDBp \rightarrow PDBeffp$ ,  $kinf$ , Elementalreaction (Change\_of\_characteristic\_of\_TDB\_in\_polymer\_phase)

Short-Long Radicals

Termination...

$P1p(s) + RL1p \rightarrow Dp(s) + Dp$ ,  $ktsl(ktsl11.fun)$ , Change (Termination)

$P1p(s) + RL2p \rightarrow Dp(s) + Dp$ ,  $ktss(ktsl12.fun)$ , Change (Termination)

$P2p(s) + RL1p \rightarrow Dp(s) + Dp$ ,  $ktss(ktsl21.fun)$ , Change (Termination)

$P2p(s) + RL2p \rightarrow Dp(s) + Dp$ ,  $ktss(ktsl22.fun)$ , Change (Termination)

$y' = f(PDBpolymerbyterminationSL.fun(y))$ , ODE-System

(Generation\_of\_double\_bonds("PDB")\_by\_termination\_in\_polymer-phase\_(short-long\_radicals))

$y' = f(TDBpolymerbyterminationSL.fun(y))$ , ODE-System

(Generation\_of\_terminal\_double\_bonds("TDB")\_by\_termination\_in\_polymer-phase\_(short-long\_radicals))